STUDIES ON MORPHOLOGY CONTROL OF POROUS SILICA THROUGH POLYMER-INCORPORATED SOL-GEL PROCESSES

KAZUKI NAKANISHI

1991

CONTENTS

GENERAL INTRODUCTION TO PHASE SEPARATION IN POLYMER-CONTAINING SYSTEMS -- 1

CHAPTER 1 SYSTEMS CONTAINING POLYACRYLIC ACID; GEL-FORMATION BEHAVIOR AND EFFECT OF SOLVENT COMPOSITION ---------- 11

CHAPTER 2 SYSTEMS CONTAINING POLYACRYLIC ACID; EFFECTS OF MOLECULAR WEIGHT AND REACTION TEMPERATURE ---------- 39

CHAPTER 3 EFFECT OF CATALYTIC CONDITION IN SYSTEMS CONTAINING POLYACRYLIC ACID ---------- 59

CHAPTER 4 EFFECT OF CHEMICAL ADDITIVES ON GEL STRUCTURE ---------- 75

CHAPTER 5 ACID-CATALYZED SYSTEMS CONTAINING SODIUM POLYSTYRENE SULFONATE ---------- 97

CHAPTER 6 ANALYSIS OF POLYMERIZATION BEHAVIOR BY SMALL ANGLE X-RAY SCATTERING ---------- 131

CHAPTER 7 PORE SURFACE CHARACTERISTICS OF MACROPOROUS SILICA GELS PREPARED FROM POLYMER-CONTAINING SOLUTION ---------- 149

SUMMARY ---------- 170

ACKNOWLEDGEMENTS ---------- 173

GENERAL INTRODUCTION TO PHASE SEPARATION IN POLYMER-CONTAINING SYSTEMS

1. INTRODUCTION

Materials with tailored structure in desired length scale are drawing increasing attention in recent years. Although various gas phase deposition processes have been explored to control the atomic level structure, most materials are still used in bulk state where their characters strongly depend on the structure in larger dimensions than molecular level. The importance of deeper understanding to the formation mechanism of middle or meso-range structure cannot be over-emphasized in order to get a true breakthrough in improving the properties of materials even for those with already controlled molecular-level structure.

Sol-gel processing of glasses, ceramics or composite materials has been rigorously studied in the past two decades because its widespread possibility of preparing materials tailored in molecular level[1]. In fact, it came true in several film or powder formation processes[2]. From the standpoint of obtaining composite materials, the low processing temperature is attractive to prepare those containing molecular level bonding between organic and inorganic components. It has also been partly realized in silica-dimethylsiloxane[3] systems, but detailed characterization[4] and control of the heterogeneity have not yet been established.

As widely known for organic polymer blends[5], the strong segregation tendency between different polymeric species results in various phase separated structures in the preparation stage. The specific structures are intentionally utilized to produce materials with improved properties. It becomes therefore important to make clear the similarity and difference in phase separation behavior of inorganic polymer systems in order to prepare the materials with controlled structure in any desired length scale. This chapter describes

the objective of the present thesis reviewing the background and related studies in the fields of glass, ceramic and polymer science.

2. SOL-GEL REACTIONS OF ALKOXY-DERIVED SILICATE SOLUTIONS

"Sol-gel reaction" is the term widely used to describe the phenomenon which accompanies the solidification of fluid substances into fluid-containing continuous solid network with temperature change or chemical reaction. The gel-formation of silicate solutions has been long investigated and reviewed extensively by Iler[6]. Recent researches are mainly concentrated on the gels prepared from alkoxysilane which can be purified by distillation. The hydrolysis and polycondensation of silicate species can be described as below.

$Si(OR)_4 + nH_2O \rightarrow Si(OR)_{4-n}(OH)_n$ (hydrolysis)

$Si\text{-}OH + Si\text{-}OH \rightarrow Si\text{-}O\text{-}Si + H_2O$ (water producing condensation)

$Si\text{-}OH + Si\text{-}OR \rightarrow Si\text{-}O\text{-}Si + ROH$ (alcohol producing condensation)

where OR denotes alkoxy group. The relative rates of hydrolysis and polycondensation depend strongly on the amount of available water and type of coexisting catalysts, resulting in silicate polymers with wide variation of molecular weight[7], hydroxy to alkoxy content[8], degree of branching[9], etc., thus influence the final gel structure in quite complex ways. An excellent review of the sol-gel process mainly based on the alkoxide route by Brinker and Scherer has been recently published[10].

3. PHASE SEPARATION IN GEL-FORMING SYSTEMS

Simple statistical thermodynamics of crosslinked system[11] yields the equivalence of the increase in the number of chemical bond to that in attractive interaction among constituents, thus the "equivalent temperature T_{eq}", defined as $T_{eq}=J/\beta$ where -J and β respectively denote the interaction energy per one pair of monomers and the correlation strength between monomers, decreases as the polymerization reaction proceeds (β increases). Since the physical state of gels prepared by irreversible reaction depends on the preparation history, sol-gel transition would be compared to the liquid-glass transition. Hence, the gel-forming reaction is physically almost equivalent to the finite-rate cooling of glass-forming systems. Furthermore, if the system has the sol-gel transition (equivalent) temperature a little above the binodal temperature, the spinodal phase separation is likely to occur on cooling (polymerizing) the system due to the reduced mobility. Consequently, the silica sol-gel reaction accompanied by the spinodal phase separation can be regarded as almost completely equivalent to the finite-rate cooling of the mixtures having UCST (Upper Critical Solution Temperature) and glass transition region in the cooling temperature range, e.g., immiscible oxide glass melts.

4. SPINODAL PHASE SEPARATION

In a given system with the miscibility gap, the line on which the second composition derivative of Gibbs' free-energy becomes zero is called spinodal curve. Since the system is unstable within the spinodal, compositional fluctuations having the wavelength larger than the critical one can spontaneously grow without requiring the activation energy for diffusion.

According to the discussion of finite-rate cooling of immiscible glass melts by Cahn and Charles based on the linearized theory of spinodal phase separation[12], the fluctuation having the fixed dominant wavelength Λ_m grows exponentially with time with the rate constant proportional to the square of quench depth, i.e., the temperature difference from the spinodal line. On the other hand, the system mobility decreases with decreasing temperature and so with quench depth in UCST system. The fluctuation wavelength having actually maximum growth rate Λ_a is then determined by these two opposing factors independent of the cooling rate. The cooling rate influences the domain size

only when it is so slow that the required fluctuations with slower growth rate can grow in substantial degree, and with the slower cooling the larger domains result. With increasing cooling rate, the attainable amplitude of fluctuation at fixed Λ_a decreases and finally becomes indistinguishable from the molecular level fluctuations with infinite cooling.

Once initiated at the fixed quench depth, the spinodal phase separation is known to follow the three successive steps[13]. The initial stage has successfully been described by the linearized theory as described above. Since the spatial fluctuation distribution is expressed by the random superpositions of sinusoidal waves with the single wavelength, so-called interconnected domain structure results when the volume fractions of phase-separating domains are comparable. In the following intermediate stage, both the dominant wavelength and amplitude of composition difference grow with time to attain equilibrium composition in each domain. The interfaces between conjugate phases becomes smooth at the end of this stage. The late stage accompanies only the morphological changes due to the coarsening of equilibrated domains. The increase in the periodical wavelength of the interconnected structure, often followed by the breaking-up and dispersion of minor phase, is observed. The rates of growth in periodical wavelength in these stages are known to increase with quench depth[13].

5. DEVELOPMENT AND FIXATION OF MORPHOLOGY IN MULTI-PHASE ORGANIC POLYMER SYSTEMS.

In the field of technology called "polymer alloying", where several kinds of organic polymers are mixed together to form special microscopic morphologies including periodical, interconnected, or finely dispersed structure, the phase separation by spinodal mechanism plays quite an important role. On the other hand, melt-quenched immiscible oxide glass systems are known to phase separate to form the interconnected or particulate morphology when subjected

to the temperature near the glass transition region. Several examples for organic polymer systems are shown below;

(1) Two incompatible polymers homogeneously dissolved in a large amount of common solvent can be made into films with interconnected morphology by casting the solution and evaporate the solvent. The periodical size of the structure can be controlled by changing the evaporation rate[14].

(2) The one-phase mixture of incompatible polymers is subjected to sudden temperature change to cause spinodal phase separation in a two-phase region and to form interconnected morphology, then either polymer is crosslinked by the chemical reaction with peroxide for the developed morphology to be fixed at arbitrary stages of structural evolution[15].

(3) Oligomers of thermosetting resin mixed with compatible rubbery (thermoplastic) polymer are cured by heating to form interconnected globular structures composed of resin and rubbery polymer. The heating rate and the kind of curing agent determine the periodical size[16].

The above examples show representative pathways to induce the spinodal phase separation and to fix the developed interconnected morphology. The first one increases the incompatibility between polymers by extracting the solvent while limiting the motion of polymers by concentrating the system. The second one induces the phase separation by the well-known temperature jump method, while the fixation of the structure depends on the chemical crosslinking reaction. Although the method of fixing the structure is different, both examples make use of rapid changes in the physical interaction among constituents to initiate the spinodal phase separation. The solvent extraction is viewed as "physical" method because neither the formation nor the breakage of chemical bonds is included in the process. From this viewpoint, the case of immiscible oxide glasses may belong to the same category as

the first example, where the driving force of phase separation is of chemical origin, but the onset of phase separation and the freezing of structure both depend on the temperature change of the system.

The last example simultaneously induces the phase separation and limits the diffusional motion of polymers by increasing the (chemical) crosslinking density of one of the polymer components. The method of inducing phase separation by promoting a chemical reaction which rapidly modifies the interaction among constituents is often termed as "chemical quenching". As shown later in Chapter 1, if we accept the equivalence of chemical bonds to attractive interactions, the above distinction between "physical" and "chemical" processes diminishes except their reversibility.

6. CHARACTERISTICS OF POLYMER-INCORPORATED SILICA SOL-GEL SYSTEM

The particular point of silica sol-gel systems which accompany phase separation is that, once the domains started to develop, the polymerization reaction in silica-rich domains would further be accelerated by the concentrating effect, which results in the decreased mobility and the formation of sharper interfaces between the domains. Hence, the interconnected porous morphology with relatively smooth pore surface is expected to form even from the incomplete domains developed in the early or intermediate stages of spinodal phase separation. The compositional differences tend to be spontaneously contrasted in the gel-forming system. And in turn, the coarsening process of the interconnected domains in the late stage will severely be restricted since it requires the bulk diffusion of constituents, while the breaking-up of the continuous domains is more or less likely to occur. Both organic polymer mixture solutions subjected to the rapid solvent evaporation[14] and cured rubber-incorporated thermosetting resins[15] give the well-defined phase morphology although the light-scattering profiles show no remarkable shift

during the domain formation. Since silica forms quite strong gel with high crosslinking density compared with organic systems, the interface formation is expected to take place much more intensively.

7. PERSPECTIVE OF THIS THESIS

The present thesis describes the application of morphology control method through phase separation to the silica sol-gel systems by incorporating water-soluble organic polymers. Since this kind of research has just started, the main purpose of this thesis is to make clear the similarity and difference in phase separation behavior of the alkoxy-derived silica sol-gel system compared with those of organic polymer systems.

In Chapter 1, the general gel-forming behavior in the system containing polyacrylic acid is extensively investigated. Possible mechanism of morphology development is discussed based on the time-resolved light scattering measurement of the reacting solution.

In Chapter 2, the effects of molecular weight of polyacrylic acid and reaction temperature on the gel morphology are described in relation to the mechanism of morphology formation discussed in Chapter 1.

In Chapter 3, the effect of catalytic condition which influences the gel formation mechanism of silica is investigated, and the results are interpreted in the same manner as in Chapter 1.

In Chapter 4, the addition effect of various organic solvents on the sol-gel system is studied. The effects of respective solvents on resultant gel morphology are discussed in terms of the solubility of polyacrylic acid and the polymerization rate of silica.

In Chapter 5, the silica system containing sodium polystyrene sulfonate (NaPSS) is investigated. Discussions are focused on the effect of low solubility of NaPSS in coexisting alcohol on the resultant gel morphology.

In Chapter 6, the polymerization behavior of silica is investigated by using the small angle x-ray scattering (SAXS) technique. The effect of coexisting polymer on the aggregation process of silica polymers are mainly discussed in relation to the identification of the dominant factor which determines the micron-range gel morphology.

In Chapter 7, the surface characteristics of gels with interconnected pores are analyzed utilizing the nitrogen adsorption and the mercury porosimetry together with SAXS. The nano-scale morphology change in wet state is demonstrated to be analogous to that of organic polymer gels.

Finally in SUMMARY, the whole results and discussions of this thesis are summarized, and the future perspectives are pointed out.

REFERENCES

[1] There are continuing series of international conferences on the sol-gel process such as "International Workshop on Gels" (1982- , every 2 years; Proceedings are *J. Non-Cryst. Solids*, **48**, 63, 82, 100, 121), "*Better Ceramics through Chemistry*" and "*Ultrastructure Processing Conference*".

[2] S.Hirano and K.Kato, *J. Non-Cryst. Solids*, **100**(1988), 538-541;
E.Matijevic in "*Science of Ceramic Chemical Processing*", eds. L.L.Hench and D.R.Ulrich (Wiley, N.Y., 1986), 463-481.

[3] J.E.McGrath, J.P. Pullockaren, J.S.Riffle, S.Kilic and C.S.Elsbernd, in "*Ultrastructure Processing of Advanced Ceramics*", eds. J.D.Mackenzie and D.R.Ulrich (Wiley, N.Y., 1988), 55-75.
Y.J.Chung, S.-J.Ting and J.D.Mackenzie, in *Better Ceramics Through Chemistry IV*, eds. B.J.J.Zelinski, C.J.Brinker, D.E.Clark and D.R.Ulrich, (Mat. Res. Soc., Pittsburgh, PA, 1990), 981-986.

[4] D.W.Schaefer, J.E.Mark, D.McCarthy, L.Jian, C.-C.Sun and B.Farago, *Mat. Res. Soc. Symp. Proc.*, vol.171(1990), 57-63.

[5] D.R.Paul and S.Newmann eds., "*Polymer Blends I & II*" (Academic Press, N.Y., 1978)

[6] R.K.Iler, "*The Chemistry of Silica*" (Wiley, N.Y., 1979).

[7] T.W.Zerda, I.Artaki and J.Jonas: *J. Non-Cryst. Solids*, **81**(1986), 365-379.

[8] L.W.Kelts, N.J.Effenger and S.M.Melpolder, *J. Non-Cryst. Solids*, **82**(1986), 57-68.

[9] C.J.Brinker, K.D.Keefer, D.W.Schaefer and C.S.Ashley, *J. Non-Cryst. Solids*, **48**(1982), 47-64.

[10] C.J.Brinker and G.W.Scherer, "*Sol-Gel Science*" (Academic Press, N.Y., 1990)

[11] P.G.deGennes, "*Scaling Concepts in Polymer Physics*" (Cornell University, Ithaca, New York, 1979).

[12] J.W.Cahn and R.J.Charles: *Phys. Chem. Glasses*, **6**(1965), 181-191.

[13] T.Hashimoto, M.Itakura and H.Hasegawa: *J. Chem. Phys.*, **85**(1986), 6118-6128.

[14] T.Inoue, T.Ougizawa, O.Yasuda and K.Miyasaka, *Macromolecules*, **18**(1985), 57-63.

[15] T.Hashimoto, M.Takenaka and H.Jinnai, *Polym. Commun.*, **30**(1989), 177.

[16] K.Yamanaka, Y.Takagi and T.Inoue, *Polymer*, **30**(1989), 1839-1844.

CHAPTER 1

SYSTEMS CONTAINING POLYACRYLIC ACID ; GEL FORMATION BEHAVIOR AND EFFECT OF SOLVENT COMPOSITION

1.1 INTRODUCTION

Phase separation in glass forming multicomponent oxide systems, especially in the spinodal region, is well known and the special application technique called the "Vycor process" is established for commercial production[1]. Among numerous studies performed recently on the sol-gel processing, most experiments have aimed to produce homogeneous phases from the gelling solutions. Although a conceptual suggestion has been given by Schaefer and Keefer on the existence and possible utilization of phase separation phenomena which occur in parallel to the polymerization of silica polymers[2], only a few studies have been made on this subject so far. Very recently it has been reported that phase separation in a range exceeding 50nm was detected in a polydimethylsiloxane-silica mixed system by SAXS and SANS measurements, and that the spinodal-like peak was recognized in 10nm range[3]. Direct SEM observations of micron-range interconnected structure of ORMOSILs[4] and partly connected globular structure prepared from highly acidic silica sols[5] have also been reported without referring to the link between structure formation and phase separation. For the systems containing colloidal silica and aqueous alkali silicate, the preparation of alkali-silicate gels with interconnected morphology is known as Shoup method[6], whose formation has been tentatively explained by the growth of silicate polymers on the colloidal silica particles working as nucleation sites.

In this chapter, the formation of micron-range interconnected porous morphology through the simple sol-gel reaction of alkoxy-derived silica system incorporated with polyacrylic acid is described. Since the solvent phase of

alkoxy-derived system is composed mainly of alcohol, water and catalysts, water-soluble polymers can coexist with silica during the polymerization and gel-forming reaction. Among various types of water-soluble polymers, polycarboxylic acids appeared to be an interesting group in that they are soluble also in less polar solvents such as alcohols. Moreover, the side chains can be partially esterified, which makes polycarboxylic acids more alcohol-soluble and may affect the compositional dependence of the phase-separation and gelation behavior of the system. In this and following three Chapters, polyacrylic acid was chosen as a polymer component and the effects of compositional parameters on the gel morphology were investigated. The simple statistical thermodynamics of phase equilibria in gel-forming systems is introduced for the phenomenological interpretation of the observed results.

1.2 EXPERIMENTAL

1.2.1 Gel Preparation

Tetraethoxysilane (TEOS) and tetramethoxysilane (TMOS), products of Shin-Etsu Chemical Co., were used as silica source. Polyacrylic acid (HPAA), product of Aldrich Chemical Co. with molecular weight of 90,000 (denoted as PA9) was used as a polymer component. Nitric acid was used as a catalyst for hydrolysis.

The sample gels were prepared as follows. First, the HPAA was dissolved in distilled water and nitric acid was added so as to adjust the solution pH. Nitric acid was added in the molar ratio to water of 0.0173, which corresponded to ca. 0.9 mol/dm^3 of acid concentration. Secondly, TMOS or TEOS was added to above solution in a short time at room temperature. Immediately the container was sealed, and after stirring for 5 min the homogeneous solution was kept at 60°C for gelation. After gelation, the gel samples were aged at the same temperature, rinsed off the polymer phase with water

and ethanol, and finally dried at 60°C. In this report, the effects on gel morphology of the compositional parameters including concentrations of HPAA and solvent compositions under fixed catalyst concentration and reaction temperature are reported. Effects of other experimental conditions will be reported in the following chapters.

1.2.2 Light Scattering Measurements

The time evolution of light scattering (LS) was measured for the gelling solution with a selected composition. The data were collected with an automated laser light scattering apparatus[7] using He-Ne laser as light source. A 38-element photo-diode array was adopted to collect finely time-resolved scattering data.

1.2.3 SEM Observation

Scanning electron microscope (S-510, Hitachi Co.) was employed for the observation of morphology of the resultant gels. For all the samples, the degree of shrinkage was almost the same because the oxide content differed less than 10% which corresponds to the linear shrinkage of less than 3%. So that the observed sizes of microstructure for the dried gels are used without any correction in the following discussion.

1.3 RESULTS

1.3.1 Sol Formation

Under vigorous stirring, transparent solution could be obtained within a few seconds for TMOS and few minutes for TEOS accompanied by an abrupt heat evolution. The important chemical reactions which take place in the reacting solution can be summarized for the TEOS-containing system as following formulae representing the hydrolysis, polycondensation and esterification reactions, respectively;

$Si(OC_2H_5)_4 + xH_2O \rightarrow Si(OC_2H_5)_{4-x}(OH)_x + xC_2H_5OH$ (1)

$-Si(OR) + -Si(OR') \rightarrow -Si-O-Si- + ROR'$ (2)

$-CH_2CHCOOH-CH_2CHCOOH- + C_2H_5OH \rightarrow -CH_2CHCOOC_2H_5-CH_2CHCOOH- + H_2O$ (3)

where -OR and -OR' denote alkoxy or hydroxy groups.

The formation of partially esterified HPAA in the course of hydrolysis seems to have little influence on the solution composition because the amount of HPAA is quite small. It is more important that HPAA molecule become more soluble in alcohol-water mixed solvent than in pure-water by the partial esterification. Though has not been determined directly, the water-insoluble precipitates found in the syneresis liquids suggests the relatively high degree of esterification of HPAA. Under the present strongly acidic condition, the esterification reaction would be efficiently catalyzed and HPAA molecules will reach nearly the most favorable degree of esterification depending on the solution composition before the onset of phase separation and gelation. Therefore, it can be postulated that the water-alcohol mixed solution acts as relatively good solvent against the partially esterified HPAA in substantially broad range of mixing ratio. More precise discussion on the solubility of HPAA will require the detailed data of the compatibility between its partially esterified form and water-alcohol mixed solvent under the specified pH condition, which is beyond the perspective of this thesis. Experimental results on the gel-forming behavior under various catalytic conditions will be reported in Chapter 3, where the effect of esterification of HPAA will be discussed in some more detail.

1.3.2 Gel Formation and Phase Separation

Figure 1.1(a) shows the typical time evolution of light scattering profile during the development of the periodic compositional fluctuation in the solution which resulted in the interconnected morphology shown as Figure 1.1(b).

Almost in parallel to the gel-formation which took place about 120min after the hydrolysis, the scattering intensity, which exhibited no obvious change until then, started to increase to form a peak corresponding to the length scale of few microns. Until about 50 s, the peak intensity increased without the shift of peak position of about q=2x10^{-3} nm^{-1}. For the following several tens seconds, the intensity increase and shift of the peak position toward smaller q occurred in parallel. After the settled peak position (q=1.5x10^{-3} nm^{-1}) is attained at 120 s, only the intensity continued to increase for several tens minutes more than an order of magnitude exhibiting a saturating tendency with the consolidation of gel-network. The periodic size of dried gel observed under SEM (2.5μm) agreed well with that calculated from the above settled peak position and linear drying shrinkage (60% of original dimension). This indicates that the micron-range morphologies of dried gels directly reflect those formed at the gel-formation stage. The above LS profiles showing continuous development of the peak at fixed position in the initial stage strongly suggest that the interconnected gel morphology was formed through the spinodal phase separation of the gelling silica solution. The main reason why the exponential growth of peak intensity with time[10] could not clearly be detected must be the steeply decreasing system mobility through the sol-gel transition, which also accounts for the continued drastic increase in peak intensity without shift of its position in contrast to the ordinary coarsening process[11].

The solutions containing larger amount of solvents lost their fluidity while they looked still transparent, and then gradually became turbid. Those with smaller amount of solvent turned turbid shortly before gelation. These observations respectively indicate the occurrence of phase separation in loosely crosslinked gel network and that in fluid phase with increasing viscosity.

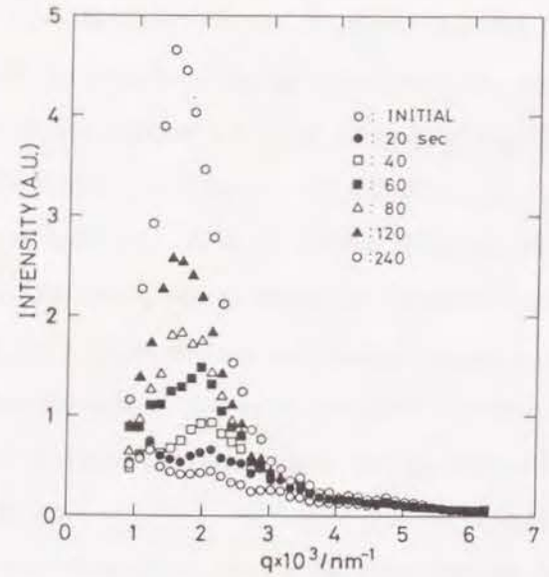

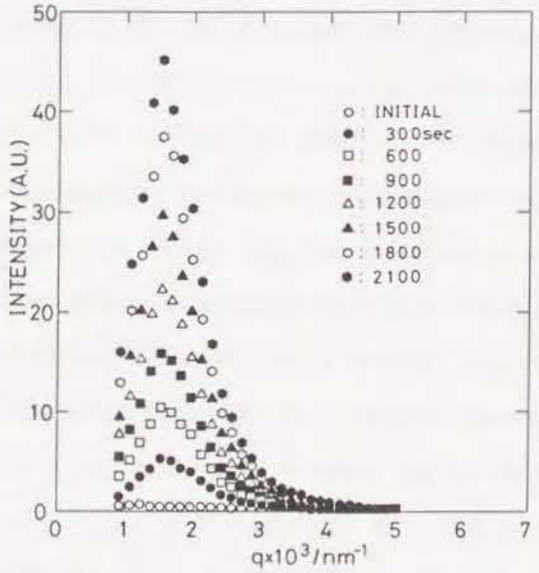

Figure 1.1(a) Time evolution of light scattering profile of the phase-separating solution resulted in the interconnected structure. Scattering intensity is plotted in linear scale against the scattering vector q defined by $q=(4\pi/\lambda)\sin(\theta/2)$ where λ is wavelength of incident beam, and θ is scattering angle. The q and intensity were corrected for refractive index and turbidity, respectively.

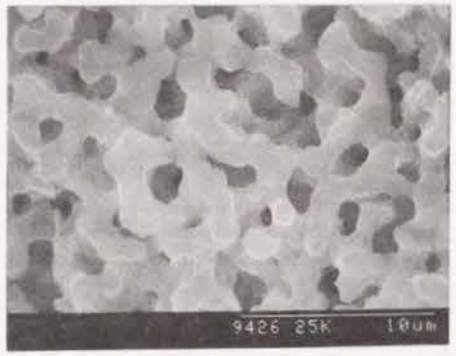

Figure 1.1(b) SEM photograph of dried gel prepared from the solution used in LS measurement. Drying shrinkage was 60%

The size and connectivity of micron-range pores and their dependence on the reaction parameters seemed to have a close relation between these sequences of gelation and phase separation, which will be further discussed below.

1.3.3 Effects of Composition and Amount of Solvent Phase.

All the gel samples were examined by SEM, and the conditions favorable for the formation of micron-range interconnected structure were extensively specified by changing the solution compositions. Hereafter, the concentration of HPAA, C, will be expressed as a molar ratio of monomeric unit of HPAA to Si in the reacting solution, and the sizes of interconnected pores are represented by the average thickness of silica skeleton L, measured directly from the SEM photographs. The values of L have been confirmed to show good agreements with those measured by mercury porosimetry.

Table 1.1 Typical starting compositions of HPAA-containing solutions.(unit:g)

Code	PA9	Water	Ethanol	Methanol	TEOS	TMOS	Nitric acid
E-1	0.35-0.45	3.0	1.59	--	6.51	--	0.31
E-2	0.30-0.50	5.0	--	--	6.51	--	0.51
E-3	0.30-0.60	5.0	2.38	--	6.51	--	0.51
M-1	0.35-0.45	5.0	--	1.87	--	4.77	0.51

The variations of L with the amount and composition of solvent phase for PA9 - TEOS systems under fixed C and catalyst concentration in water phase, are plotted in a composition triangle of water, ethanol and silica as Figure 1.2. The compositions are calculated by assuming that the hydrolysis and condensation of TEOS are completed by the time of gelation, which implies the consumption of 2 mol of water and the generation of 4 mol of ethanol per unit mole of TEOS in the system. Since considerable amount of -OH group is known to exist on the gel surfaces, the real solvent composition may somewhat shift to ethanol-rich field. General trends are that with an increase of solvent phase, irrespective of water or ethanol, L decreases, and that smaller pores are obtainable somewhat ethanol-rich region of the composition field.

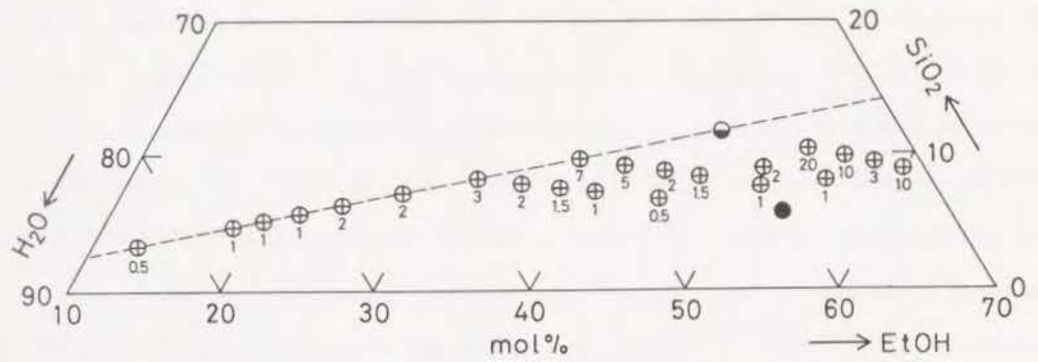

Figure 1.2 Variation of gel morphology with solvent phase composition prepared with fixed PA9 concentration C=0.177 at 60°C. Averaged pore sizes are indicated on respective symbols. Solvent phase compositions were calculated as described in the text.

● :microporous gels, ⊕ :interconnected structure,

◒ :macroscopic two-phase

1.3.4 Gelation Time

The gelation time, t_g was determined for several selected samples by simply tilting the containers as the moment when the bulk fluidity was lost. Figure 1.3 shows t_g for three ethanol-containing and one methanol-containing solvent compositions with varying C as shown in Table 1.1. At almost the same oxide concentrations, the E-2 composition showed longer t_g because of lower catalyst-water ratio and higher ethanol concentration than E-1. The t_g of TMOS-containing samples fell on the intermediate values between those of compositions E-1 and E-2. For E-3 composition t_g became longer than any other composition because of lower oxide concentration together with the higher ethanol fraction in solvent phase. In all cases t_g decreased with increasing HPAA content. This acceleration of gelation with the coexistence of polymer is similar to that of NaPSS-containing systems as evidenced by SAXS described in Chapter 6, which is tentatively interpreted as the result of enhanced aggregation of primary silica oligomers by the increased segregation tendency of the system.

1.3.5 Effect of HPAA Concentration

Figure 1.4 shows the variation in L with C for three different TEOS-containing compositions listed in Table 1.1. The symbols indicating the periodic size were plotted only for the C-values at which the interconnected porous morphology could be obtained. The gel morphologies respectively obtained in lower and higher C-ranges were continuous silica matrix with isolated micron-range pores and the aggregation of spherical silica particles in E-1 and E-2 compositions. The overall morphology change for E-2 composition in broad C-range is shown by SEM photographs as Figure 1.5. The spherical silica particles were observed only at higher C values and their size distribution was relatively broad. With an increase of relative ethanol amount at

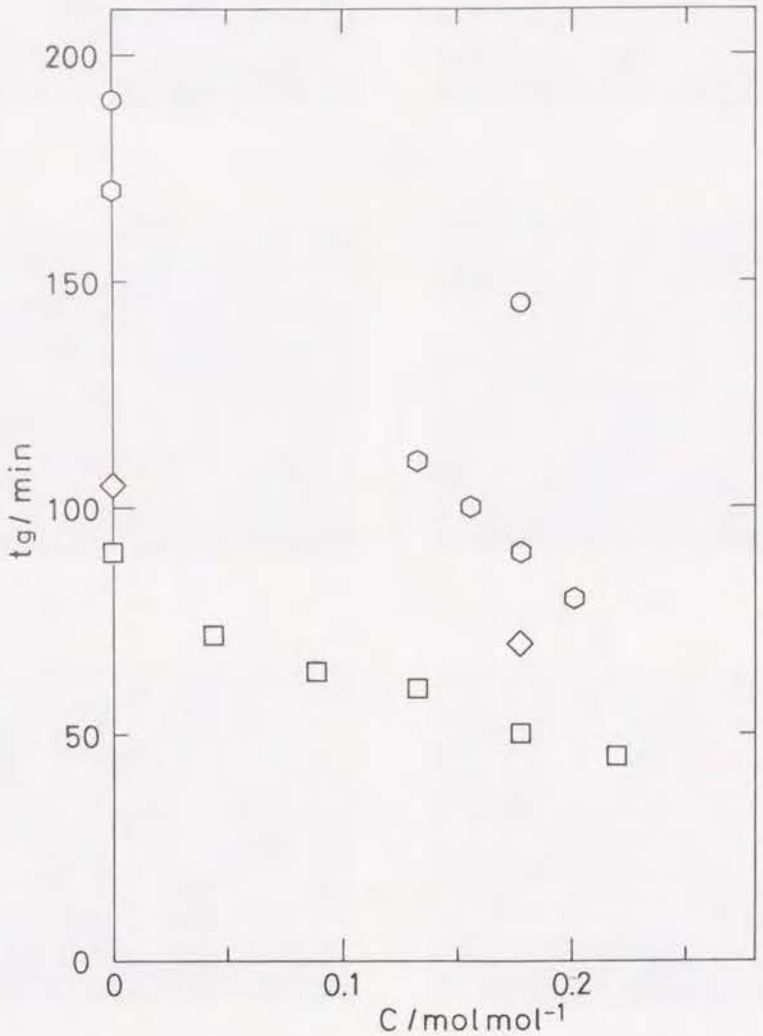

Figure 1.3 Dependence of gelation time t_g on PA9 concentration C for varied solvent compositions at 60°C. ○:E-1, □:E-2, ○:E-3, ◇:M-1.

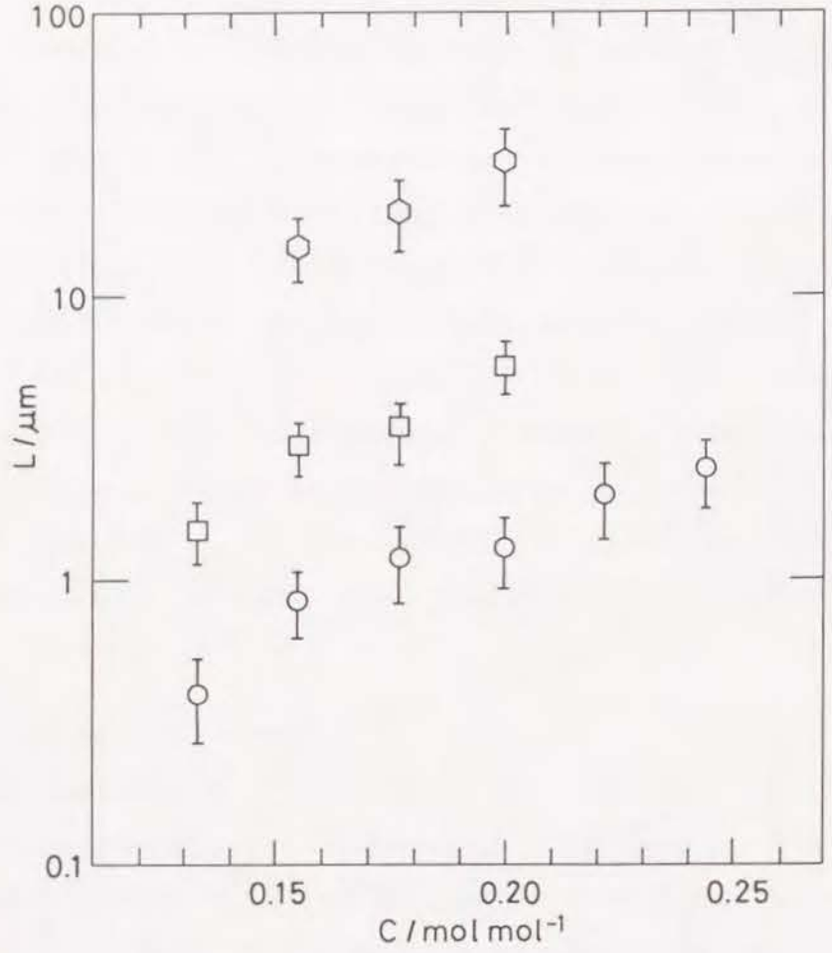

Figure 1.4 Dependence of average pore size L on PA9 concentration C for varied ethanol-containing solvent compositions at 60°C. ○:E-1, □:E-2, ○:E-3.

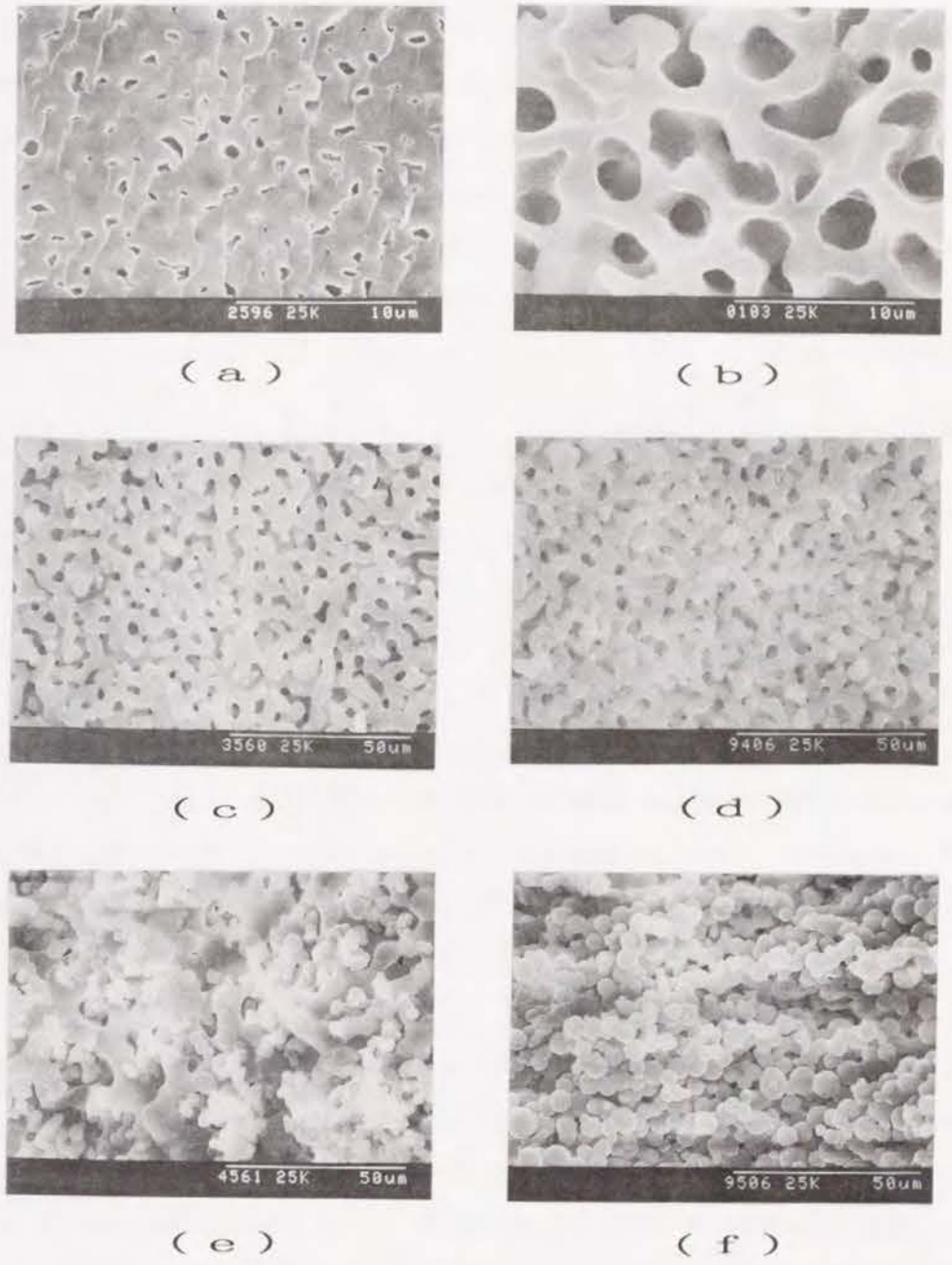

(a) (b) (c) (d) (e) (f)

Figure 1.5 SEM photographs of gel morphologies prepared from E-2 composition at 60°C.

(a):C=0.111, (b) 0.133, (c) 0.155, (d) 0.177, (e) 0.200, (f) 0.222.

fixed volume of the solvent phase, both t_g and L increase accompanied by the narrowing of the C-range of interconnected structure. On the other hand, the addition of ethanol brings also the increase in t_g but decrease in L in an extended C-range. In the lower C-range than plotted in Figure 1.3, microporous gels without SEM-detectable pores resulted. In all compositions, the increase in C slightly reduced t_g as described above, but always resulted in the increase in L.

1.3.6 Effect of Kind of Alkoxysilane

Figure 1.6 shows the variation in L with C for the compositions E-2 and M-1. To M-1 composition, methanol was added to the mixtures of HPAA, water, catalyst and TMOS in order to make their total volume and oxide content equivalent to that of E-2 for the same C-values. Larger L and narrower C-range of interconnected structure than that of E-2 resulted by simply substituting ethanol with methanol. For M-1 series, SEM photographs are shown as Figure 1.7. The inclusion of spherical particles from lower C-values than E-2 to increase and dominate the whole morphology can be recognized. The results of M-1 and E-1 are analogous including the morphological change and slight increase in t_g.

The solutions prepared from 1 : 4 molar ratio of TMOS : ethanol and TEOS : methanol gave the identical t_g and interconnected gel structures with identical pore size, which proved that the difference in the rates of hydrolysis and of trans-esterification among species including HPAA between TMOS- and TEOS-containing systems are negligible in the present gel-forming reactions, and that the substitution of TEOS with TMOS essentially means the change in solvent composition.

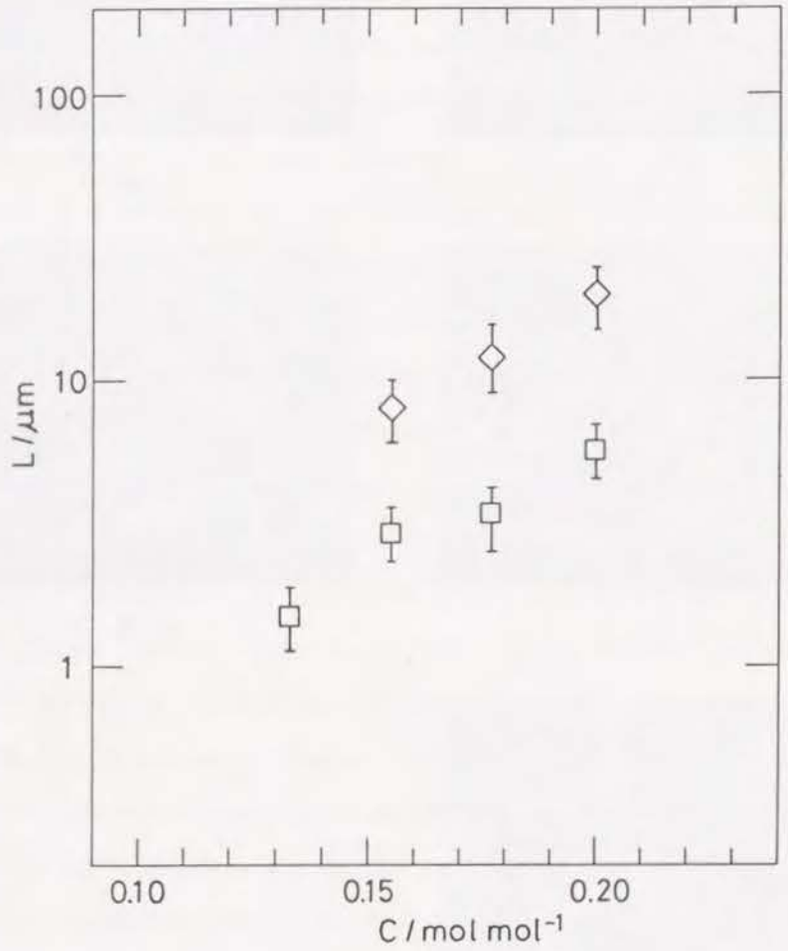

Figure 1.6 Dependence of average pore size L on PA9 concentration C for methanol- and ethanol-containing solvent compositions at 60°C. □:E-2, ◇:M-1.

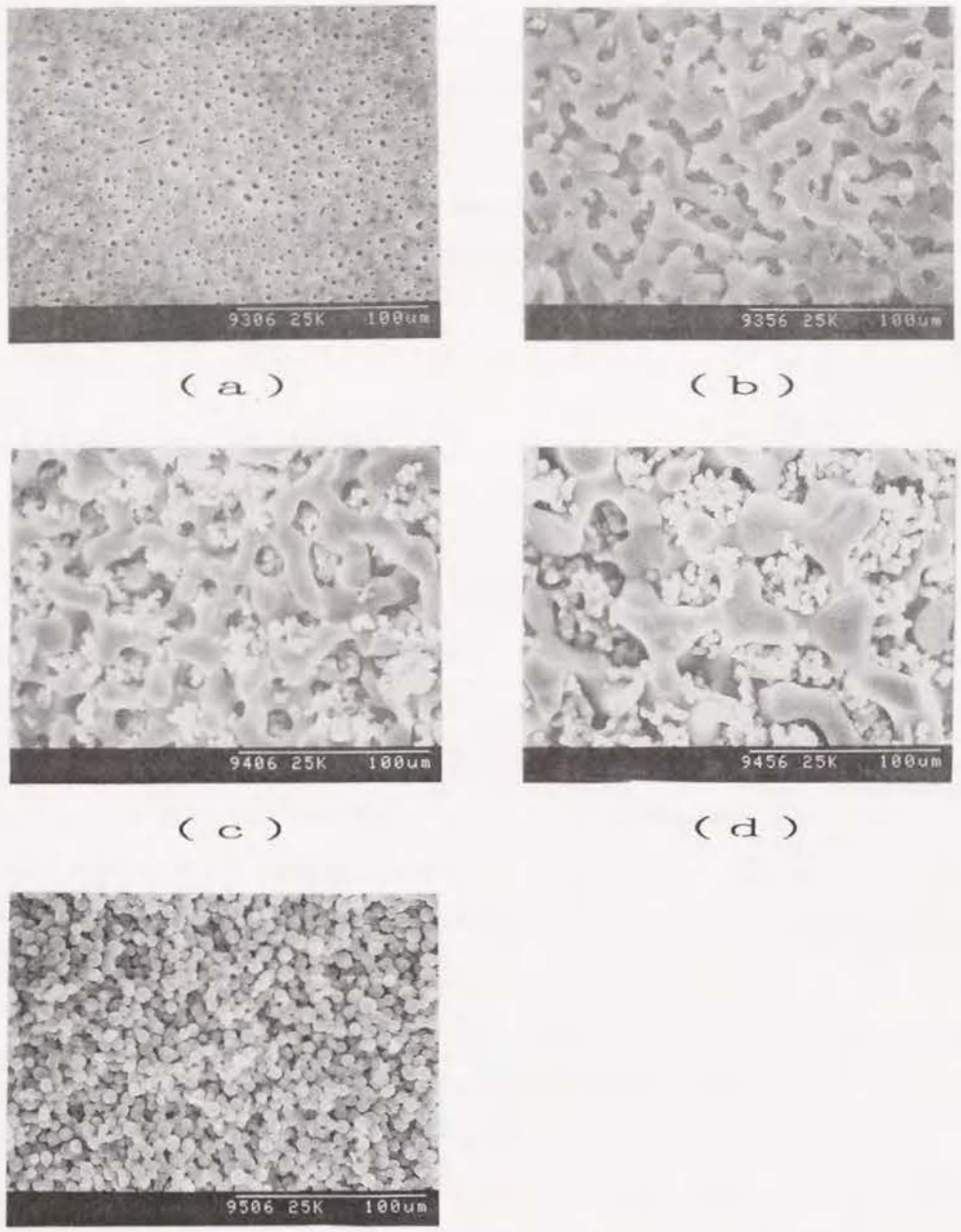

Figure 1.7 SEM photographs of gel morphologies prepared from M-1 composition at 60°C.

(a) C=0.133, (b) 0.155, (c) 0.177, (d) 0.200, (e) 0.222.

1.4 DISCUSSION

1.4.1 Spinodal Phase Separation in Polymerizing Systems

Spinodal phase separation can be initiated by several different ways of "quenching" the system which thrust the single-phase mixture into two-phase region of the phase-diagram rapidly enough to prevent the nucleation-growth type phase separation. "Physical quench" is the most convenient and popular method represented by the rapid cooling or heating of the system (temperature jump). One of the other possibilities to attain "quenching" is to polymerize certain component and extend the two-phase region to include the starting composition and temperature. In the absence of strong affinity between molecules or a large amount of co-solvent, different kind of polymers easily become immiscible (segregation occurs) with an increase of molecular weight of either component due to the decreased combinatorial entropy gain on mixing. Thus, the one-phase solution containing one originally polymeric and another polymerizable specie can favorably be used to realize the polymerization-induced spinodal phase separation if the polymerization proceeds rapidly enough. This method can be called "chemical quench" as the chemical reaction drives the free-energy change. In initiating the spinodal phase separation by the finite-rate changes in physical or chemical conditions, a parallel reduction in the mobility of the system is favored in order to avoid the inclusion of the nucleation-growth process because it is relatively slow process requiring the activation energy for diffusional motions[8,9]. However, the over-reduction of the system mobility inhibits also the spinodal phase separation and leads the incomplete domain formation.

According to the treatments of phase equilibria in gel-forming systems based on statistical thermodynamics[8], the increase in the number of chemical bond is equivalent to that in attractive interaction among constituents, thus the "equivalent temperature T_{eq}", defined as $T_{eq}=J/\beta$ where -J and β

respectively denote the interaction energy per one pair of monomers and the correlation strength between monomers, decreases as the polymerization reaction proceeds (β increases). During the polymerization reaction the viscosity increases gradually and diverges at the sol-gel transition. Taking into consideration that the system turns from viscous to elastic without a evolution of latent heat and that the physical state of gels depends on the preparation history, amorphous sol-gel transition would be compared to the liquid-glass transition rather than liquid-crystal transition. Hence, the gel-forming reaction is physically equivalent to the finite-rate cooling of glass-forming systems. It has been further discussed by deGennes[8] that if the system has the sol-gel transition (equivalent) temperature a little above the binodal temperature, the spinodal phase separation is likely to occur on cooling (polymerizing) the system due to the reduced mobility. The situation is represented by Figure 1.8(b). Consequently, the present polymer-incorporated silica sol-gel reaction can be regarded as nearly equivalent to the finite-rate cooling of the mixtures having UCST (Upper Critical Solution Temperature) and glass transition region in the cooling temperature range, e.g., immiscible oxide glass melts. The correspondences between several factors of finite-rate cooling of glass melts and sol-gel transition are shown in Table 1.2.

Table 1.2 Correspondence between important parameters affecting the phase separation process in finite rate cooling and sol-gel transition

System	Origin of Free-energy Change	Origin of Mobility Change
Finite-Rate Cooling of UCST System	Temperature	Viscosity Change with Temperature
Sol-Gel Transition	Mixing Entropy	Crosslink Density

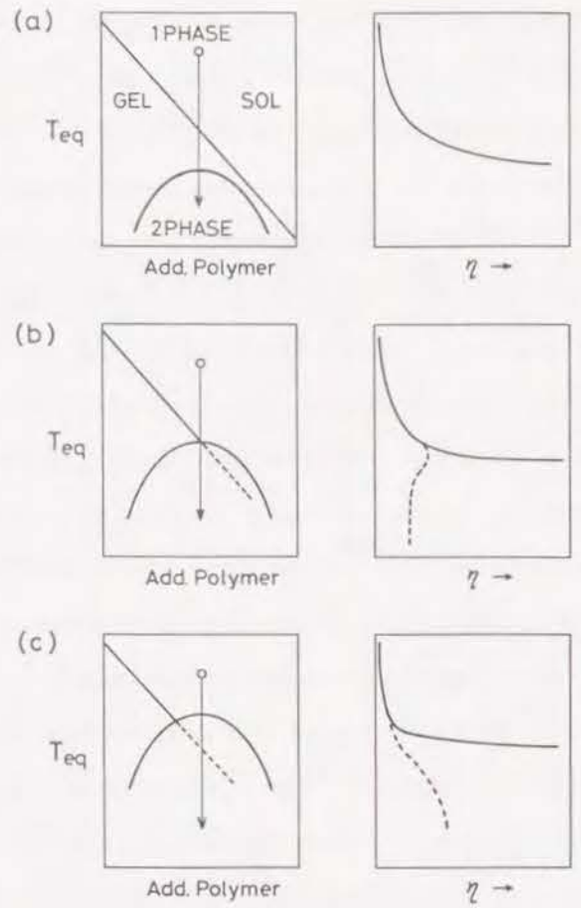

Figure 1.8 Schematic phase diagrams of quasi-binary, (silica-solvent) and (polymer-solvent) systems which exhibit sol-gel transition (boundaries are shown as right-downward line) and UCST type phase separation. (Modified from the Figure V.14 in ref.[8]) The ordinate is expressed by the equivalent temperature T_{eq} (see text); (a) weak segregation, (b) moderate segregation, (c) strong segregation. Arrows indicate the cooling (polymerization) processes from one-phase sol down to two-phase gel state. Accompanying increases in viscosity η are shown in right-side figures, where solid and broken lines respectively denote η in silica- and polymer-rich phases. In the case (b), a cooling of the starting composition (o) allows gel-formation and phase separation to occur in parallel.

1.4.2 Fixation of Phase Separated Structure by Gelation

Once initiated at the fixed quench depth, the spinodal phase separation is known to follow the three successive steps. (Figure 1.9) The initial stage has successfully been described by the linearized theory which predict the exponential amplitude growth of fixed dominant fluctuation wavelength[10]. The dominant wavelength and time constant of amplitude growth have inverse correlations with the quench depth. Since the spatial fluctuation distribution is expressed by the random superpositions of sinusoidal waves with the dominant wavelength, so-called interconnected domain structure results when the volume fractions of phase-separating domains are comparable. In the intermediate stage, both the dominant wavelength and amplitude of composition difference grow with time to attain equilibrium composition in each domain. The interfaces between conjugate phases become smooth at the end of this stage. The late stage accompanies only the morphological changes due to the coarsening of equilibrated domains. The increase in the periodic wavelength of the interconnected structure, often followed by the breaking-up and dispersion of minor phase, is observed[11]. The rates of growth in periodic wavelength in these stages are known to increase with quench depth[12].

The most particular point of the present system is that, once the domains started to develop, the polymerization reaction in silica-rich domains would further be accelerated by the concentrating effect, which results in the decreased mobility and the formation of sharper interfaces between phases. Hence, the interconnected porous morphologies with relatively smooth pore surface are expected to form even from the domains with diffuse interfaces developing in the early or intermediate stages of spinodal phase separation, i.e., the compositional differences tend to be enhanced in the gel-forming system. And in turn, the coarsening process of the interconnected domains in the late stage will severely be restricted since it requires bulk diffusion of

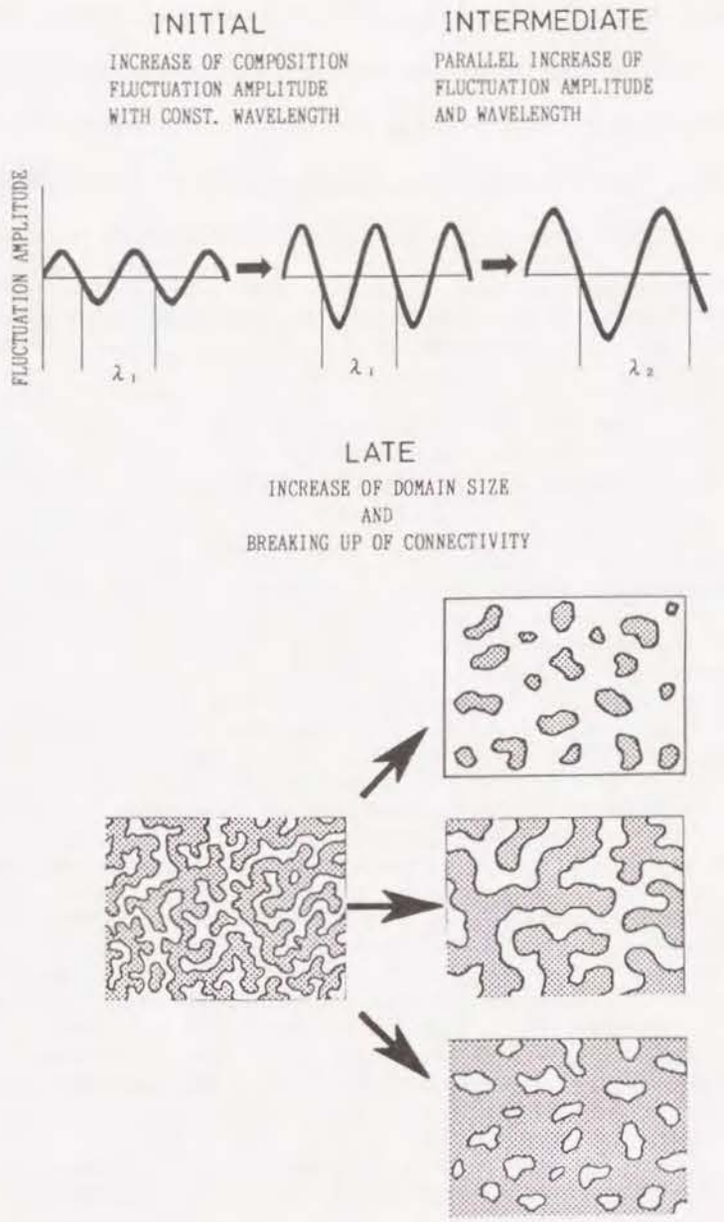

Figure 1.9 Time evolution of spinodally phase-separating system in successive three stages of domain growth[10]. For detail, see text.

the constituents, while the breaking-up of the domains is more or less likely to occur in earlier stages of gel-formation. As shown in Figure 1.1(a), the preliminary LS data for the smooth pore sample which exhibited only a slight peak shift accompanied by the marked increase in intensity support the above speculation.

1.4.3 Correspondence of Processing Parameters between Finite-Rate Cooling and Gel-Formation.

Under the normalized polymerization rate, i.e., the constant increase rate of bridging Si-O-Si bonds, the experimental systems are categorized into two general cases; (a) weak segregation ($T_{eq,g} > T_{eq,b}$; where $T_{eq,g}$ and $T_{eq,b}$ respectively denote the temperatures of sol-gel transition and phase separation) and (c) strong segregation ($T_{eq,g} < T_{eq,b}$). These conditions are graphically represented by T_{eq} vs. added polymer concentration, and by T_{eq} vs. η diagrams as Figure 1.8(a) and (c). The polymerization rate affects the time scale of free-energy change, thus can be regarded as the cooling rate. $T_{eq,g}$ can be compared to the glass transition temperature both of them represent the temperature ranges with transitional properties depending on the relation between β and T_{eq}. For example, the gel-formation with fewer bridging bonds (at high T_{eq}) results in less steep viscosity change against T_{eq} and exhibits broader transition range. The segregation strength determines the T_{eq} at which the system becomes "not-stable" in the overall polymerization process, hence it corresponds to the binodal temperature.

According to the discussion of Cahn and Charles based on the linearized theory of spinodal phase separation[9], the fluctuation wavelength with maximum growth rate Λ_m grows exponentially with time whose rate constant proportional to the square of quench depth. On the other hand, the system mobility decreases with decreasing temperature and so with quench depth in

UCST system. The fluctuation wavelength having actually maximum growth rate Λ_a is then determined by these two opposing factors independent of the cooling rate. The cooling rate influences the domain size only when it is so slow that enough time is given for the fluctuations with slower growth rate to grow in substantial degree, and the slower cooling the larger domains result. With increasing cooling rate, the attainable amplitude of fluctuation at fixed Λ_a decreases and finally becomes indistinguishable from the molecular level fluctuations with infinitely rapid cooling. In the present case, although the mobility decrease can take place far more drastically at sol-gel transition, the above discussion on glass-forming systems would be valid.

In condition (a), phase separation takes place in already crosslinked network, and the lowered mobility effectively suppresses the growth of composition fluctuation with longer wavelength than the narrowing mesh size of the network. Accordingly the final wavelength fixed in the gel structure would only weakly depend on the polymerization rate. It will be harder for spinodal phase separation to step into the intermediate and late stages since they require the substantial network mobility. In condition (c), phase separation proceeds well above the sol-gel transition temperature, the fluctuation wavelength whose time scale of amplitude growth exceeds that of polymerization rate becomes dominant. The intermediate and late stages will follow until the gel-formation depending on the cooling rate. Hence, the polymerization rate significantly affects the final morphology of these kinds of gels.

1.4.4 Effect of Solvent Phase Composition

Since the present experimental systems are limited in water-rich and strong acid-catalyzed ones, the fully-hydrolyzed silica oligomers gradually form polymerized clusters with high number-average molecular weight[12], and the sol-gel transition takes place steeply against the t_g-normalized reaction

time. Hence, the effect of polymerization rate on gel-morphology show a large variation depending on the relation between $T_{eq,g}$ and $T_{eq,b}$.

As will be described in detail in Chapter 3, at fixed C-value of 0.177 with E-2 composition, the periodic size L exhibited almost the constant value against the several times' variation in t_g by catalyst concentration. Thus the increased L in E-1 and M-1 compositions are at least partly due to the increased $T_{eq,b}$ caused by the variation in solvent composition. In the case that $T_{eq,b}$ is considerably lower than $T_{eq,g}$, phase separation proceeds under the limited mobility which results in the weaker dependence of L on the polymerization rate. Provided that $T_{eq,b}$ increased reflecting the lowered solvent quality to exceed $T_{eq,g}$, the system experiences longer duration in the metastable state and attains only a shallow quench depth with the slow polymerization rate. In that case, the time-consuming nucleation-growth process can take place to result discrete silica particles with relatively broad size distribution, and the spinodally developing domains will be large and slowly growing ones. The above process results in the coarser continuous gel structure incorporated with discrete spherical particles. This mechanism is supported by the SAXS results which detected the formation of extremely large-sized particles in the high-$T_{eq,b}$ solution long before the gel-formation.

In contrast, with an increased amount of solvent, finer interconnected pores could be obtained in an extended C-range in spite of the increased t_g. An increased solvent fraction contributes both to slow down the polymerization by diluting the system and to decrease the segregation tendency, i.e., to decrease $T_{eq,b}$ relative to $T_{eq.g}$. Although these changes have opposing effects on the pore size, the latter effect overcomes the former to result finer morphology by drastically lowering the system mobility in which the domain formation occurs. It can be concluded that the mobility of the gelling network in which the coarsening proceeds largely determines the size of final gel

morphology at least in the present water-rich highly acidic system. The observation supports the above discussion that submicron morphology always resulted from the gel initially transparent and gradually turned opaque.

1.4.5 Effect of HPAA Concentration

With an increase of C at the fixed amount of solvent, the polymerization-induced phase separation is expected to take place at earlier stages of growth process of silica as long as the solvent-HPAA interaction remains essentially constant. As described above, earlier phase separation leads the system to shallower quench depth and longer coarsening to form coarser morphology. The volume fraction of pores is closely related to that of HPAA-rich phase. Moreover, earlier occurrence of phase separation results in the lower volume fraction of polymerizing silica clusters. Consequently, the volume fraction of pores and their average size increase with C.

The dependence of the width of C-range of interconnected structure on the solvent composition can be explained by the mechanism described in the preceding section. Since the fragmentation of domains proceeds in the coarsening stage of spinodal phase separation, a system having lower mobility during coarsening can fix the interconnected structure in more extended C-range.

1.5 CONCLUSIONS

(1) By hydrolyzing alkoxysilane with an acid catalyst under the coexistence of HPAA, gels with micron-range interconnected pores were obtained.

(2) Morphology of the macroporous gels could be controlled in wide range of volume fraction, connectivity and size of pores by changing the solvent composition and HPAA concentration at the fixed temperature.

(3) The preliminary light scattering experiment suggested that the gel morphology is formed by spinodal phase separation in the gelling silica solution which was subsequently fixed by consolidation of gel network.

(4) The dependence of gel morphology on the compositional reaction parameters could be explained in analogy to the finite-rate cooling of immiscible glass melts by taking the segregation tendency and polymerization rate in the former system respectively as the binodal temperature and cooling rate in the latter.

SUMMARY OF CHAPTER 1

The phase separation of gelling solutions have been investigated for the acid catalyzed alkoxy-derived silica systems containing polyacrylic acid. The occurrence of spinodal phase separation and the formation of micron-range interconnected porous morphology were observed. Steep decrease in the mobility of gelling silica network was considered to be responsible for the remarkable increase in light-scattering intensity after the settlement of peak position. Experimental results on the effects of HPAA concentration and solvent composition suggested that the relative rates of phase separation and gel-formation are the most important parameters to determine the quench depth and resulting periodic size of the interconnected gel morphology.

REFERENCES

[1] H.P.Hood and M.E.Nordberg, U.S.Pat. 2215039 (Sept. 17, 1940).

[2] D.W.Schaefer and K.D.Keefer, in; *Better Ceramic Through Chemistry*, eds. C.J.Brinker, D.E.Clark and D.R.Ulrich,(Elsevir-North-Holland, N.Y., 1984), 1-13.

[3] D.W.Schaefer, J.E.Mark, D.McCarthy, L.Jian, C.-C.Sun and B.Farago, *Mat. Res. Soc. Symp. Proc.*, vol.171(1990), 57-63.

[4] Y.J.Chung, S.-J.Ting and J.D.Mackenzie, in *Better Ceramics Through Chemistry IV*, eds. B.J.J.Zelinski, C.J.Brinker, D.E.Clark and D.R.Ulrich, (Mat. Res. Soc., Pittsburgh, PA, 1990), 981-986.

[5] H.Kozuka and S.Sakka, *Chem. Lett.* (1987), 1791-94.

[6] R.D.Shoup, *J. Colloid Interf. Sci.*, **3**(1976), 63-69.

[7] T.Hashimoto, J.Kumaki and H.Kawai: *Macromolecules*, **16**(1983), 641-648.

[8] P.G. deGennes:*"Scaling Concept in Polymer Physics"* (Cornell University, Ithaca, New York, 1979).

[9] J.W.Cahn and R.J.Charles: *Phys. Chem. Glasses*, **6**(1965), 181-191.

[10] J.W.Cahn:*Acta Metal.*, **9**(1961), 795-800.

[11] T.Hashimoto, M.Itakura and H.Hasegawa: *J. Chem. Phys.*, **85**(1986), 6118-6128.

[12] T.Hashimoto, M.Itakura and N.Shimidzu: *J. Chem. Phys.*, **85**(1986), 6773-6786.

[13] T.W.Zerda, I.Artaki and J.Jonas: *J. Non-Cryst. Solids*, **81**(1986), 365-379.

CHAPTER 2

SYSTEMS CONTAINING POLYACRYLIC ACID ; EFFECTS OF MOLECULAR WEIGHT AND REACTION TEMPERATURE

2.1 INTRODUCTION

In the previous Chapter, demonstrated were the phase separation and gelation in the systems containing polyacrylic acid (HPAA) and alkoxysilane. Macroporous silica body with well-defined morphology could be prepared. The interconnected morphology was formed in an increasingly broad range of HPAA concentration with an increase of solvent phase, which could be explained in terms of the decreased segregation strength allowing the spinodal phase separation at the increased quench depth with extended composition range to occur.

In good contrast to an addition of alcohol which decelerate the polymerization, an increase in reaction temperature usually accelerates both hydrolysis and polycondensation of alkoxysilane[1], while that in molecular weight contributes to mainly reduce the solubility of HPAA in the reacting solution. It is therefore expected that the effect of polymerization rate on the formation and fixation process of interconnected structure will be made clear by comparing the effects of solvent composition and of temperature or molecular weight. Rigorous examination on this point was carried out by preparing the gel samples in an extended temperature range from 40 to 80°C using HPAA with four different molecular weights.

2.2 EXPERIMENTAL

Tetraethoxysilane (TEOS), product of Shin-Etsu Chemical Co., was used as silica source. Polyacrylic acid (HPAA), products of Aldrich Chemical Co. having the molecular weights of 90,000 (denoted hereafter as PA9) and 250,000

(PA25), and those synthesized by Toa Gosei Chemical Industry Co. Ltd. with average molecular weights of 10,000(PA1) and 30,000(PA3), were used as polymer component. Nitric acid was used as a catalyst for hydrolysis.

The sample gels were prepared by hydrolyzing TEOS with acidic aqueous solutions containing various amount of HPAA as described in the previous chapter. Gelation and aging were conducted under tightly sealed condition in air circulating baths at temperatures ranging from 40 to 80°C. The gelation time t_g was measured by simply tilting the container to determine the time at which the bulk fluidity of the solution was lost. The t_g was not measured when solutions exhibited macroscopic two-phase appearance accompanied by the sedimentation. After leaching out the polymer phase with water and ethanol, samples were finally dried at 60°C and subjected to SEM observation.

Hereafter, the concentration of HPAA will be expressed by C defined as the molar ratio of monomeric HPAA to Si in the reacting solution, which is proportional to their weight ratio.

Table 2.1 Typical starting compositions of HPAA-containing solutions.(unit:g)

Code	Water	Ethanol	TEOS	Nitric acid
E-1	3.0	1.59	6.51	0.31
E-2	5.0	--	6.51	0.51
E-3	5.0	2.38	6.51	0.51

2.3 RESULTS

2.3.1 Solvent Composition Dependence of Pore Size at Varied Temperature.

Figure 2.1 shows the dependence of L at three reaction temperature T=40, 60 and 80°C on the composition of solvent phase while the molar ratio of HPAA to

TEOS and catalyst concentration being fixed. For clarity, each measured value of pore size is not plotted on the figure, the deduced curves expressing equal pore-sizes are drawn instead. With an increase of T, the pore size decreases at any composition, i.e., the iso-pore size line shifts towards silica-rich field. The overall shape of the iso-pore size lines, however, shows no remarkable change with T especially in the lower silica content field, indicating that the compositional dependence of partially esterified HPAA is affected little by T.

Figure 2.2(a) shows the dependence of L on T for three selected compositions listed in Table 1. The T-dependence becomes strong with an increase of L, which in turn means the weakened composition dependence of L at increased temperature corresponding to the broadening of the composition region of smaller L in Figure 2.1. SEM photographs for E-2 composition are shown in Figure 2.2(b).

2.3.2 HPAA Concentration Dependence of Pore Size at Varied Temperature

With an increase of the reaction temperature, the gelation time t_g at fixed concentration drastically decreased. Typical sample having the composition shown in Table 2.1 as E-2 with C=0.177 showed t_g's of 35, 50 and 220 min at 80, 60, 40°C, respectively.

Figure 2.3 shows the dependence of L on C at three different reaction temperatures. The enlargement of C-range of interconnected structure can be seen with drastically decreased values of L with an increase of temperature. At lower temperatures the HPAA-poor and HPAA-rich compositions respectively resulted in the morphologies with isolated pores and those with particle aggregates. Both of the discontinuous morphologies resembled to those obtained with E-1 solvent composition shown in chapter 2.1. SEM photographs of the gels prepared at 80°C are shown as Figure 2.4.

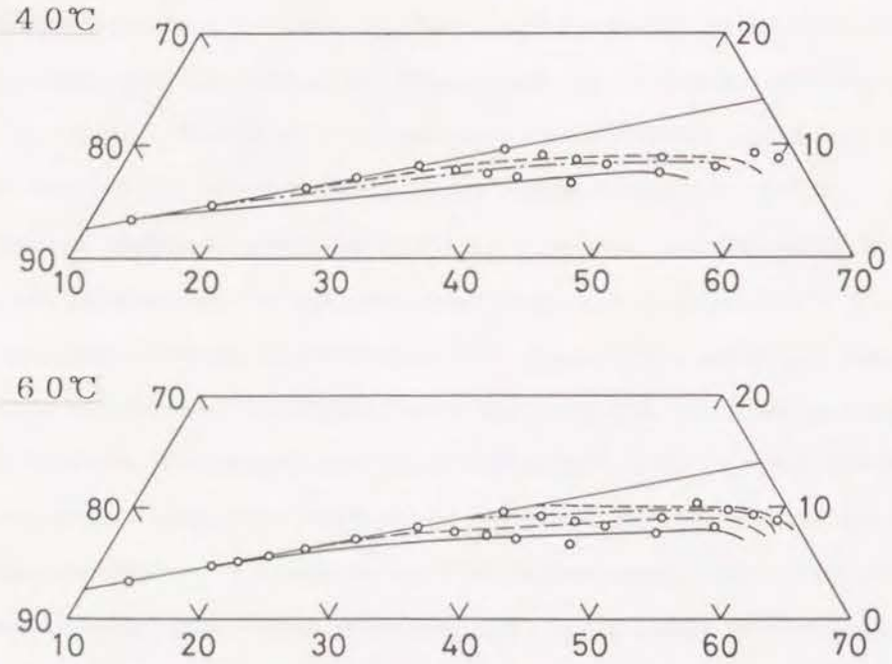

Figure 2.1 Dependence of average pore size L on solvent phase composition at fixed PA9 concentration of C=0.177 at different temperatures. Solvent compositions were calculated with 2 mol decrease of water and 4 mol increase of ethanol per 1 mol TEOS from the starting composition. The curves denote the equal pore size compositions. ———:1μm, — — —:2μm, —·—·—:5μm, ------- :10μm.

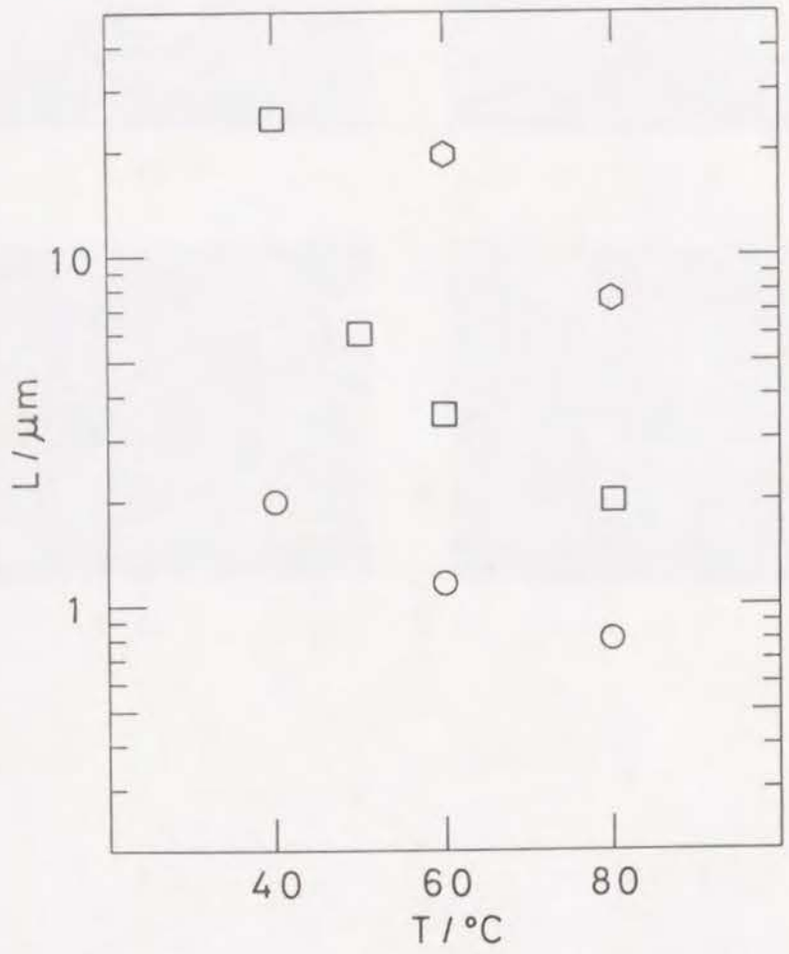

Figure 2.2(a) Dependence of average pore size L on reaction temperature T for selected solvent compositions. C=0.177. ⬡:E-1, □:E-2, ○:E-3.

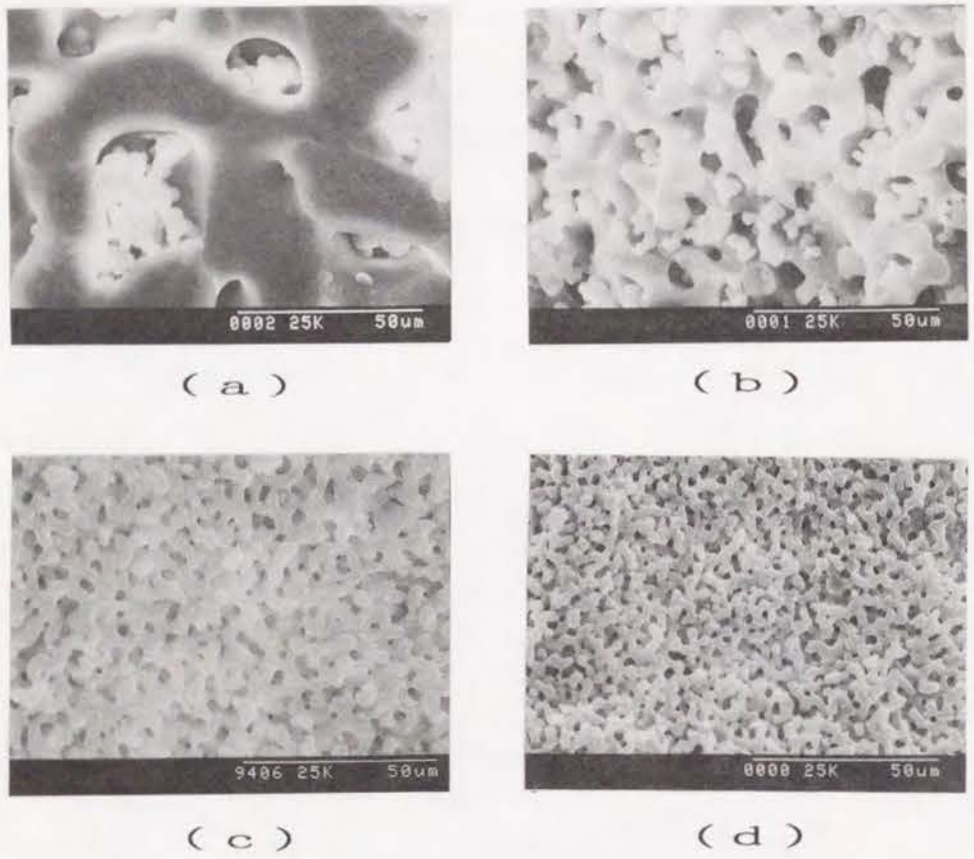

(a) (b)

(c) (d)

Figure 2.2(b) SEM photographs of gel morphologies prepared from composition E-2. C=0.177. (a) 40°C, (b) 50°C, (c) 60°C, (d) 80°C

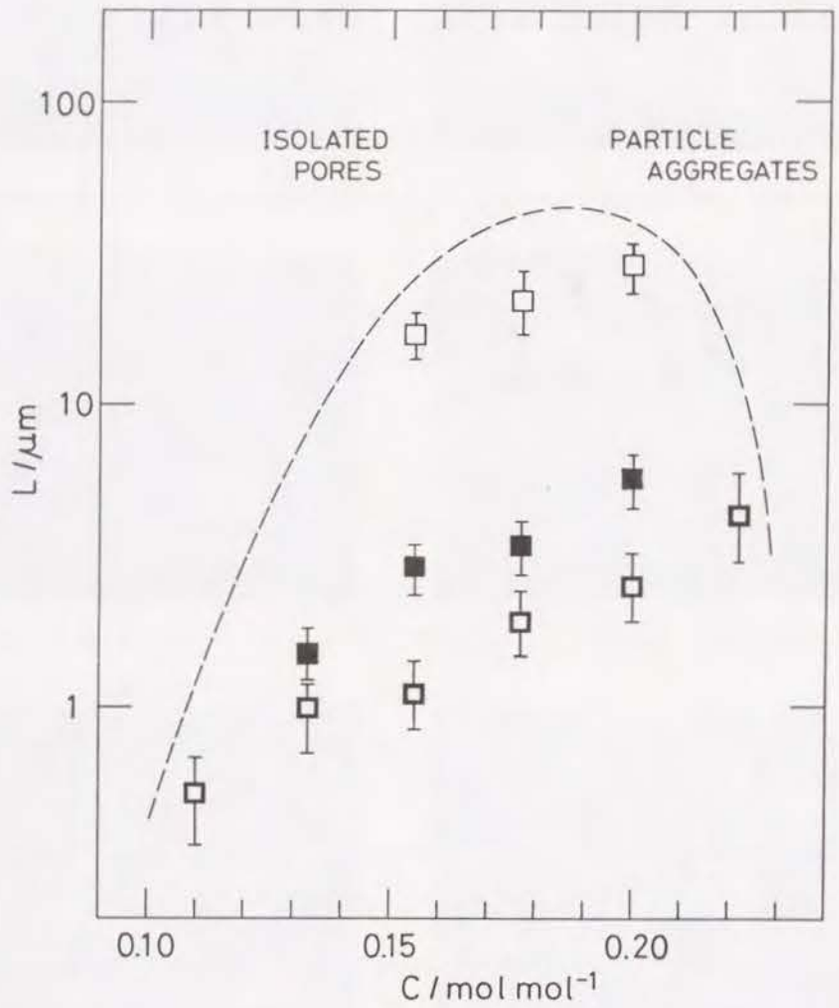

Figure 2.3 Dependence of average pore size L on C at different reaction temperatures. The starting composition is E-2.

□ :40°C, ■ :60°C, ◘ :80°C.

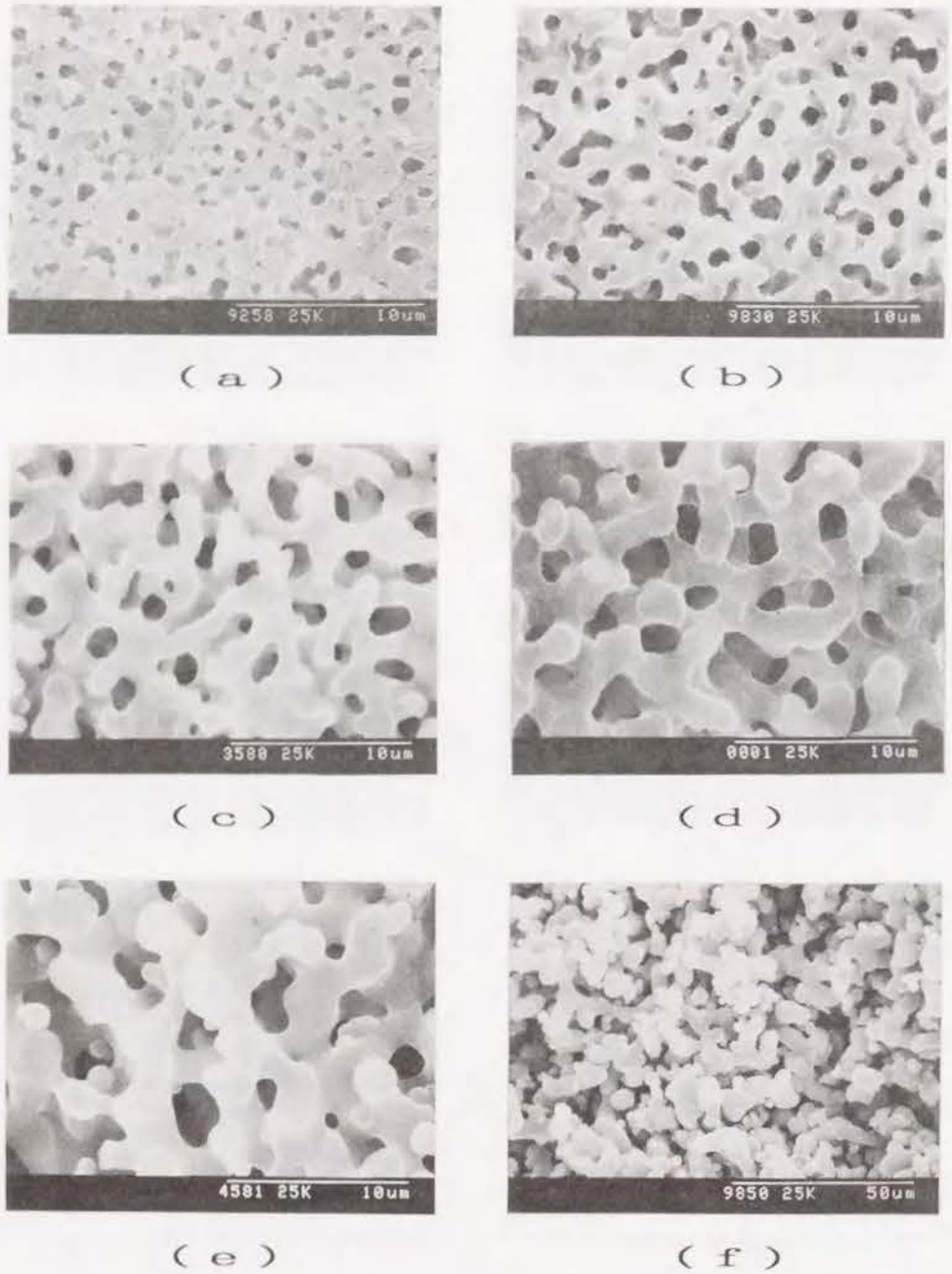

(a) (b)

(c) (d)

(e) (f)

Figure 2.4 SEM photographs of gel morphologies prepared with varied PA9 concentration with composition E-2 at 80°C.
(a):C=0.111, (b) 0.133, (c) 0.155, (d) 0.177, (e) 0.200, (f) 0.222.

1.3.3 Effect of Molecular Weight of HPAA.

Figure 2.5 shows the *C*-dependence of t_g having E-2 composition at 60°C. With an increase of molecular weight of HPAA *P*, the degree of acceleration of gel formation per unit added weight of HPAA increases. It seems, however, that t_g shows almost the same values around 50 to 60 min in the *C*-range where the interconnected structure is formed. The phase separation and gel formation sequence was also found to vary depending not only on *C* but also on *P*. As described in Chapter 1, the gelation occurs prior to phase separation in relatively low *C*-range and the relative emergence of phase separation becomes earlier with an increase of *C*. When compared at the central part of the *C*-range of interconnected structure shown in Figure 2.6, for PA1 and PA3 system the gradual increase of translucency was observed *after* the soft gel formation, while in PA9 the gelation and clouding occurred in almost in parallel. In PA25 system, although the exact comparison is rather difficult due to the exceptionally high viscosity of the starting solution, gelation seemed to take place after the clouding.

Figure 2.6 shows the log-log plots of *P* and morphology of the resultant gels from the solutions containing TEOS and HPAA (PA1, PA3, PA9 and PA25) under E-2 composition at 60°C. The molar ratio of water to TEOS was fixed at 8.54, and that of a catalyst to water at 0.0173. The interconnected micron-range morphology can be obtained over 25-fold of molecular weight range. Through the *C*-ranges of interconnected structure, a straight line with a slope of -0.5 can be drawn although some discrepancy can be recognized for PA1-system. The figure also shows that the morphology with isolated micron-range pores is formed with relatively high molecular weight HPAA, while only the nanometer-range pores can be seen in low molecular weight systems.

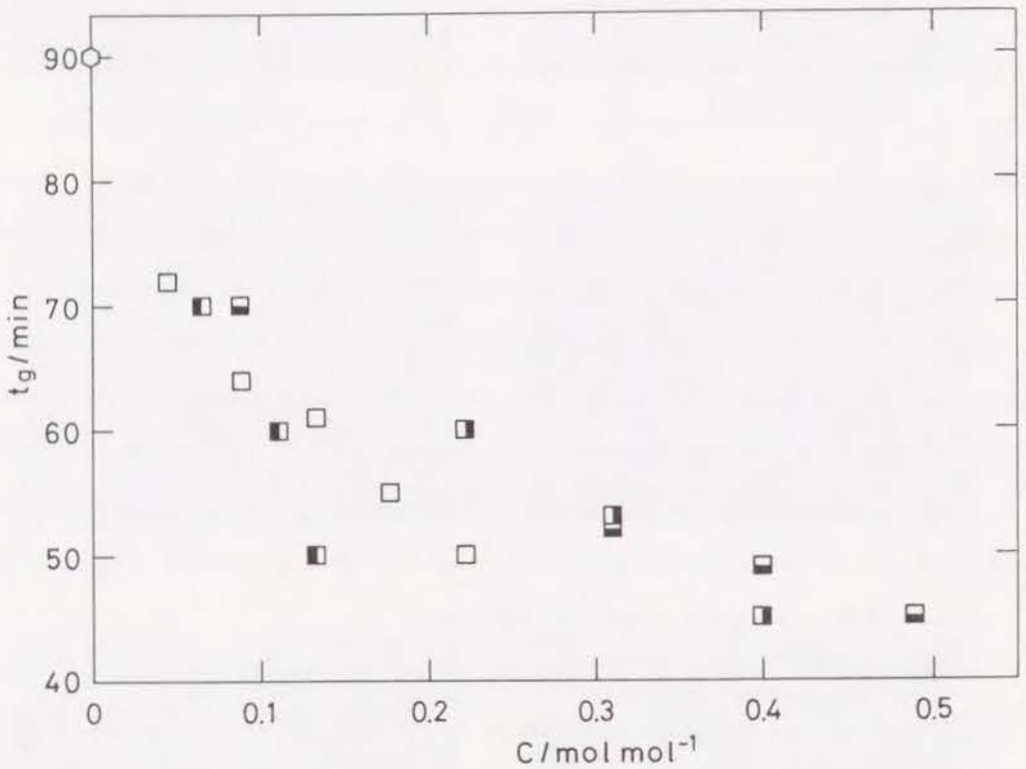

Figure 2.5 Dependence of gelation time t_g on HPAA concentration C with starting solvent composition E-2 at 60°C.

◒ :PA1, ◨ :PA3, □ :PA9, ◧ :PA25.

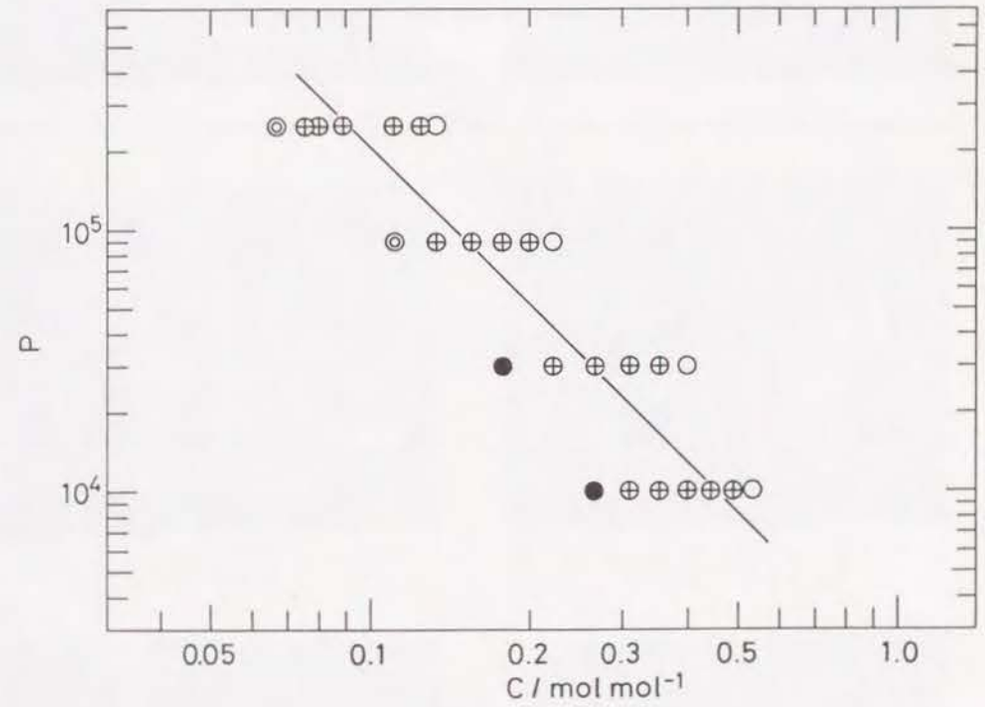

Figure 2.6 Log-log plots of molecular weight of HPAA P against concentration C with indications of resultant morphology. Starting solvent composition is E-2 prepared at 60°C.

◎ :isolated pores, ⊕ :interconnected structure,

○ :particle aggregates, ● :microporous gels.

Figure 2.7 shows the variation of L with C for four different molecular weights of HPAA at E-2 composition at 60°C. For PA1 and PA3, L gradually increases with an increasing C, while the dependence becomes somewhat stronger for PA9. For PA25 a reversed and weaker dependence can be seen in fairly large size range near 100μm. The size range of L and the concentration range of interconnected structure are respectively increasing and decreasing function of molecular weight. SEM photographs of the gels prepared with PA1 are shown as Figure 2.8.

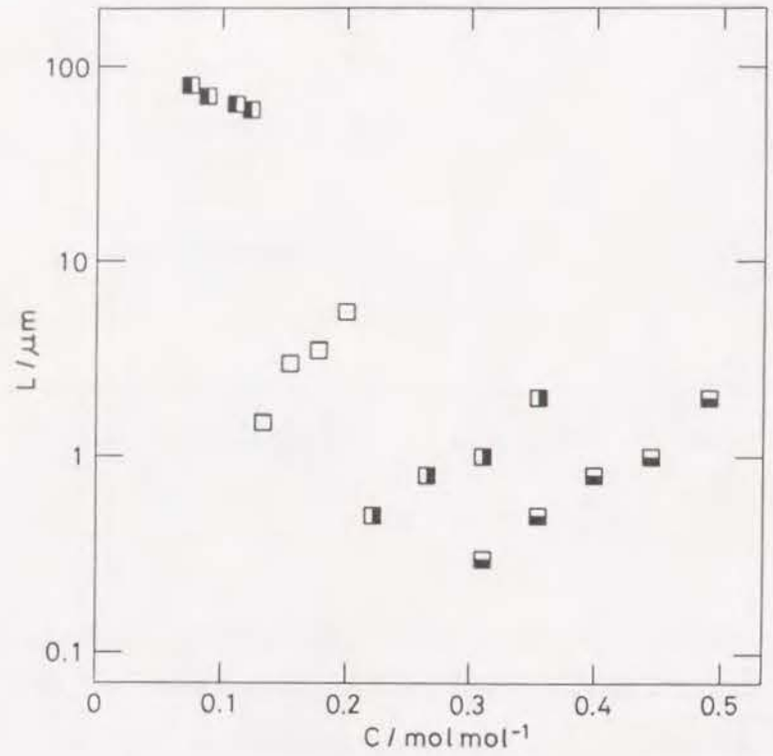

Figure 2.7 Dependence of average pore size L on HPAA concentration C for four kinds of molecular weight. Starting composition is E-2 prepared at 60°C. ◒:PA1, ◨:PA3, □:PA9, ◧:PA25.

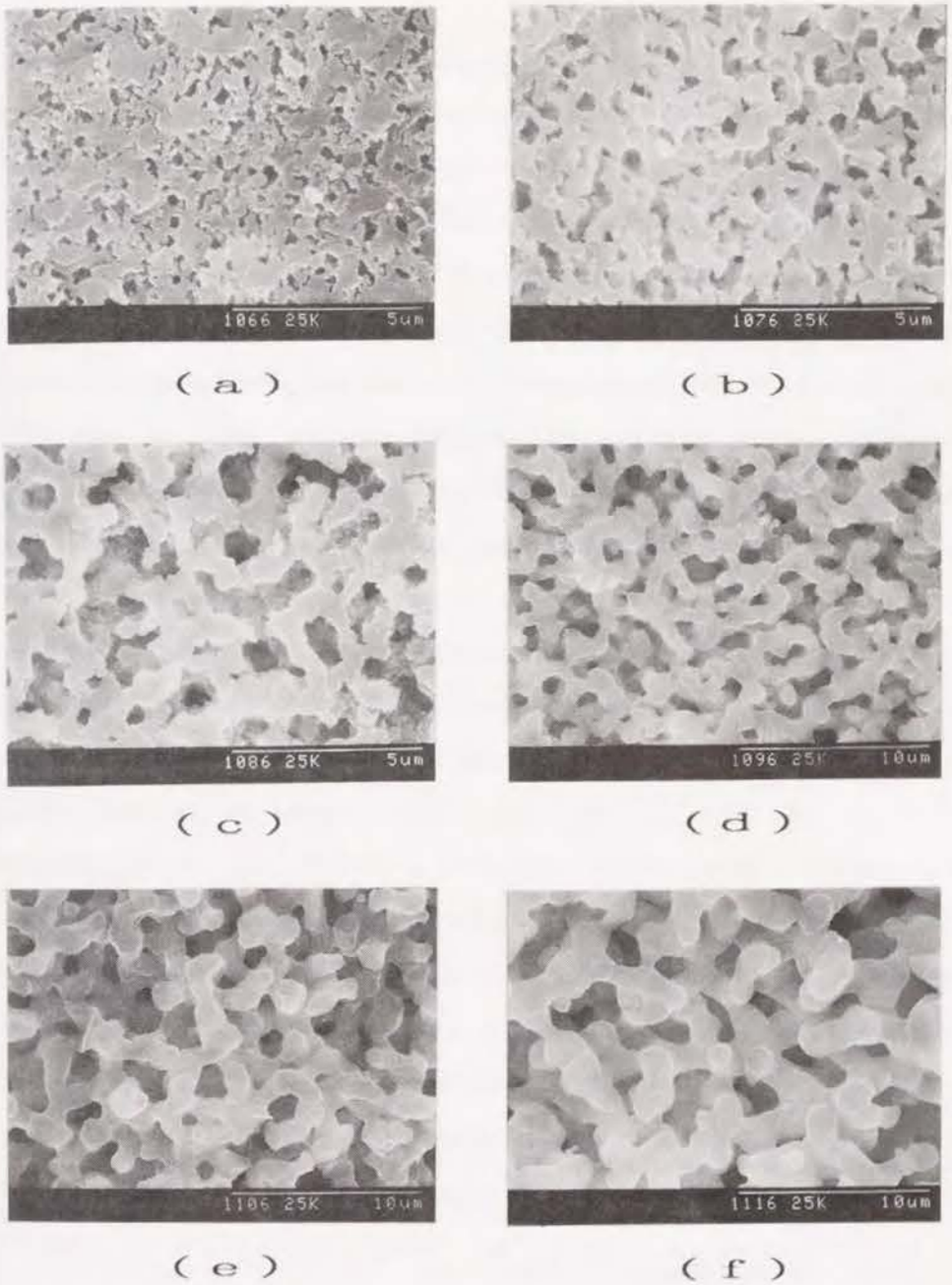

Figure 2.8 SEM photographs of gel morphologies prepared from PA1-TEOS system with E-2 composition at 60°C.
(a):C=0.266, (b):0.311, (c):0.355, (d):0.399, (e):0.444, (f):0.488.

2.4 DISCUSSION

2.4.1 Relative Rates of Polymerization and Phase Separation.

It has been reported that an increased temperature accelerates both hydrolysis and polycondensation of alkoxysilane resulting in almost exponential dependence of t_g on $1/T$[1]. At the same time, the mutual solubility of solutes increases at higher temperature. HPAA did not exhibit lower critical-type solution behavior below 100°C in the concentration range studied, while the concentrated aqueous solutions became cloudy at room- or lower temperatures. These effects of increased temperature to accelerate polymerization and decrease the segregation strength certainly allow the system to be thrust deeply into the spinodal region.

The increase in the molecular weight of HPAA, on the other hand, is expected to mainly decrease the solubility of HPAA rather than affect the polymerization process. In fact, the polymerization process was also affected by the presence of HPAA or other polymers to accelerate the aggregation of hydrolyzed silica, which will be described in Chapter 7. Quite fortunately in the present system, t_g was found to be almost constant in the concentration range where the interconnected structures are formed. It is therefore justified that by changing P one examines almost solely the effect of solubility, i.e., segregation strength on the resultant gel morphology.

2.4.2 Fixation of Developed Periodical Structure.

As already discussed in Chapter 1, the phase separation and gel-formation induced by the chemical polymerization reaction is physically equivalent to the cooling of immiscible glass melts[3], where the correspondences between the rates of polymerization and cooling, the segregation strength and binodal temperature, the sol-gel transition and the liquid-glass transition, can clearly be recognized. The viscosity of the solution will play an important role in

determining the dependence of L on C in relation to the length scale of the developing domains. In PA1 and PA3 systems, the clouding occurred after the loose gel formation, while in PA9 system the increase in turbidity and gel formation occurred almost in parallel. This difference arises from the increased segregation strength with molecular weight which effectively decreases the chemical "cooling" rate leading the C-dependence of L in PA9-system somewhat stronger. The apparent reversed dependence of L on C in PA25-containing samples can be explained partly by the change in the volume fractions of skeletons and pores, that is, the pore fraction increases with C to lead apparent decrease in the thickness of the skeletons even at fixed periodic size. In these samples, the phase separation results in the quite coarse domain formation due to the strong segregation of the system. Remaining possibility is that as the viscosity of sample solutions steeply increases with C, it becomes easier for high-C samples to be deeply thrust into the spinodal region, leading to the reversed dependence of L on C.

The effectiveness of decreased segregation strength in obtaining finer interconnected morphology compared with that of polymerization rate can be recognized in the compositional dependence of L at varied temperature (Figure 2). The very weak dependence of L on T for E-3 composition compared with that for E-1 indicates that the gel-formation rate itself has relatively little effect in the system where the decrease of segregation strength allows the spinodal phase separation in a crosslinked network. The same tendency of the dependence of L on polymerization rate was seen in the systems containing varied amounts of acid catalyst, which will be further described in the next chapter.

2.4.3 Macro-Pore Fraction and Volume of Incorporated Polymer.

The fraction of micron-range pore volume is obviously related to the

volume of HPAA because silica polymer and HPAA molecule completely exclude each other due to the increased molecular weight of silica near the gel point. For the nanometer-range porosity, on the other hand, the interaction between silica and solvent phase plays more important role, which will be reported in Chapter 7. The slope showing the value of around -0.5 through 25-fold of molecular weight range indicates the important feature of the present system. Although the polymerization behavior of silica depends on the amount and molecular weight of coexisting HPAA, t_g showed very close values in the C-range of interconnected morphology. This fact seems to justify to provide, in these respective C-ranges, that hydrolyzed TEOS polymerizes in almost the same rates and manner to occupy almost the same volume fractions in the solutions near the gel point during the development of interconnected domains. Accepted that the interconnected phase-separated structure keeps its connectivity longer in the coarsening process when the volume fractions of conjugate phases are comparable*, the power of -0.5 suggests that the volume of HPAA-rich phase varies with P analogously to that of polymers in theta solvent[2]. The slope value is about -0.25 in NaPSS-TMOS systems described in Chapter 5 and becomes positive in the systems containing polyethylene glycol(PEG)[4]. Considering that alcohols are non- or poor-solvent of NaPSS and PEG, the volume of polymer-rich phase depends more strongly and in more complicated manner on molecular weight in general. The comparable solvent qualities of water and ethanol against the partially esterified HPAA possibly have realized the effectively constant interaction between HPAA and mixed solvent in broad P-range to give the "normal" power of -0.5. The weaker dependence of HPAA-solvent interaction can be recognized also on the reaction temperature, which resulted in the fixed central C-values of interconnected structure at varied temperature in contrast to the whole shift of C-range in NaPSS-TMOS systems (Chapter 5).

If the above discussion exactly explains what is occurring during phase separation and gel-formation, it will further become possible to extend the solution chemistry of organic polymers in solvents to the inorganic polymer - organic polymer - solvent or inorganic polymer - solvent systems. The real meaning of the slope should further be studied comparatively using different kind of polymers in the future work.

* This becomes true when the quasi-two component diagram of silica-solvent and HPAA-solvent represented against volume-fraction axis shows symmetrical binodal and spinodal lines of which critical composition results conjugate phases with equal volumes.

2.5 CONCLUSIONS

(1) Silica gels with micron-range interconnected pores could be prepared by the polymer-incorporated sol-gel process using HPAA having molecular weight between 10,000 and 250,000. The amount of HPAA most suitable to obtain the interconnected gel morphology decreased in proportion to the inverse square root of their molecular weight.

(2) With an increase of reaction temperature, both the solvent composition and HPAA concentration range of interconnected structure extended, and the pore size decreased.

(3) The relation between polymerization rate and segregation strength could well explain the experimental results. The increase in reaction temperature accelerated the polymerization which could bring the system deep into the spinodal region, while the increased molecular weight lead the earlier emergence of immiscibility through the decreased solubility of HPAA resulting in the coarser periodic structure.

SUMMARY OF CHAPTER 2

The phase separation phenomena of gelling solutions have been investigated for the acid catalyzed alkoxy-derived silica systems containing polyacrylic acid. The effects of solvent composition, molecular weight of polyacrylic acid and reaction temperature on phase separation and gelation behaviors were examined through the morphology observation by SEM. All the effects could well be explained by considering respective influences on the factors which determine the phase separation and gel-formation behaviors such as segregation strength and volume fraction of polymer, polymerization rate of silica and total mobility of the phase separating system.

REFERENCES

[1] For the recent comparative studies see for example, M.W.Colby, A.Osaka and J.D.Mackenzie: *J. Non-Cryst. Solids*, **99**(1988), 129-139

[2] P.J.Flory: *"Principles of Polymer Chemistry"*, (Cornell University, Ithaca, New York, 1971).

[3] P.G. deGennes: *"Scaling Concept in Polymer Physics"* (Cornell University, Ithaca, New York, 1979).

[4] K.Nakanishi, H.Komura and N.Soga, unpublished data.

CHAPTER 3

EFFECT OF CATALYTIC CONDITION IN SYSTEMS CONTAINING POLYACRYLIC ACID

3.1 INTRODUCTION

Through the discussions in the previous chapters, the phase separation and gel-formation induced by the chemical polymerization reaction was shown to be physically equivalent to the finite-rate cooling of immiscible glass melts. Quite analogous to that viscosity - temperature curves of glass-forming melts show wide variation depending on the type and strength of the interaction among constituent molecules or ions, various reaction route can be applied to obtain gels through polymerization even when the chemical composition of the gel phase is fixed. In the case of alkoxy-derived silica, the solution pH greatly affects both hydrolysis and polycondensation reactions, and resultant gel structure below and above isoelectric point (IEP) differs substantially each other.

Tetramethoxysilane (TMOS) is far more easily hydrolyzed than tetraethoxysilane (TEOS) to result clear homogeneous solution even under solvent-free and weakly acidic conditions. Thus phase separation and gel-formation behavior between below and above IEP can be compared with ease. In addition, the lack of acid catalyst limits an *in situ* esterification reaction of HPAA with coexisting alcohols, which greatly influences on the compatibility of HPAA in the water-alcohol mixed solvents.

In this chapter, the effect of acid catalyst concentration on the pore size have been first examined for HPAA-TMOS and HPAA-TEOS systems from strongly acidic pH condition up to IEP, then the phase separation and gelation behavior was extensively investigated in HPAA-TMOS systems hydrolyzed and polymerized a little above IEP.

3.2 EXPERIMENTAL

TMOS and TEOS, products of Shin-Etsu Chemical Co., were used as received. HPAA, products of Aldrich Chemical Co., having the molecular weight of 90,000 (PA9) and 250,000 (PA25) were used without further purification.

The representative solution compositions adopted are listed in Table 3.1. Compositions M-1 and E-2 have almost equal solution volume and silica content, and together with E-4 they were used to systematically compare the effect of catalyst concentration below IEP of silica in PA9-containing system. Compositions M-2 was chosen as the most suitable ones to obtain the interconnected porous gels in PA25-containing system. For this composition no acid was added and the hydrolyzed solutions showed constant pH of 2.4 throughout the HPAA concentration range examined.

The sample gels were prepared as follows. First, the HPAA was dissolved in mixtures of distilled water and various amounts of alcohols followed by the addition of concentrated nitric acid solution. Secondly, TMOS or TEOS was added to above solution in a short time. Immediately the container was sealed, the solution was vigorously stirred at room temperature to promote emulsification and hydrolysis reaction. The time required to reach the homogeneous and transparent state differed substantially depending on the kind of alkoxysilane and catalyst concentration. After having turned transparent, the solution was additionally stirred for 5 min, then kept at constant temperatures for gelation. After gelation, the gel sample was aged at the same temperature, rinsed off the organic phase with water, and finally dried at 60°C.

The microstructures of dried gels were examined by a scanning electron microscope (S-510, Hitachi Co.), using the fractured surfaces. The average thickness of silica skeleton L was measured directly from the SEM photograph.

Table 3.1 Starting Compositions of sample solutions (unit:g)

Composition	HPAA	Water	Methanol	TMOS or TEOS
M-1	0.40*1	5.0	1.87	TMOS 4.77
M-2	0.30-0.55*2	5.0	none	TMOS 5.15
E-2	0.40*1	5.0	--	TEOS 6.51
E-4	0.40*1	4.0	--	TEOS 6.51

*1:Molecular weight = 90,000, *2:Molecular weight = 250,000

3.3 RESULTS

3.3.1 Sol and Gel Formation

Under strongly acidic conditions, the hydrolysis of alkoxysilane occurred within few minutes to result transparent solution accompanied by the heat evolution. With decreasing acidity of water phase, increasingly longer time was required under the fixed stirring condition before the complete transparency could be achieved. Especially for the TEOS-containing solutions with lower acid concentration below 0.1 moldm^{-3}, mixtures were kept ca. 40°C in water bath in order to accelerate the hydrolysis process. In the case of pH=2.4, the initially mixed solutions became finely dispersed only gradually, it took more than 40 min to get the solution once transparent. Shortly after the transparency observed the solution again turned cloudy, and it took another 10 min to obtain completely transparent solutions. On the other hand, for the composition M-1, the time required to obtain transparent solution was within few tens seconds due to the existence of methanol working as co-solvent.

The time required for gelation t_g was measured from the moment when the solution turned transparent with heat evolution. Figure 3.1(a) shows the dependence of t_g on acid concentration in water phase for the composition M-1

and E-2. The gel times seem to have their maxima at acid concentration around 0.1 moldm^{-3}. According to Corriu et al. the acidity function of water methanol mixed solution is about an order of lower than the original pH of the water phase[1], which coincides with the fact that the gelation is the slowest at IEP of silica. Almost the same trends were observed for the composition E-4, where the hydrolysis time depends rather strongly on acid concentration leading the absolute value of gel time somewhat ambiguous.

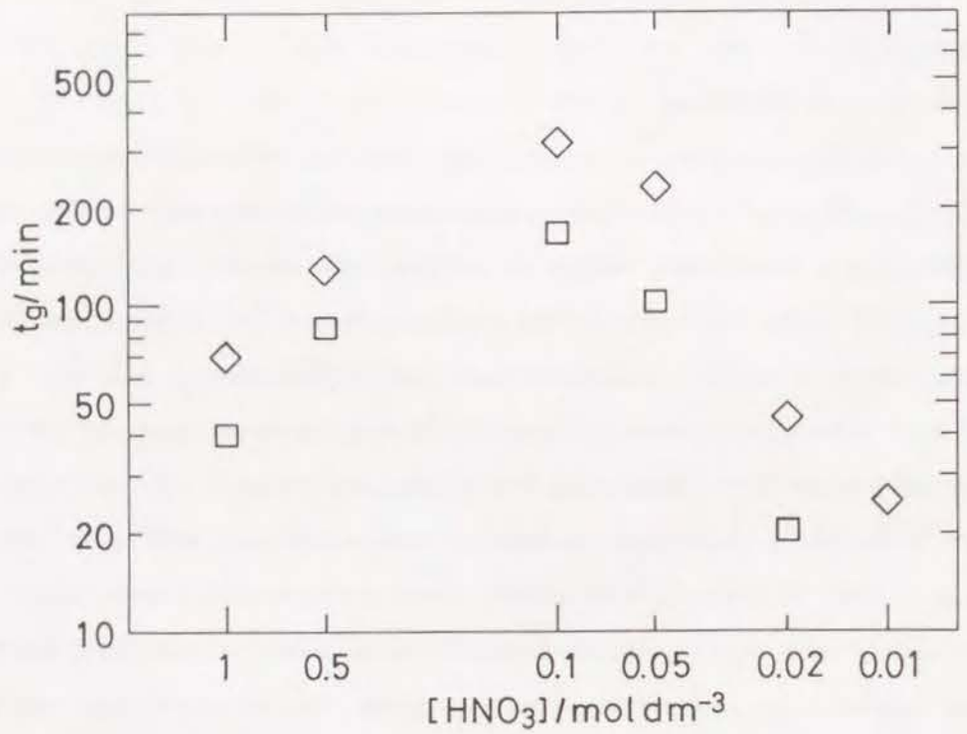

Figure 3.1(a) Dependence of gel time t_g on catalyst concentration of aqueous solution used for hydrolysis at 60°C;
◇:composition M-1, □:composition E-2.

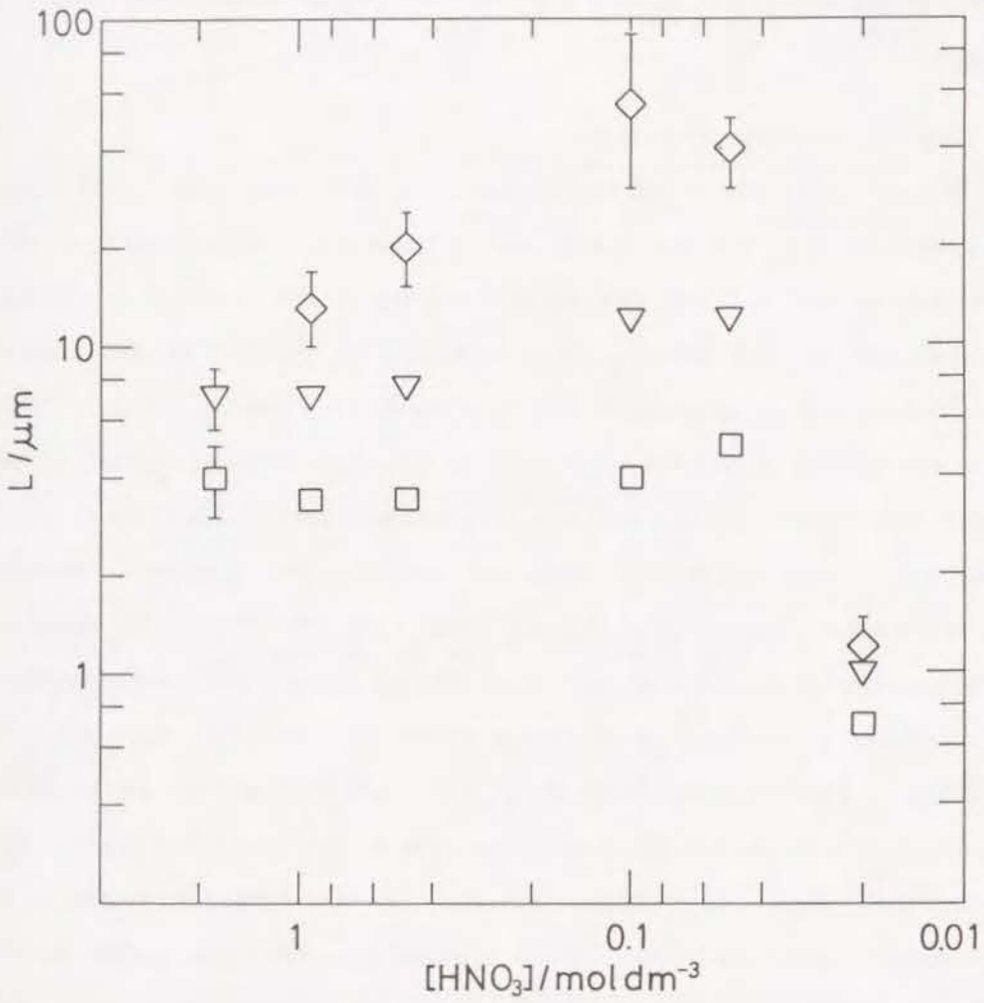

Figure 3.1(b) Dependence of periodic size L on catalyst concentration of aqueous solution used for hydrolysis at 60°C;
◇:composition M-1, □:composition E-2, ▽:composition E-4.

The emergence of translucency or opacity was observed in parallel to the gel-formation of the samples. Some turned opaque while the sample still retains fluidity and others became gradually translucent after the formation of soft gels.

3.3.2 Effect of Catalyst Concentration.

Figure 3.1(b) shows the dependence of L on the catalyst concentration in compositions M-1, E-2 and E-4 shown in Table 3.1. All compositions show the maxima between 0.1 and 0.05 moldm^{-3} acidity of the hydrolyzing solution. In composition M-1, L and t_g behave almost in parallel against catalyst concentration, but in composition E-2 L depends only weakly on t_g. These results are in good agreement with those in previous chapters indicating that systems with weaker segregation tendency showed weaker dependence on the polymerization rate. The morphology of resulting gel changes remarkably when the catalyst concentration becomes lower than 0.05 moldm^{-3} to which the IEP of this system roughly corresponds. Though micron-range interconnected gels could not be obtained in pH range above IEP when PA9 was used, PA25 was found to form interconnected pores at pH=2.4 in TMOS-system when the composition with somewhat lower solvent fraction and higher HPAA concentration, shown as M-2, was used. In the following sections, the morphological variations with solvent composition, HPAA concentration and reaction temperature were examined for the compositions around M-2, with reference to those in the strongly acidic systems.

3.3.3 Effect of Solvent Composition

Figure 3.2(a) and (b) show the dependence of gel morphology on the solvent phase composition near M-2 under fixed C at 40 and 60°C. The solvent phase compositions were calculated assuming the complete hydrolysis and condensation of TMOS by the time of gel-formation and phase separation

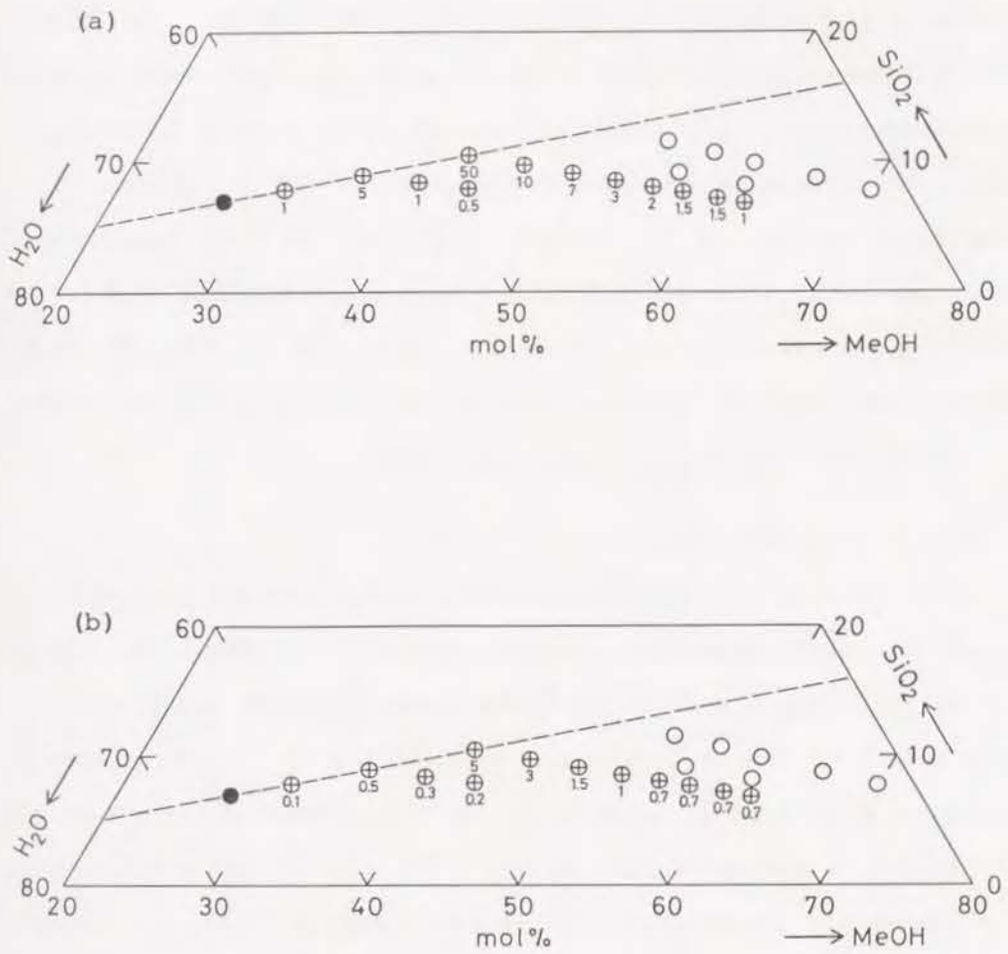

Figure 3.2 Dependence of gel morphology on solvent composition at (a) 40°C and (b) 60°C. HPAA concentration was fixed at C=0.164. Solvent compositions were calculated by assuming 2 mol decrease of water and 4 mol increase of methanol per 1 mol of TMOS from starting composition. Average pore sizes are plotted on symbols for the samples with interconnected structure; ● :microporous gels ⊕ :interconnected structure, ○ :particle aggregates.

because more than twice amount of water for complete hydrolysis was used[2]. The actual compositions may exist in somewhat methanol-rich field as silica polymers carries considerable amount of hydroxy groups even at gel-formation. Compared with PA9-system with composition E-2 shown in Chapter 2, L depends more strongly on the solvent composition at both temperatures. Moreover, the smaller pores are obtainable in somewhat water-rich region when the silica concentration was fixed, which is opposite to the strongly acidic system. In methanol-rich region with higher silica concentration the particle aggregates of silica were obtained even at low temperature.

3.3.4 Effect of HPAA Concentration

Figure 3.3 shows the C-dependence of L at fixed solvent composition at 40 and 60°C. Again compared with strongly acidic PA9 systems, the dependence is by far stronger and the obtainable L-range exceeds one order. The absolute amount of PA25 in composition M-2 which gives the interconnected morphology is about twice as large as that in composition E-2 in spite of the smaller amount of expected solvent phase. SEM photographs are shown for 60°C in Figure 3.4, which exhibit the analogous change to that in strongly acidic PA1 system shown in Chapter 2 from low-fraction fine pores to globular interconnected skeletons except the extended L-range in the present system.

3.3.5 Effect of Temperature

The above results show also the strong temperature dependence of L except substantially diluted cases. As shown in Figure 3.3, the SEM-detectable interconnected porous structure resulted in the same C-range at both temperatures. This behavior differs from that observed in strongly acidic systems where the C-range extended with increasing temperature (Chapters 2 and 5).

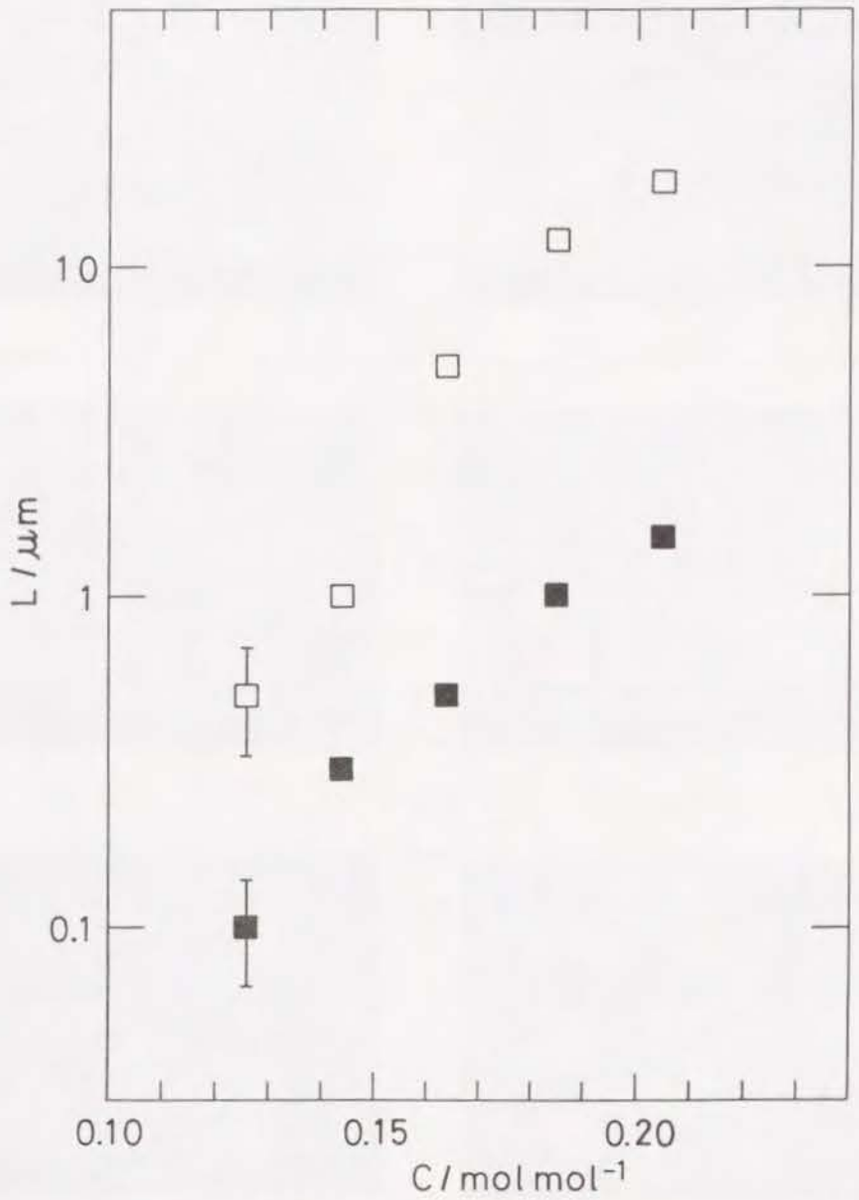

Figure 3.3 Dependence of average pore size L on PA25 concentration C. Starting composition was fixed at M-2. □:40°C, ■:60°C.

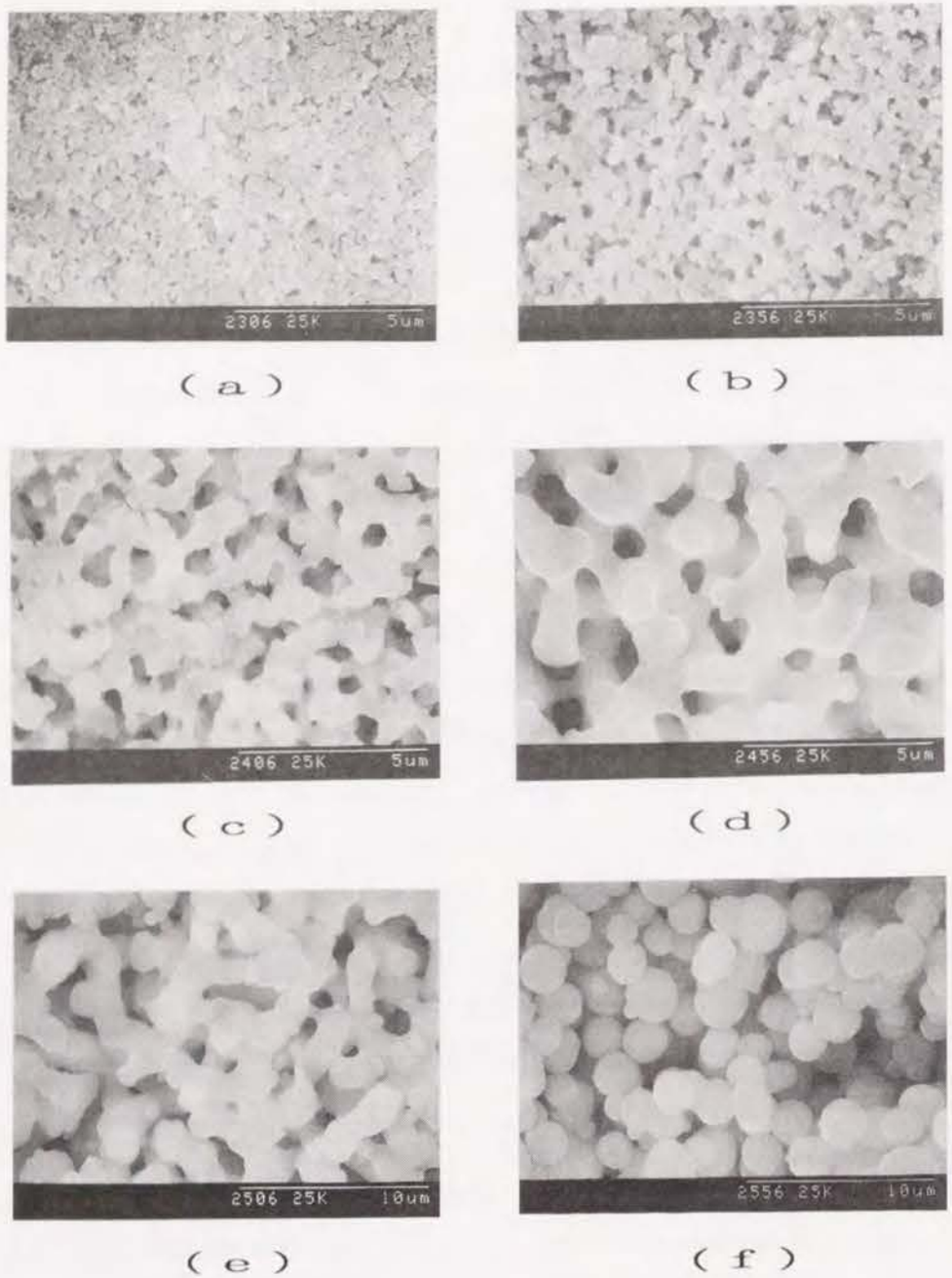

Figure 3.4 SEM photographs of the gel morphologies obtained from PA25-TMOS systems with varying C at 60°C. Starting composition is M-2. (a) C=0.123, (b) 0.144, (c) 0.164, (d) 0.185, (e) 0.205, (f) 0.226.

3.4 DISCUSSION

3.4.1 Expected Variation in Gel Forming Behavior with Catalytic Condition

It has been confirmed by NMR[3] that under strongly acidic conditions the polymerization proceeds relatively slowly between highly hydrolyzed species, and that the reduction of acid catalyst leads the decreased hydrolysis rate and preferential condensation between already hydrolyzed species. The acceleration of polymerization relative to hydrolysis result in the decreased fraction of polymeric species, i.e., the increased polydispersity of molecular weight of silica polymers from the oligomeric state[4] to the moment of gel formation[5]. Thus, as-gelled structure of strongly acidic samples can be described by compact packing of large-sized loosely crosslinked silica clusters with relatively narrow molecular weight distribution containing essentially no oligomeric species, while that of low acid or basic gels by loose packing of exceptionally large highly crosslinked clusters containing considerable amount of lower molecular weight fractions among them. If one plots the gel-fraction against t_g-normalized reaction time, the low acid or basic system will show broader sol-gel transition range than strongly acidic one.

3.4.2 Comparison of Gel-Formation and Phase Separation Behaviors Above and Below IEP

The dependences of L and t_g on catalyst concentration shown as Figures 3.1(a) and (b) exhibit increased influence of t_g on L in the system with higher segregation tendency. The same trend could be recognized when the systems with various solvent compositions were prepared at different temperature[2]. It is thus considered that the gel-forming mechanism is essentially the same in pH condition below IEP under the present water-rich condition. The characteristic behavior of gel-formation and phase separation in the highly acidic and above-IEP systems can be summarized respectively as

follows. In the highly acidic systems the ratio of weight-average to number-average molecular weight of silica polymers N_w/N_n throughout the polymerization reaction is relatively small[4,5]. As the free-energy of polymer-containing mixture is estimated from N_n, while the viscosity of the system is related to N_w, the segregation strength and viscosity steeply increase in parallel at sol-gel transition. Since N_n may reach considerably large value before the gel-formation, the coexistence of polymers having lower molecular weight and of a large amount of solvent is required in order to induce the phase separation in parallel to the gel-formation.

In the above-IEP system the ratio N_w/N_n is large. Although the mobility of the solution is reduced from the early stage of polymerization due to the high average N_w, the prolonged consolidation continues by slow reaction between the gel-network and unreacted or oligomeric species even after the gel-formation. Due to the coexistence of a large fraction of low molecular weight species, the averaged free energy of the system remains low at the gel-formation. Hence, the coexisting organic polymer with higher molecular weight is required to cause the phase separation and gelation in parallel and the smaller amount of solvent is enough to keep the system one-phase until gelation.

According to the analogy adopted in the previous chapters, the slow polymerization of already loosely gelled network corresponds to the slow cooling of mixture across the broad glass transition region, where the system remains homogeneous well below the binodal temperature. An addition of PA25 to this system causes the drastic increase in viscosity and in the segregation strength which sensitively reflects the change in N_n. The same amount of addition to M-1 composition causes phase separation in very early stage of polymerization resulting in the macroscopic two phase liquids long before the gel-formation. Hence, the polymerization of M-2 composition is regarded as

equivalent to the high-binodal and highly viscous glass melt subjected to the slow cooling. Since the amount of PA25 strongly affect the segregation strength, much stronger C-dependence of L than E-2 is reasonably explained. The high viscosity of dissolved PA25 helps the present system to exhibit still moderate dependence on the above parameters by suppressing the coarsening.

3.4.3 Effect of Esterification

The lack of esterification makes HPAA more soluble to water than to alcohol, which result in the opposite dependence of periodic size on water-alcohol ratio of solvent phase to that observed in highly acidic conditions. An increase in alcohol fraction reduces the solubility of HPAA and decelerates hydrolysis and polymerization, which allows the interconnected structure to coarsen into globular morphology before the completion of solid-gel phase as shown in Figure 3.2.

3.5 CONCLUSIONS

(1) Silica gels with interconnected porous morphology could be prepared both in above- and below-IEP conditions by the polymer-incorporated alkoxy-derived sol-gel process. Above IEP, the system with PA25 and TMOS was most suitable to obtain samples with controlled morphology.

(2) The results were interpreted by treating the gel-forming polymerizing system analogously to the immiscible glass-forming mixture subjected to the finite-rate cooling.

(3) The differences in the dependence of morphology on several reaction parameters between above- and below-IEP conditions could well be explained by considering the different gel-forming mechanism of alkoxy-derived systems.

SUMMARY OF CHAPTER 3

The phase separation of gelling solution was investigated in an extended acid catalyst concentration range for the systems containing polyacrylic acid (HPAA) and tetraalkoxysilane. In spite of the considerable differences in the polymerization rate and gel-forming behavior of silica, analogous phase separation and gelation behavior to that in the highly acidic systems has been observed even under the pH condition higher than the isoelectric point of silica. The difference in the weight- and number-average molecular weights of silica polymers at gel-formation well explained the changes in the relations between reaction conditions and gel morphology.

REFERENCES

[1] R.J.P.Corriu, D.Leclercq, A.Vioux, M.Pauthe and J.Phalippoou, in "*Ultra-structure Processing of Advanced Ceramics*" eds. J.D.Mackenzie and D.R.Ulrich (Wiley, N.Y., 1988), 113-126.

[2] J.C.Pouxviel, J.P.Boilot, J.C.Beloeil and J.Y.Lallemand: *J. Non-Cryst. Solids*, **89**(1987), 345-360.

[3] L.W.Kelts, N.J.Effinger and S.M.Melpolder: *J. Non-Cryst. Solids*, **83**(1986), 353-374.

[4] W.G.Klemperer and S.D.Ramamurthi in "*Better Ceramics Through Chemistry III*", eds. C.J.Brinker, D.E.Clark and D.R.Ulrich (Mat. Res. Soc., Pittsburgh, Pa., 1988), 1-14.

[5] T.W.Zerda, I.Artaki and J.Jonas: *J. Non-Cryst. Solids*, **81**(1986), 365-379.

CHAPTER 4

EFFECT OF CHEMICAL ADDITIVES ON GEL STRUCTURE

4.1 INTRODUCTION

In the previous chapters, described were the formation of silica gels with sharply controlled micron-range interconnected pores through simple hydrolysis of alkoxysilane under coexistence of water-soluble polymers with various proportions of solvent phase and an acid catalyst.

It has been well known that additions of various organic solvents to the reaction mixture of alkoxysilane, alcohols and water lead to the wide variety of changes in the resultant gel structure, i.e., average pore size and porosity, by influencing the both hydrolysis and gelation processes[1,2]. An addition to HPAA-TEOS system of such kind of organic solvent that influences both the polymerization rate of silica and the solubility of coexisting HPAA is expected to give the experimental evidences required to confirm the principles of formation of interconnected macroporous gels, which have been discussed in the previous chapters. From this standpoint, most of the organic solvents were chosen from those already have been used as DCCA, whose effects on the polymer-free silica sol-gel systems are well-known. The results are discussed mainly on the respective effectiveness of the solvents in the acceleration of polymerization reaction of silica relative to the improvement of the solubility of HPAA molecules which is possibly in partially esterified form between hydroxy-containing solvents.

4.2 EXPERIMENTAL

Tetraethoxysilane (TEOS), product of Shin-Etsu Chemical Co., was used as silica source. HPAA, products of Aldrich Chemical Co., having the molecular weights of 90,000 (PA9), 250,000(PA25) and 750,000 (PA75) were used as polymer

component. PA75 was used only to qualitatively compare the solvent power between ethanol and DMF. Nitric acid was used as a catalyst for hydrolysis.

The sample gels were prepared as follows. First, HPAA was dissolved in distilled water and nitric acid was added so as to adjust the solution pH. In most cases, nitric acid was added in the molar ratio to water of 0.0173, which corresponded to ca. 0.9 moldm^{-3}. Secondly, TEOS was added to above solution in a short time. Immediately the container was sealed, and after stirring for 5 min the solution was kept at constant temperatures for gelation. After gelation, the gel samples were aged at the same temperature, rinsed off the organic phase with water and ethanol, and finally dried at 60°C.

Scanning electron microscope (S-510, Hitachi Co.) was employed for the observation of morphology of the resultant gels. For all the samples, the degree of shrinkage was almost the same (shrank linearly about 60% of original size) because the oxide content in the same series of samples differed less than 10% which corresponds to the linear shrinkage of less than 3%. The observed sizes of microstructure for the dried gels are used without any correction in the following discussion, accordingly.

4.3 RESULTS AND DISCUSSION

4.3.1 Effect of Additional Solvents to PA25-System

Figure 4.1 shows the selected SEM photographs of gel morphology obtained from the solutions containing several kinds of additional organic solvent with equal volume fractions, ca. 30% of total volume at 80°C. The compositions of starting materials are shown in Table 4.1 as A-2. Figure 4.2 shows the correlation between the average thickness of silica skeleton L determined from SEM photographs and the solubility parameters δ_s of added solvents listed in Table 4.2. Abbreviated expression of solvents and gelation times t_g in minutes are respectively shown on the top and bottom of the symbols. Although a

Table 4.1 Starting compositions of sample solutions.
(units ; upper line : g, lower line : ml)

Code	HPAA	Water	Solvent	TEOS	Nitric acid
A-2	PA25 0.20	5.0	---	6.51	0.51
		5.0	5.0	7.0	0.37
R-1	PA9 0.25-0.50	4.0	---	6.51	0.41
		4.0	1.0	7.0	0.29
R-2	PA9 0.25-0.50	3.0	---	6.51	0.31
		3.0	2.0	7.0	0.22
R-3	PA9 0.25-0.50	2.0	---	6.51	0.20
		2.0	3.0	7.0	0.15
E-2	PA9 0-0.50	5.0	0	6.51	0.51
		5.0	0	7.0	0.37

Table 4.2 Solubility parameter and miscibility with HPAA, water and ethanol of various solvents.

Solvent (Abbreviation)		Solubility Parameter δ_s ((cal cm^{-3})$^{1/2}$)	Miscibility with HPAA*1	Water	Ethanol
(1) Ethyl Acetate	(AcOEt)	9.1	Poor	Poor	Good
(2) Acetic Acid	(AcOH)	10.1	Poor	Good	Good*2
(3) 1,4-Dioxane	(DOX)	10.0	Good	Good	Good
(4) 1-Butanol	(BuOH)	11.4	Good	Poor	Good
(5) 2-Propanol	(PrOH)	11.5	Good	Good	Good
(6) Ethanol	(EtOH)	12.7	Good	Good	--
(7) Propylene Glycol	(PG)	12.6	Good	Good	Good
(8) Ethylene Glycol	(EG)	14.6	Good	Good	Good
(9) Glycerol	(Gly)	16.5	Good	Good	Good
(10) N,N-Dimethyl Formamide	(DMF)	12.1	Good	Good	Good
(11) N-Methyl Formamide	(MMF)	16.1	Good	Good	Good
(12) Formamide	(FA)	19.2	Good	Good	Good
(13) Water		23.4	Good	Good	Good

*1 Judged from the appearance of solution containing 2.0g of PA25 and 50ml of solvent.
*2 Esterification is possibly included under strongly acidic condition.

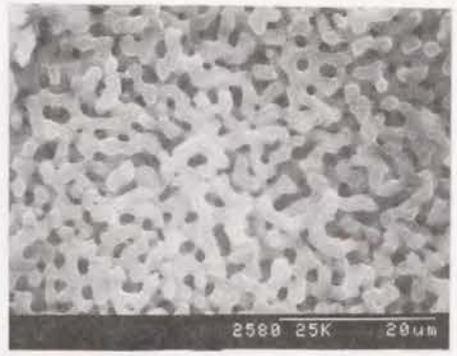

FA

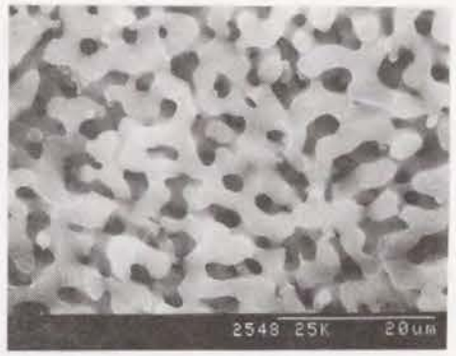

MMF

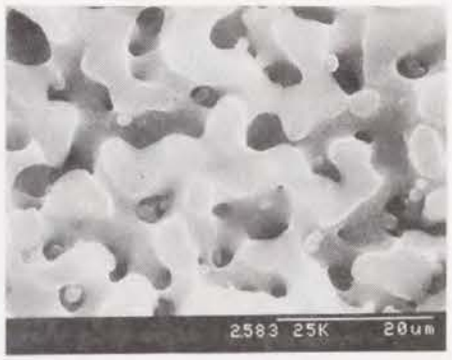

DMF

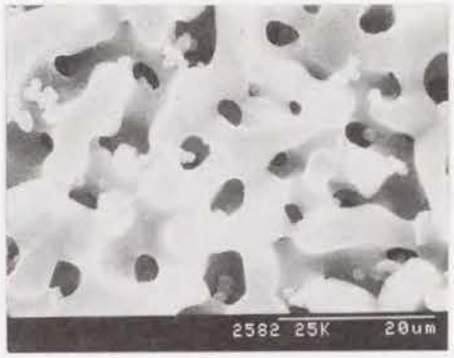

Gly

EG

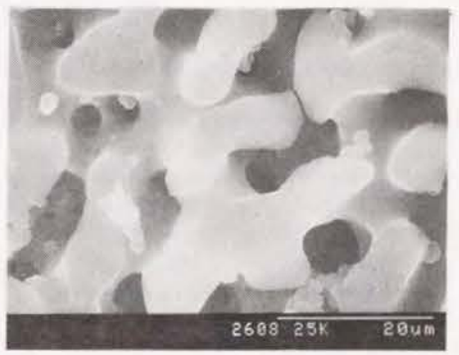

PG

Figure 4.1 SEM photographs of gel morphology prepared from PA25-TEOS system with additions of various kind of organic solvents at 80°C. Starting composition is shown as A-2 in Table 4.1. The names of solvents are indicated in the abbreviated form listed in Table 4.2.

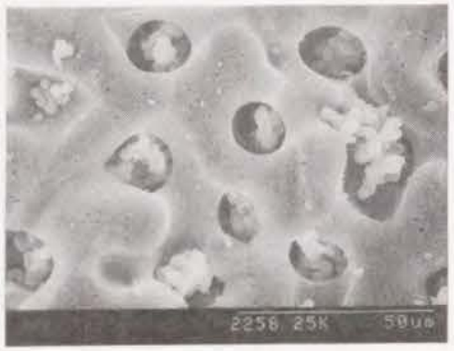

EtOH

PrOH

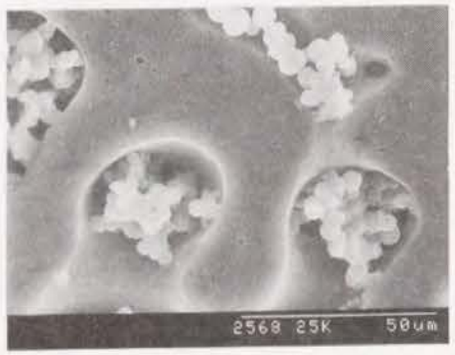

DOX

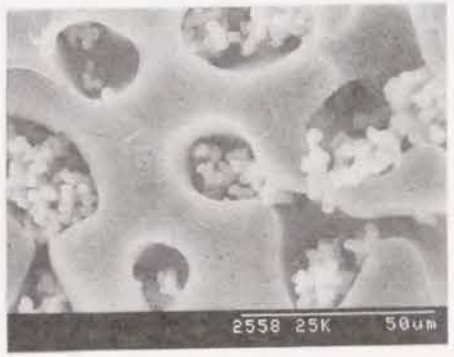

AcOEt

Figure 4.1 SEM photographs of gel morphology (Continued).

roughly reversed correlation can be recognized, at lower δ_s values the distribution of L is broad showing the increase with t_g. Figure 4.3 shows the correlation between L and t_g. There are several exceptional samples deviating from those exhibit good positive correlation. The above results indicate that neither δ_s nor t_g solely plays the decisive role to determine the morphology, but that the specific characters of respective solvents must be taken into account regarding their contribution to the segregation tendency of HPAA and the acceleration of polymerization reaction of silica.

As has been demonstrated in the previous chapters, any factor which leads the later occurrence of phase separation with respect to the gel-formation of the system resulted in the finer morphology. Among the systems showing similar gel-formation behaviors, rapid polymerization was favorable for the finer morphology. In other words, the reaction parameters which accelerate the polymerization or gel-formation, or those increase the solubility of HPAA can decrease the periodic size of the interconnected structure, and *vice versa*. For example, samples prepared at higher temperature exhibit finer morphology mainly due to the accelerated polymerization reaction, those prepared under coexistence of higher molecular weight HPAA result in coarser morphology due to the decreased solubility (increased segregation) of HPAA. The situation has been shown to be physically equivalent to the finite-rate cooling of immiscible glass melts, in which the cooling rate corresponds to the polymerization rate, the binodal temperature to the segregation tendency, and the gel-formation induced by the crosslinking polymerization to the liquid-glass transition with decreasing temperature. Therefore, the effect of additional solvents should be interpreted in terms of their influence on the polymerization or gel-forming rate and HPAA solubility. It has been evidenced that the gel-forming mechanism remains essentially unchanged in pH condition below isoelectric point of silica in Chapter 3. We here assume that the

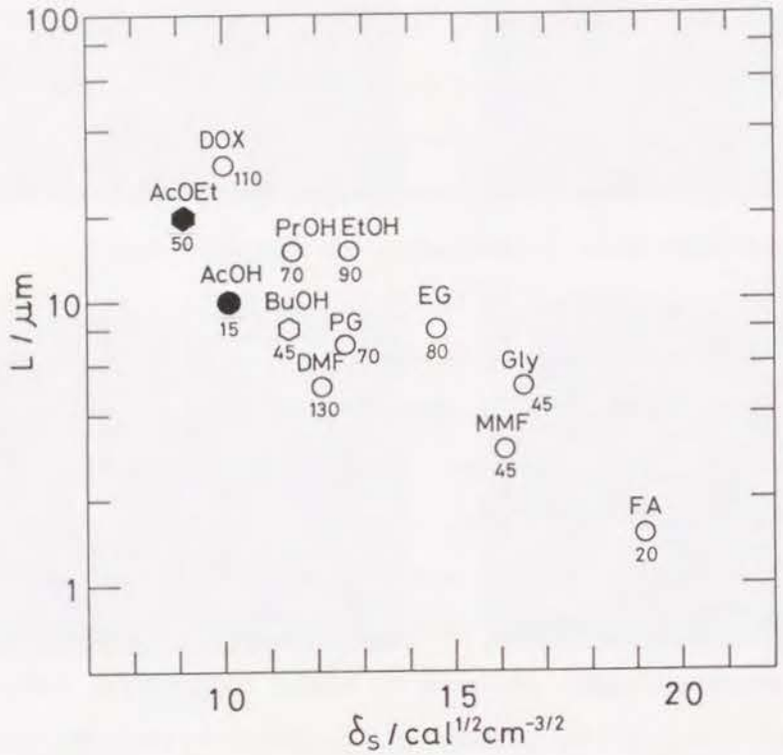

Figure 4.2 Correlation between average pore size L and solubility parameter δ_s. Gelation time t_g is indicated under each symbol. Different symbols indicate the compatibility of each solvent with water or HPAA shown in Table 4.2. Filled symbols and hexagons respectively indicate poor compatibility with water and HPAA.

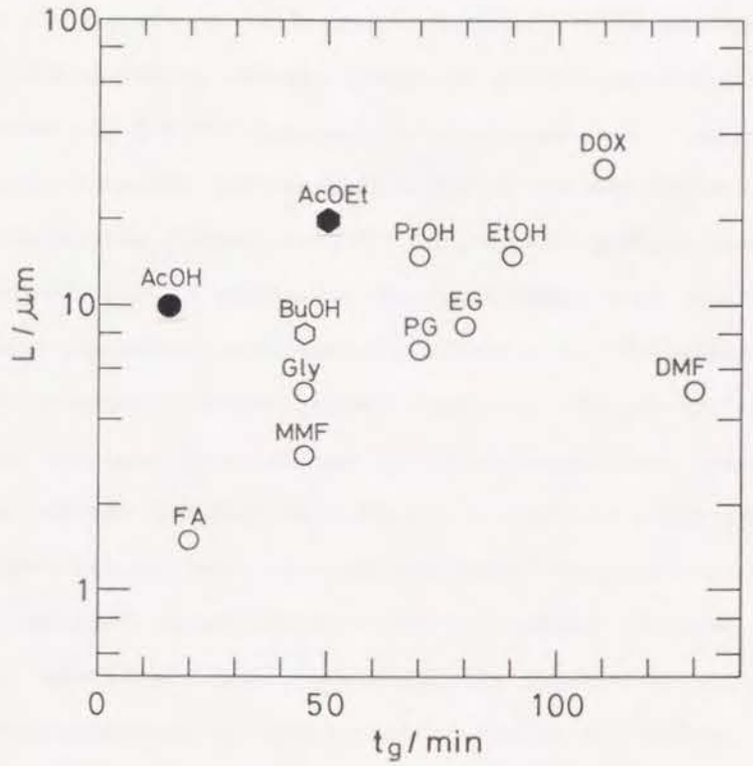

Figure 4.3 Correlation between average pore size L between gelation time t_g at 80°C. Symbols have the same meaning as in Figure 4.2.

additional solvents affect mainly on the polymerization rate and HPAA solubility and neglect the difference in the gel-forming mechanism such as observed for acid- and base-catalysis.

The effects of additional organic solvents to silica sol-gel systems on the micro-morphology and polymerization mechanism have been reported mainly under neutral condition using electron microscope, Raman spectroscopy[3], and gas chromatography[4]. The solvents used to improve the gel strength against the drying stress can be classified into several groups in view of polarity and hydrogen-bonding character[3]. The most famous and pronounced example is formamide[5] whose acceleration of polymerization of silica under acidic condition is attributed to the gradual decomposition to generate ammonia and formic acid[6]. For the acid-catalyzed systems, protic solvents act as a stabilizer to the protonated silanol-containing species, which results in the acceleration of condensation reaction. It is thus expected that for the protic solvents the effectiveness to accelerate polymerization can be estimated by their polarity, i.e., solubility parameter. On the other hand, HPAA tends to dissolve in hydrogen-bonding polar solvents as shown in Table 4.1, and in the cases of polyatomic alcohols, the esterified part of HPAA retains hydrophilicity and high solubility in polar protic solvents. Therefore, both the polymerization rate of silica and solubility of HPAA increase with increasing δ_s, which explains the overall trend of Figure 4.2.

Several exceptionally deviated samples seen Figure 4.3, which correspond to those scattered around low δ_s region, can be categorized as follows;

(1) Large L with shorter t_g. (AcOH)

(2) Small L with longer t_g. (DMF)

(3) Shorter t_g in less polar solvents. (AcOEt, BuOH)

First two can be explained by considering that the chemical cooling rate is related to both the polymerization rate and segregation tendency. In the first

case, although added AcOH acts simultaneously to increase the segregation tendency of HPAA and to accelerate the polymerization reaction of silica, the former effect is strong enough to cause the phase separation in even earlier stage of the gel-formation to result the final gel morphology with larger L. This corresponds to the increased cooling rate in parallel to the addition of strongly miscibility-reducing component in a immiscible glass system to phase separate well above the glass transition region.

The second case resembles that observed in PA9-containing system, where in spite of the increased t_g the interconnected morphology with smaller L was obtained with an addition of ethanol. In the present case, if we compare the effects of ethanol and DMF addition in Figure 4.3, the latter gives by far smaller L in spite of longer t_g. In addition, although dioxane shows nearly the same t_g as DMF, it gives the largest L of all. Ethanol did not show complete miscibility with PA75 at room temperature, and dioxane is known to become non-solvent of HPAA at higher temperature (LCST system), while DMF completely dissolved PA75 in broad ambient temperature range. Accordingly, a probable explanation is that the segregation tendency of HPAA is so drastically lowered by the addition of DMF that even with the very slow gel-formation the development of phase-separating domains proceeds in already crosslinked gel network to result the final gel morphology with finer pores than other systems exhibiting more rapid gel-formation. This corresponds to the slow cooling of a UCST system below the glass transition region.

The third result is rather confusing, but the important point is that the additives are incompatible with water. It is tentatively explained that the gel-forming rate is related to the rate of aggregation of silica clusters which reflects the compatibility of silica with solvent phase. Under water-rich and acidic condition, TEOS can be almost completely hydrolyzed and the polymeriz-

ing clusters carry considerable amounts of hydroxy groups giving high hydrophilicity to the clusters. As a result, the tendency to eliminate the highly hydrophobic solvent phase becomes strong in BuOH or AcOEt systems leading to the enhanced aggregation and accelerated gel-formation of silica. The SAXS results obtained for NaPSS-containing sols showing the formation of larger aggregates and earlier gel-formation may support the above speculations on the effect of coexisting incompatible components. Substantially smaller L for BuOH compared with AcOEt or other alcohols shown in Figure 4.2 indicate that as far as the segregation tendency of HPAA is not significantly changed, the accelerated polymerization results in the finer morphology irrespective of the origin of acceleration.

4.3.2 Effect of Replacement of Water with Other Solvents in PA9-System

In order to close up the characters of each solvent, the water-poor compositions with PA9 were prepared with either formamide, DMF, dioxane, acetic acid or ethanol shown as R-2 in Table 4.1. In the case of ethanol, the composition is identical to E-1 in Chapter 1. Figure 4.4(a) shows the dependence of L on HPAA content C. The results of E-2 composition with higher water- and catalyst-concentration are also plotted for comparison. The logarithmically normalized dependence of L on C is strong in DMF- and DOX-systems and quite weak in FA- and AcOH-systems although the respective L-ranges are considerably different. Figure 4.4(b) shows the C-dependence of t_g plotted in linear scale. The long t_g in DMF- and DOX-systems and short t_g in FA- and AcOH-systems respectively correspond well to the strong and weak C-dependences of L.

The strong C-dependence of L in DMF- and DOX-systems can be attributed to their extremely slow polymerization. Due to relatively low solvent power (high segregation tendency) of DOX to DMF against HPAA, the L of the

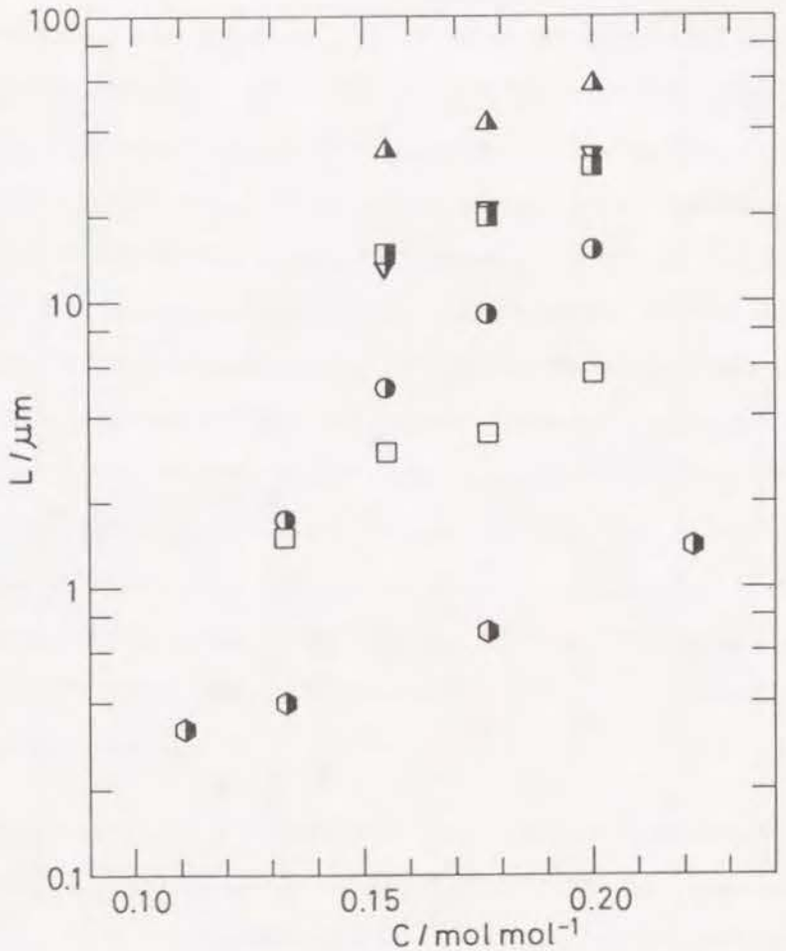

Figure 4.4(a) Dependence of average pore size L on PA9 concentration C prepared from composition R-2 with AcOH, DOX, DMF, FA and EtOH as additional solvents at 60°C.

▲:AcOH, ▼:DOX, ◑:DMF, ◑:FA, ◨:EtOH, □:E-2 composition.

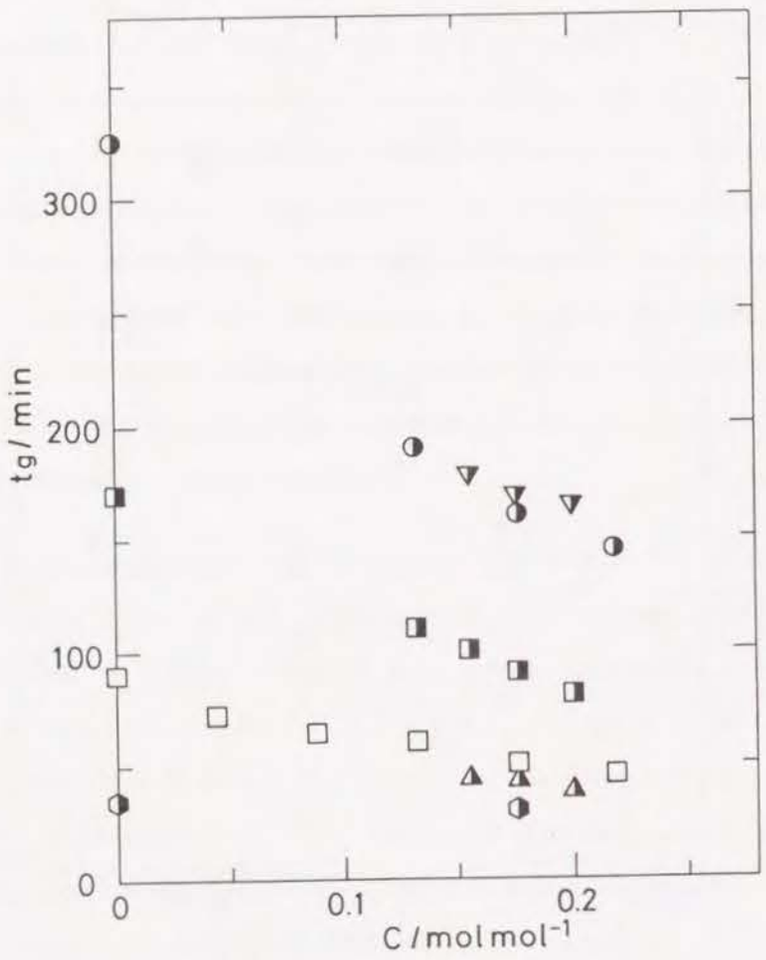

Figure 4.4(b) Dependence of gelation time t_g on PA9 concentration C for the same samples shown in Figure 4.4(a). Symbols have the same meaning as in Figure 4.4(a).

former system is quite large. Because the slow polymerization corresponds to the slow cooling, DOX- and DMF-systems are respectively regarded as the high- and low-binodal systems. An increase of C induces the increase of segregation tendency to significantly increase the mobility at the phase separation, which is equivalent to the decrease in cooling rate. In the slow polymerizing systems the relatively small change in the segregation tendency changes the effective cooling rate and strongly influences the wavelength of composition fluctuation allowed to grow. The closeness between the results of ethanol and DOX in Figure 4.4(a) in contrast to the considerable difference in Figure 4.2 indicates that slight difference in the polymerization rate becomes indistinguishable in the system with lower segregation tendency.

In the rapidly polymerizing system, on the other hand, the effective cooling rate is not strongly affected by C resulting in the weak C-dependence of L. Since the spinodal region extends with the increasing quench depth, FA-system with lower segregation tendency gives an extended C-range of interconnected structure.

4.3.3 Effect of Formamide Fraction in Solvent Phase in PA9-System

Figure 4.5 shows the C-dependence of L in the systems containing varied proportions of formamide shown as R-1, R-2 and R-3 in Table 4.1. The results of E-2 composition are also plotted as formamide-free reference. While L decreases only slightly between R-1 and R-2, the drastic increase in L and narrowing of C-range of interconnected structure can be recognized between R-2 and R-3. As t_g monotonously decreased with increasing formamide content, the increase in L in R-3 composition is to be attributed to the increased segregation tendency in spite of the accelerated polymerization as observed in AcOH-system.

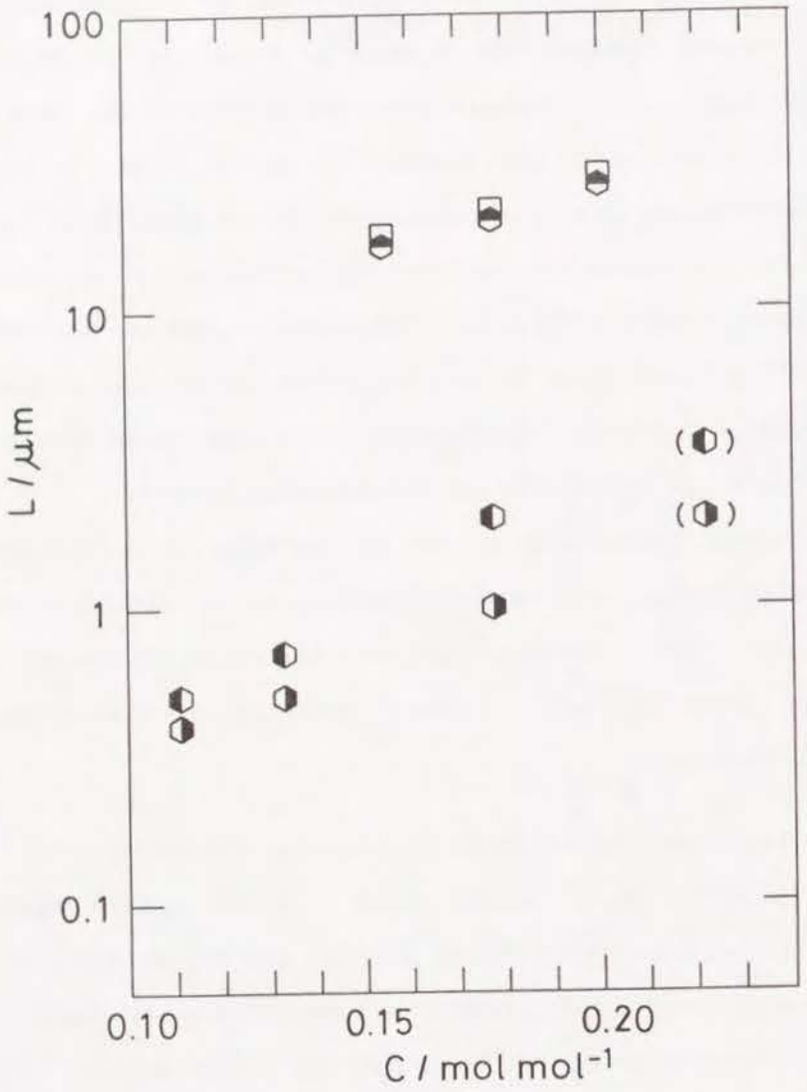

Figure 4.5 Dependence of L on C for the compositions containing varied fraction of formamide at 40°C. Symbols in parentheses indicate continuous but globular interconnected structure.
◐:R-1, ◑:R-2, ◓:R-3, □:E-2.

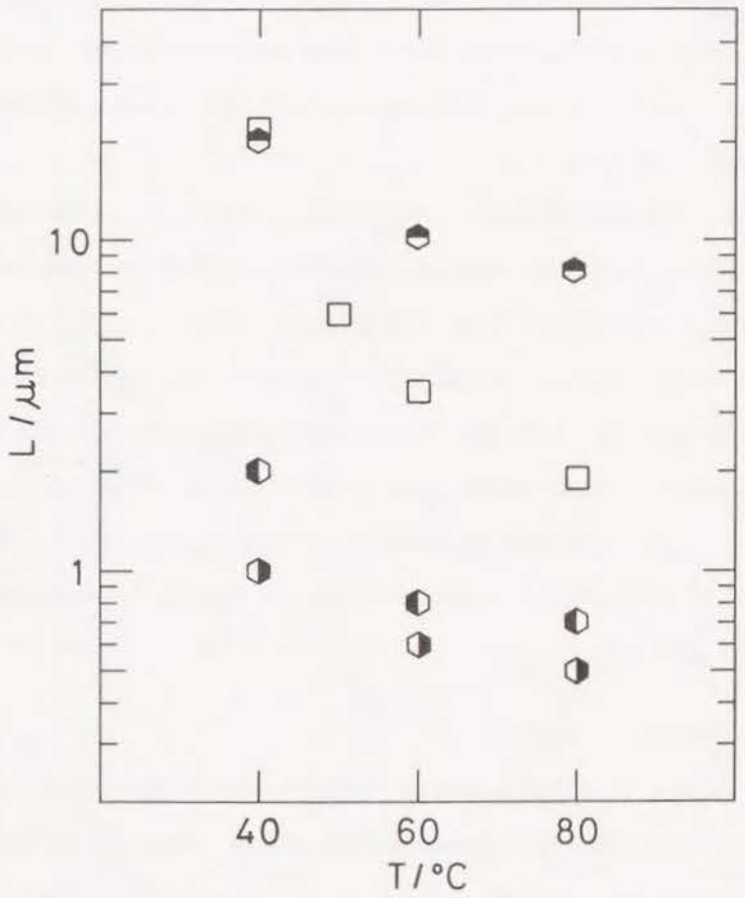

Figure 4.6 Dependence of average pore size L on reaction temperature T for the samples containing various amount of formamide at fixed PA9 concentration C=0.177. Symbols are the same as in Figure 4.5.

Figure 4.6 shows the dependence of L on the reaction temperature T for varied formamide fractions at fixed C. Compared with E-2 composition, the existence of formamide suppresses the T-dependence even when comparable L are observed. E-2 and R-3 compositions can respectively be categorized as the slow polymerization - weak segregation and the rapid polymerization - strong segregation systems.

Quite similar to PA25-system, the interconnected morphology with smaller L could also be prepared by adding formamide to E-2 composition. Almost analogously to the ethanol addition, the C-range of interconnected structure broadened and shifted toward higher C. The particular result observed for formamide system was that with increasing amount of formamide, the surface of interconnected pores became rough in submicron range. This can be explained by the increased polymerization rate and decreased segregation, which inhibited the growth of composition fluctuation in so tightly crosslinked, rapidly solidifying silica network.

4.3.4 Effect of Addition of Sorbitol

Sorbitol is one of sugar-alcohols having the analogous molecular structure to glycerol. It has been reported that the addition of various kind of mono- or polyatomic alcohols significantly affect the activity of hydronium ions to modify the acid catalyzed hydrolysis and polycondensation rate of silica to result in wide range of t_g[7]. Since sorbitol was suggested to be one of the effective additives to accelerate polymerization by increasing the activity of acid catalysts, the effects of sorbitol addition to E-2 composition including 0.40g of PA9 or 0.20g of PA25 (solvent-free composition of A-2) were examined. Figure 4.7 shows the resultant L and t_g for varied temperature. As sorbitol is in solid state at room temperature, the added amount is expressed by the molar ratio to Si similarly to HPAA concentration. For example, C_S=0.2 roughly

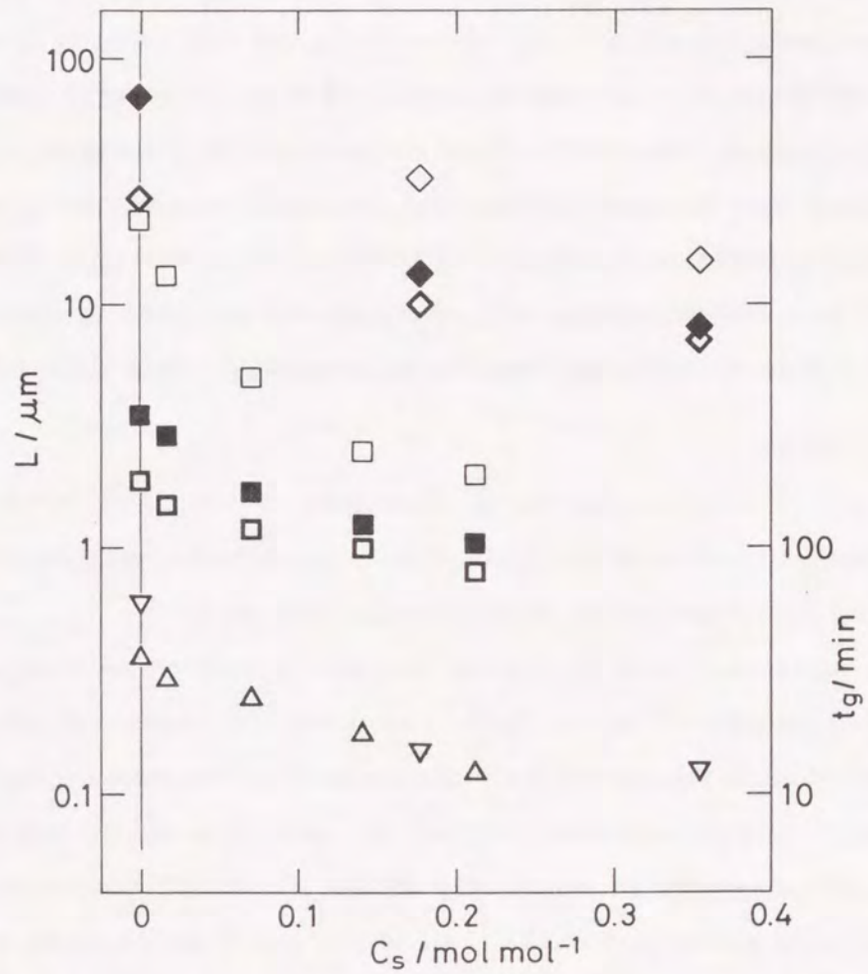

Figure 4.7 Effect of sorbitol addition to E-2 solvent composition with PA9 (C=0.177) or PA25(C=0.089). Sorbitol concentration is expressed by the molar ratio to starting TEOS. Square and triangle symbols respectively denote the average pore size L and gelation time t_g.
□ :PA9, 40°C, ■ :PA9, 60°C, ◘ , ▲ :PA9, 80°C,
◇ :PA25,40°C, ◆ :PA25,60°C, ◈ , ▼ :PA25,80°C.

corresponds to an addition of 1.20g against E-2 composition. With increasing sorbitol addition, both t_g and L gradually decrease and the effect is more marked at lower temperature. In other words, the difference in L with T becomes smaller with an addition of sorbitol, which is similar to the effect of formamide shown in Figure 4.6. When compared by the normalized addition weight, sorbitol is far more effective than formamide in reducing t_g and L. The important reason why sorbitol exhibited such an outstanding effect may be that it has high compatibility with water, alcohols and HPAA because of its highly hydrogen-bonding polar character as discussed in Section 4.3.1.

4.4 CONCLUSIONS

(1) The size of interconnected porous morphology of silica gels prepared by the polymer-incorporated sol-gel process could be controlled with additions of various organic solvents in an extended length scale range.

(2) Finer morphology could be obtained with the solvents which decrease the segregation tendency of HPAA. Among them those also accelerated the polymerization of silica resulted in less concentration- or temperature-dependent morphology. Coarser morphology resulted with those increase the segregation of HPAA, the concentration dependence of gel morphology became stronger with decreasing polymerization rate. All of the above results could well be explained by treating the polymer-containing gel-forming systems as analogous to the immiscible glass-forming melts subjected to various rates of cooling.

(3) Sorbitol was found to be the most effective additive among those investigated in preparing finer morphology with the present HPAA-containing system due to its ability to accelerate polymerization of silica and high compatibility with other constituents.

SUMMARY OF CHAPTER 4

The effects of additions of various organic solvents on the porous gel structure have been investigated for the acid catalyzed systems containing polyacrylic acid (HPAA) and tetraethoxysilane(TEOS). The changes in the segregation tendency of HPAA and in the polymerization rate of silica influenced the overall phase separation and gelation process. The efficiency of additional solvents which reduce the segregation strength and accelerate polymerization, such as formamide, to form interconnected structure in an extended composition range has been demonstrated.

REFERENCES

[1] G.Orcel and L.Hench, *J. Non-Cryst. Solids*, **79**(1986), 177-194.

[2] G.Orcel, L.L.Hench, I.Artaki, J.Jonas and T.W.Zerda, *J. Non-Cryst. Solids*, **105**(1988), 223-231.

[3] I.Artaki, T.W.Zerda and J.Jonas, *J. Non-Cryst. Solids*, **81**(1986), 381-395.

[4] A.Yasumori and M.Yamane, *Phys. Chem. Glasses*, **30**(1989), 193-201.

[5] S.Wallace and L.L.Hench, in "*Better Ceramic Through Chemistry*" eds. C.J.Brinker, D.E.Clark and D.R.Ulrich (North Holland, N.Y., 1984), 47-52.

[6] H.Rosenberger, H.Burger, H.Schutz, G.Scheler and G.Maenz, *Zeitschrift fur Physikalische Chemie Neue Folge*, **153**(1987), 27-36.

[7] R.J.P.Corriu, D.Leclercq, A.Vioux, M.Pauthe and J.Phalippoou, in "*Ultra-structure Processing of Advanced Ceramics*", eds. J.D.Mackenzie and D.R.Ulrich (Wiley, N.Y., 1988), 113-126.

CHAPTER 5

ACID-CATALYZED SYSTEMS CONTAINING SODIUM POLYSTYRENE SULFONATE

5.1 INTRODUCTION

In the preceding chapters, examined were the effects of various preparation parameters on gel morphologies formed through spinodal phase separation in alkoxy-derived silica systems containing polyacrylic acid (HPAA). Since the water-soluble polymers having strong ionic character exhibit very poor solubility against alcohols, the phase separation and gelation behavior with such kind of polymer is expected to be different from that in HPAA-systems. In this chapter, the composition and molecular weight ranges of sodium polystyrene sulfonate (NaPSS) which result in the interconnected structure have been specified for tetramethoxysilane(TMOS)-based system, and the variations of their periodic size with several compositional parameters and reaction temperature are extensively investigated.

5.2 EXPERIMENTAL

Tetramethoxysilane (TMOS), product of Shin-Etsu Chemical Co., was used as received. NaPSS aqueous solutions having the molecular weight range between 10,000 and 30,000 (coded as PS1), 50,000 and 100,000 (PS5), 400,000 and 600,000 (PS50) were kindly supplied by Toso Co. The sample codes, molecular weights, viscosity and solution pH's are shown in Table 5.1. Nitric acid was used as a catalyst for hydrolysis.

As has been reported previously[1], dropwise addition of NaPSS aqueous solution to TMOS-methanol solution sometimes results in the temporal formation of polymer precipitates. In order to assure the homogeneous mixing and better reproducibility, the following procedure was chosen to prepare the starting solutions. First, the NaPSS aqueous solution was diluted to an

Table 5.1: Properties of NaPSS

Sample Code	Mol.Wt. $x10^{-4}$	$\eta x10^3$/Pa s*1	pH*1
PS 1	1 - 3	6.9	8.3
PS 5	5 - 10	25	8.0
PS 50	40 - 60	480	8.0

*1: Viscosity η and pH's are for 20wt% aqueous solutions at 25°C.

Table 5.2: Typical Starting Compositions (unit: g)

	NaPSS	WATER	62%HNO_3aq.	Methanol	TMOS
S-1	Var.*1	5.0	0.51	--	5.15
S-2	PS5 1.30	5.0	0.51	Var.*1	5.15
S-3	PS5 1.30	Var.*1,2	Var.*1,2	--	5.15
S-4	PS5 1.30	5.0	Var.*1	--	5.15

*1: Varied in appropriate ranges shown in Figure Captions.
*2: The molar ratio of HNO_3/H_2O was kept constant at 0.0173.

appropriate concentration and nitric acid was added at the same time. Methanol was also added in some cases. Then TMOS was mixed with the above solution in a short time. Typical starting compositions are listed in Table 5.2. Under vigorous stirring, the hydrolysis reaction started in a few seconds accompanied by heat evolution. For the purpose of avoiding evaporation loss, the container was closed and sealed immediately after the addition of TMOS. After stirring for 5 min, the solution was kept at 40 and 60°C in the sealed container. After gelation, the sample was aged at the same temperature and immersed in distilled water for more than 10h to rinse off the organic phase, finally dried at 60°C.

All samples were dried at 60°C before the morphology observation with SEM (S-510, Hitachi Co.). The as-observed periodic size was used for comparison because the drying shrinkage ratios were almost the same among the samples with SEM detectable morphology (see Table 5.3).

Light scattering (LS) experiments have been performed for the selected reacting solutions in order to assure the phase separation mechanism. The measuring apparatus was the same as that described in Chapter 1.

5.3 RESULTS

5.3.1 Sol and Gel Formation

As described in the experimental section, the hydrolysis reaction started few seconds after mixing. Even in the case of no methanol addition, the solution gave heterogeneous appearance for only first few seconds.

The appearance of the solution thus prepared changed in several different ways during the polymerization period. The solutions containing very small amount of NaPSS showed no change in their transparency even after gelation, however, some turned translucent or opaque after several days' or weeks' drying. These kind of gels had no pores observable by SEM (> 20nm).

With an increasing NaPSS content, after the formation of transparent gels the eventual increase in translucency was observed, and the final extent of translucency increased with NaPSS content. These gels often gave submicron-range porous structures. The solutions containing relatively large amount of NaPSS turned turbid before the systems lose their fluidity. Among the samples which turned turbid, some showed supernatant and sedimentary layers before gelation and the others gelled without particular change in their appearance. In the former case, the sedimentary layer lost its fluidity shortly after the phase separation while the supernatant required longer time to gel. The samples which gelled without macroscopic phase separation exhibited micron-range (up to 100μm) structures including interconnected pores and skeletons, particle aggregates and isolated pores as listed in Table 5.3.

Table 5.3 also shows that times required for the emergence of turbidity (t_t) and for gelation (t_g) are strong functions of NaPSS molecular weight and concentration. With relatively small amounts of NaPSS addition, t_g increases from that of NaPSS-free reference solution. Acceleration of gelation is observed with further increase of NaPSS and becomes significant when the turbidity emerges before gelation. This suggests that the domain formation due to phase separation certainly affects the overall gel-formation process. Detailed SAXS studies concerning this kind of acceleration of silica gel formation by the phase separation are described in detain in the next chapter and those for colloidal silica systems are reported elsewhere[3].

After gelation, syneresis has been observed in all the samples during the aging period, resulting in the linear shrinkage about 90%. NaPSS phase was extracted from the aged gel pieces by immersing them in distilled water. No serious fracture of the wet gel monoliths was observed, and the translucent gels gradually increased their opacity during the immersion due to dissolution of organic phase.

Table 5.3: Time required for emergence of turbidity (t_t) and gelation (t_g) at 40°C, linear shrinkage ratio (l/l_0), appearance and SEM-observed morphology after drying at 60°C for samples prepared with varied NaPSS concentration. Starting composition is S-1 in Table 2.

NaPSS(g)	C	t_t(min)	t_g(min)	l/l_0(%)	Appearance	Morphology
PS1						
0.40	0.057	--	162	56	Translucent	Homogeneous*1
0.80	0.115	--	177	55	Translucent	Homogeneous*1
1.20	0.172	--	170	55	Translucent	Homogeneous*1
1.50	0.215	165	165	61	White Opaque	Isolated Pores
1.60	0.230	145	158	61	White Opaque	Isolated Pores
1.70	0.244	130	148	61	White Opaque	Isolated Pores
1.80	0.258	110	138	61	White Opaque	Interconnected Pores
PS5						
0.60	0.086	--	153	56	Translucent	Homogeneous*1
1.00	0.143	145	145	55	Translucent	Homogeneous*1
1.10	0.158	130	138	59	White Opaque	Isolated Pores
1.20	0.172	120	130	59	White Opaque	Interconnected Pores
1.30	0.187	100	122	60	White Opaque	Interconnected Pores
1.40	0.201	80	120	65	White Opaque	Particle Aggregates
PS50						
0.40	0.057	--	148	55	Translucent	Homogeneous*1
0.80	0.115	135	135	61	White Opaque	Continuous Pores
1.00	0.143	100	130	64	White Opaque	Particle Aggregates
1.20	0.172	80	105	64	White Opaque	Particle Aggregates
Reference						
0	0	--	145	54	Transparent	Homogeneous*1

*1: Pores larger than 20nm were not observed.

5.3.2 Development and Freezing of Periodic Domains in Gel-Forming Solution Evidenced by Light Scattering Measurement

Figure 5.1(a) shows the time evolution of LS profiles for the gelling solution which gave the gel morphology as shown in Figure 5.1(b) after drying. In very early stages, the peak intensity grew almost exponentially accompanying the peak shift toward smaller q. Then both the growth and shift of the peak gradually slowed down, and finally only the peak intensity increased at the fixed peak position. These evolutions of LS profile indicate the development of periodic domains from initially homogeneous solution and subsequent freezing of the structure by gelation. The above results possibly suggest the occurrence of spinodal phase separation in parallel to the gel-formation although further confirmation will be desirable. If the whole domain formation process is diffusion-controlled, i.e. the nucleation-growth occurs, the growth rate will monotonically decrease in such gel-forming systems due to the increasing restriction to the diffusional motion.

The periodic size of dried gel determined by the SEM observation (4μm) corresponded well with that calculated from the peak position in LS pattern of the as-gelled sample (5μm) and the linear drying shrinkage ratio (80%). Therefore, the periodic structures observed under SEM for dried gels are considered to directly reflect the wet gel structures originating from those in phase-separating solutions. It was also confirmed that the immersion in water had no effect on the micron-range morphology of the solidified gels on drying, and TG-DTA measurements proved that more than 90% of NaPSS removal after the immersion treatments.

5.3.3 Effects of Molecular Weight of NaPSS and Reaction Temperature

Figures 5.2 and 5.3 show the variations in the morphology of resultant gels with concentration of PS5 expressed by C, the molar ratio of monomeric units of NaPSS to TMOS in the starting solution. The catalyst concentration,

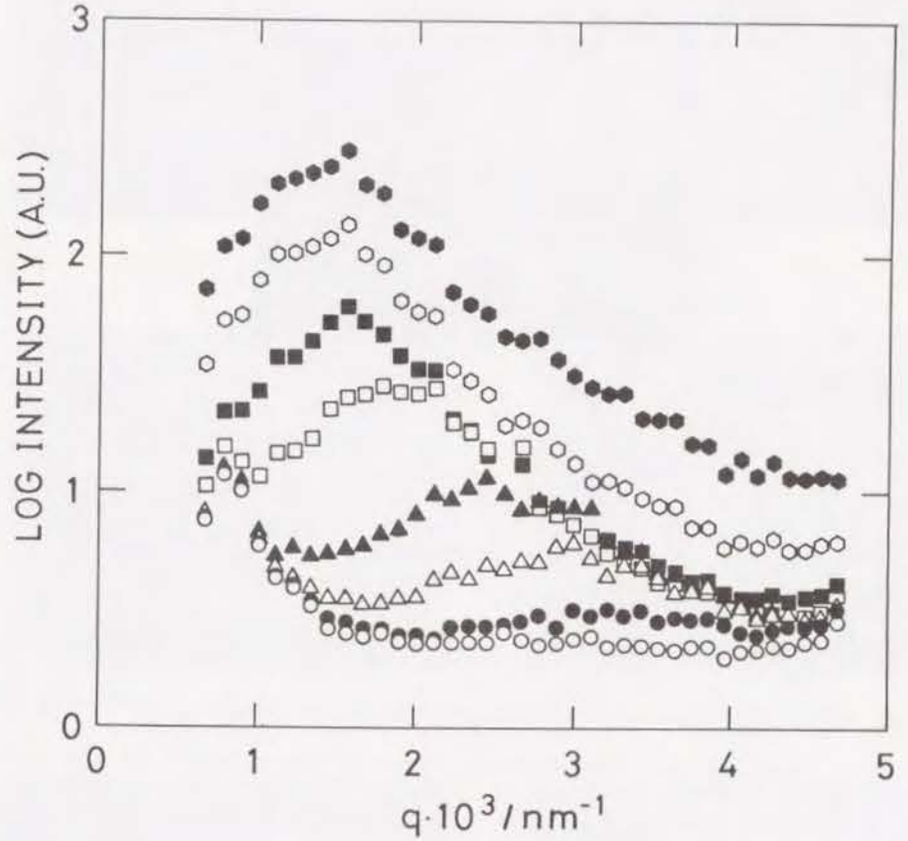

Figure 5.1(a) Time evolution of LS profile of gelling solution at 40°C. Solution composition is S-1 with C=0.172. The abscissa is scattering vector, $q=(4\pi/\lambda)\sin(\theta/2)$ where λ is wavelength of incident beam, and θ is scattering angle. The scattering vector and intensity were respectively corrected for refractive index and turbidity. Time zero was arbitrarily chosen;
○:initial, ●:20s, △:40s, ▲:60s, □:100s, ■:140s, ○:300s, ●:600s.

Figure 5.1(b) SEM photograph of dried gel piece used in the light-scattering experiment. I/I_0 was 80% in this piece.

water to TMOS ratio were kept constant at S-1 composition shown in Table 5.2.

At both temperatures the interconnected morphology with well-defined periodicity was obtained. The periodic size, L, represented by the thickness of the skeleton or diameter of the aggregated spheres measured from the photographs are plotted against C as Figure 5.4. The steep increase of L with C in more than two orders of magnitude can be recognized with only 20% increase in C at 40°C. The L increases with C in an upward concave manner in logarithmic scale which implies the explosive increase at higher C values. Though at 60°C the dependence of L on C is weaker and the maximum size of interconnected structure decreases, the upward concave nature of L vs. C remains the same. At both temperatures, the higher C than those plotted in the figures resulted in the aggregates of spherical silica particles to those shown in Figure 5.2 (f) and Figure 5.3 (e) with their size almost independent of C.

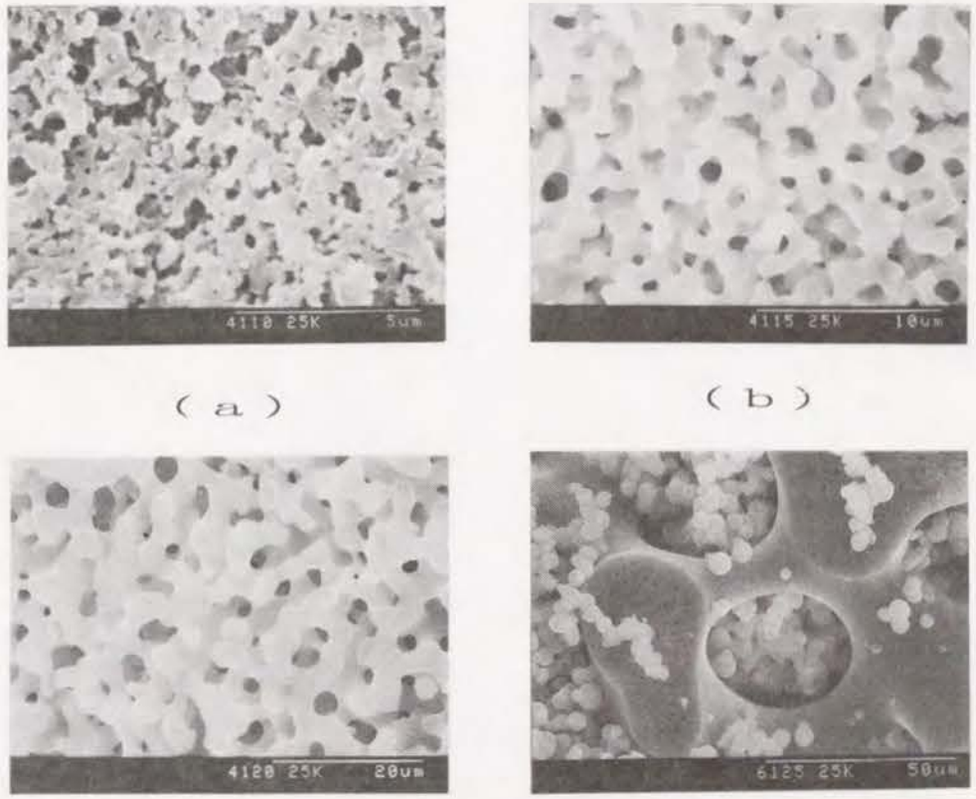

(a) (b) (c) (d) (e) (f)

Figure 5.2 Variations in gel morphology of PS5-system with C at 40°C. (a) C=0.158, (b) 0.165, (c) 0.172, (d) 0.179, (e) 0.187, (f) 0.194.

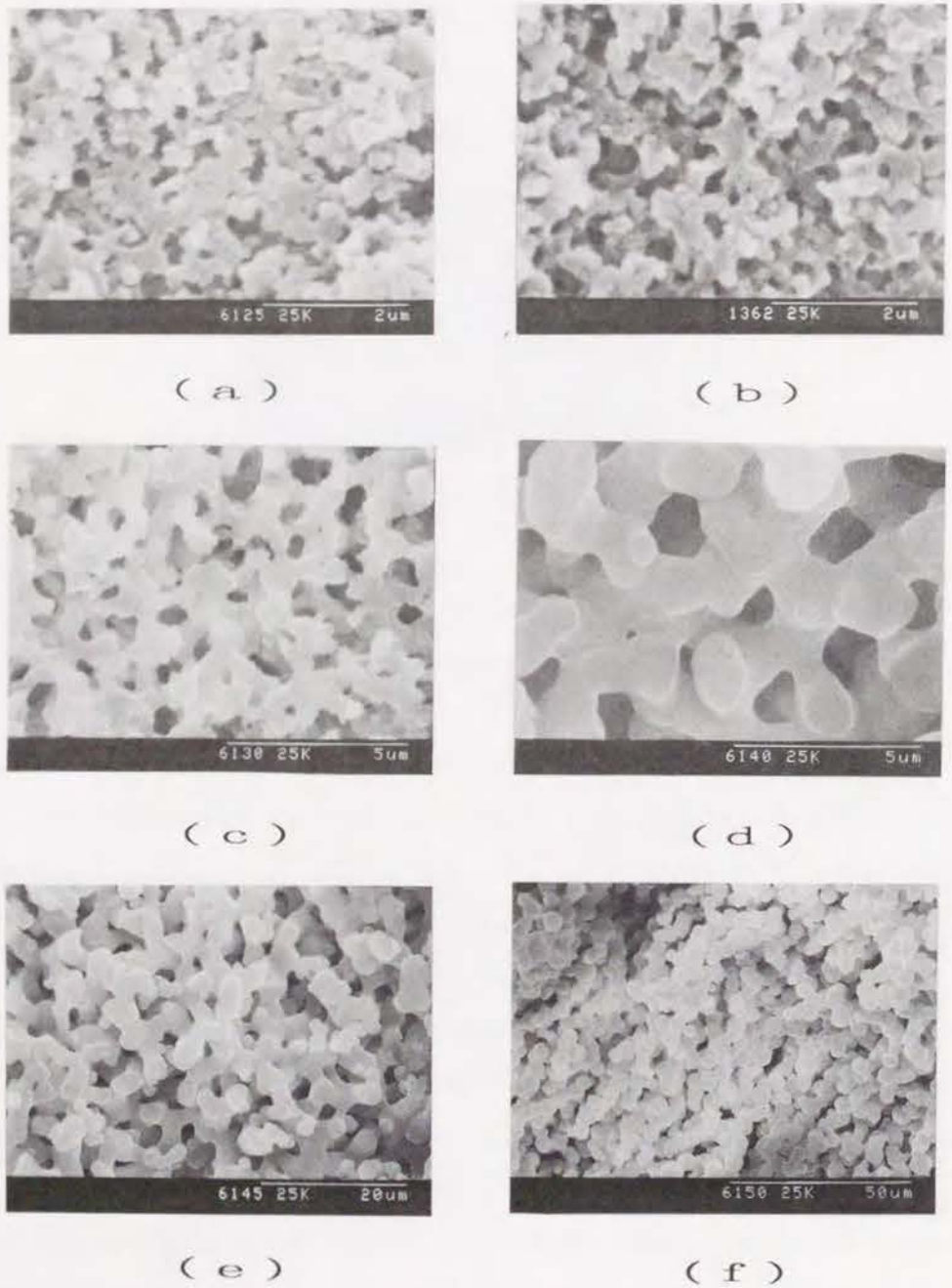

Figure 5.3 Variations in gel morphology of PS5-system with C at 60°C.
(a) C=0.179, (b) 0.187, (c) 0.194, (d) 0.201, (e) 0.208, (f) 0.215.

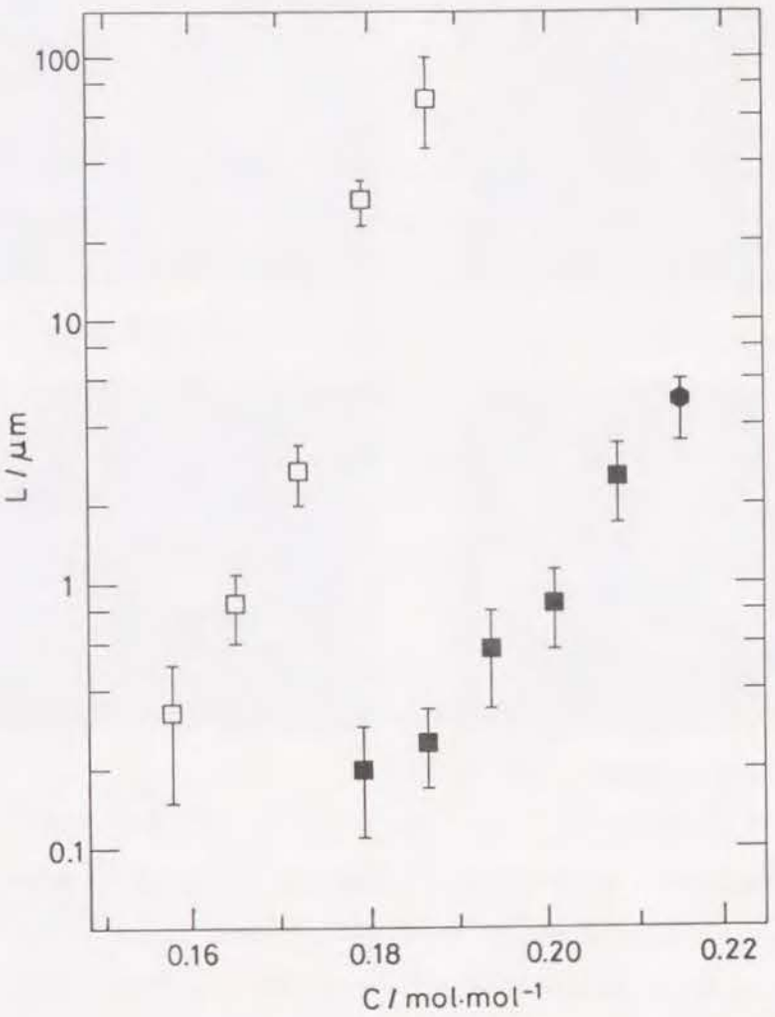

Figure 5.4 Variations of periodic size L with NaPSS content C in PS5-containing system. C is defined by molar ratio of NaPSS to TMOS in starting composition. L was directly measured from photographs; Molar ratios were fixed at H_2O/TMOS = 8.53 and HNO_3/H_2O = 0.0173 □ :40°C, ■ :60°C. Hexagon indicates the particle aggregates.

When NaPSS with higher or lower molecular weight than PS5 was used, the morphologies with isolated domains were obtained especially at lower temperature. Figures 5.5 and 5.6 show the morphology of the gels prepared from PS1-containing solution at 40 and 60°C, respectively. At 40°C, with increasing NaPSS content the volume fraction and average size of the isolated pores increased (Figure 5.5 (a) to (c)), and finally formed the interconnected structure in the length scale exceeding 100μm (Figure 5.5 (d)). Aggregated spherical silica particles could be seen between the developed silica skeletons, while isolated pores of micron-range were distributed within them. At higher C-values the solution formed sedimentary and supernatant layers before the homogeneous gelation occurred. After gelation, isolated pores in a continuous silica matrix and aggregated silica particles in micron-range were respectively observed in sedimentary and supernatant phases. On the other hand at 60°C, the interconnected structures formed (Figure 5.6) which were analogous to those seen in PS5-containing system at 40°C. The dependence of L on C for both temperatures is shown in Figure 5.7.

Figures 5.8 and 5.9 show the morphology of the gels prepared from PS50-containing solution at 40 and 60°C, respectively. At 40°C, with increasing NaPSS content the fine porous structure in 100nm range turned into the chainlike aggregates of spherical silica particles (Figure 5.8). Their average size increased with C up to ca. 3μm in diameter. At higher C-values, particle aggregates with essentially the same size and size distribution as shown in Figure 5.8 (e) were obtained. On the other hand at 60°C, the chainlike aggregates increased their connectivity to some extent (Figure 5.9 (a) to (c)), and then turned into particle aggregates with their size smaller than those at 40°C (Figure 5.9 (d)). The dependence of particle size or thickness of skeleton, L, on C is shown in Figure 5.10.

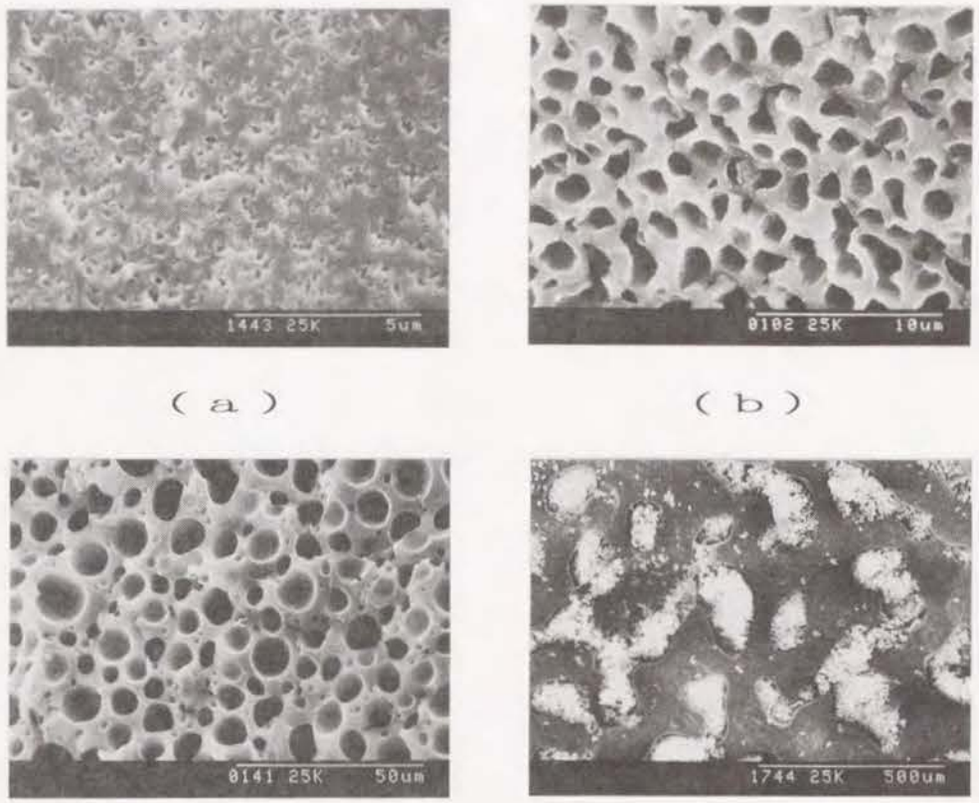

Figure 5.5 Variations in gel morphology of PS1-system with C at 40°C.
(a) C=0.210, (b) 0.224, (c) 0.243, (d) 0.249.

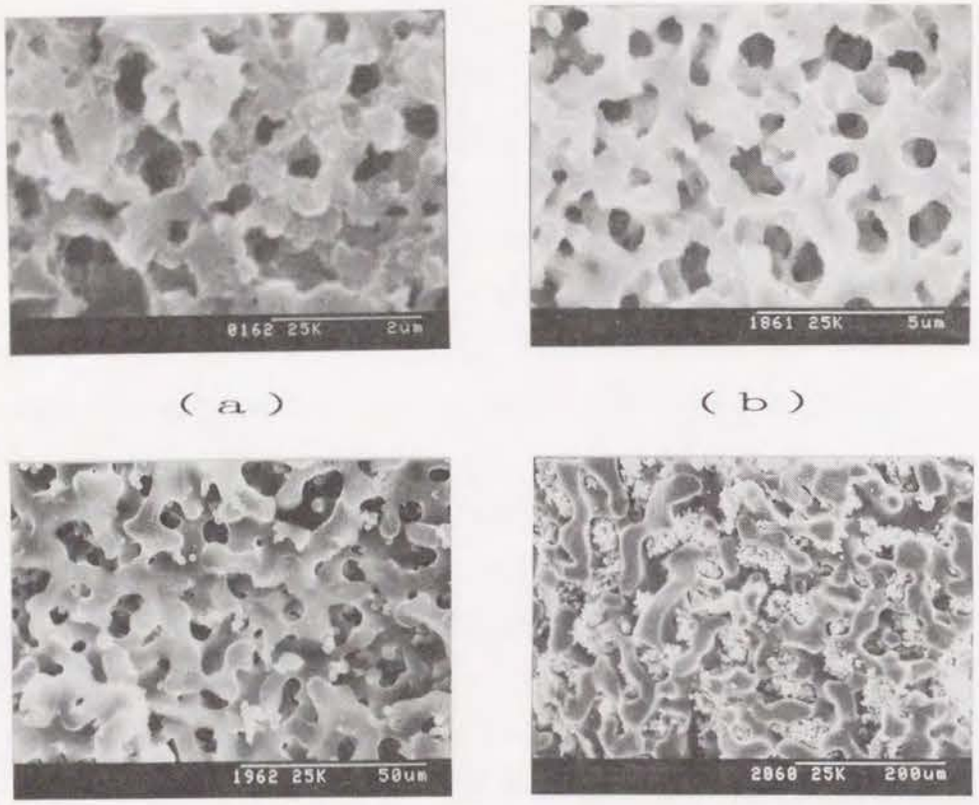

(a) (b)

(c) (d)

Figure 5.6 Variations in gel morphology of PS1-system with C at 60°C. (a) C=0.260, (b) 0.267, (c) 0.282, (d) 0.296.

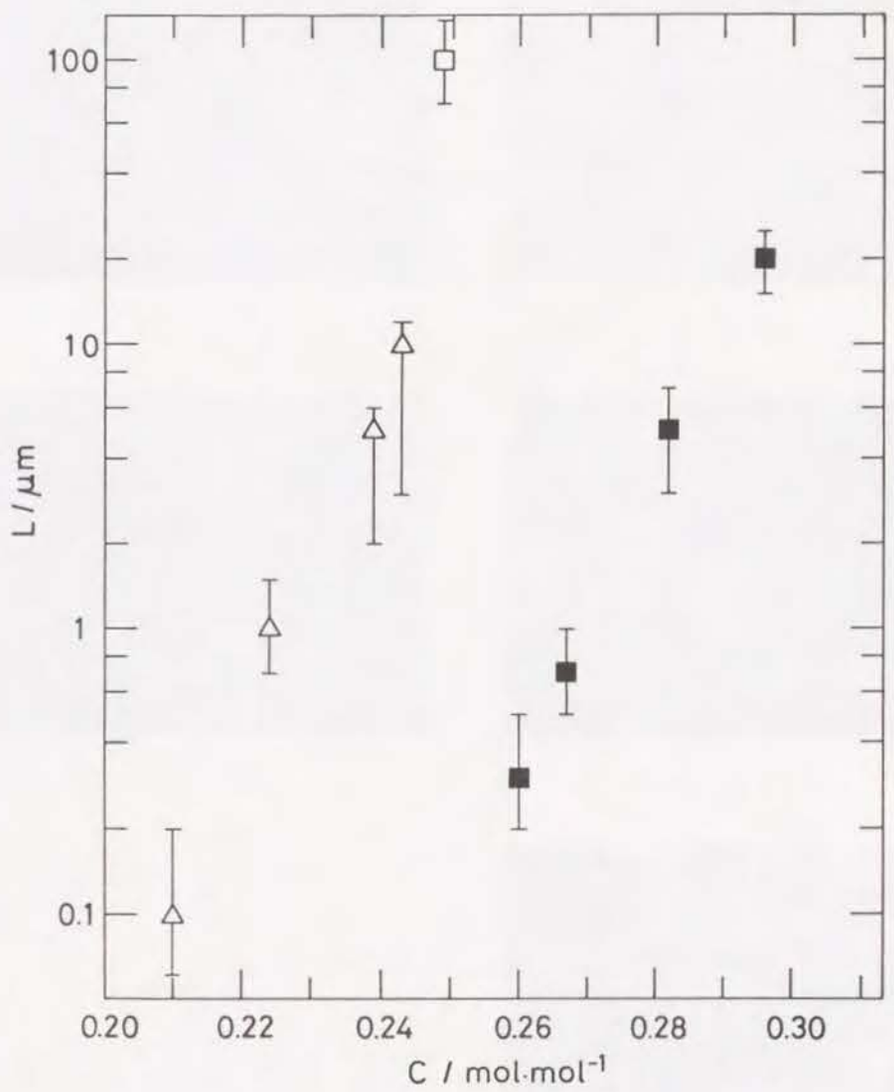

Figure 5.7 Variations of periodic size L with NaPSS content C in PS1-containing system; □, △ :40°C, ■ :60°C. Triangles indicate the morphology with isolated pores.

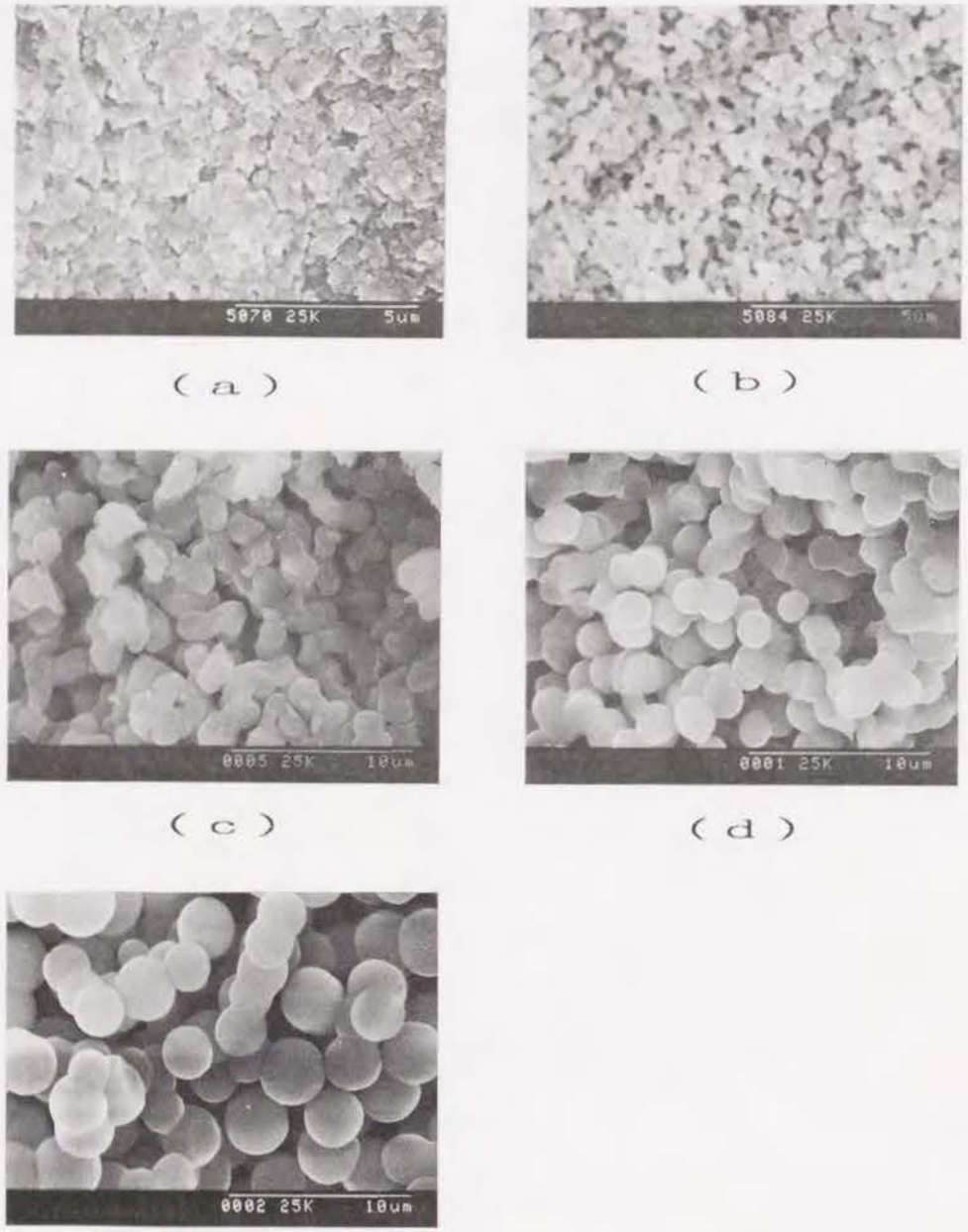

(a) (b)

(c) (d)

(e)

Figure 5.8 Variations in gel morphology of PS50-system with C at 40°C.
(a) C=0.110, (b) 0.126, (c) 0.134, (d) 0.142, (e) 0.158.

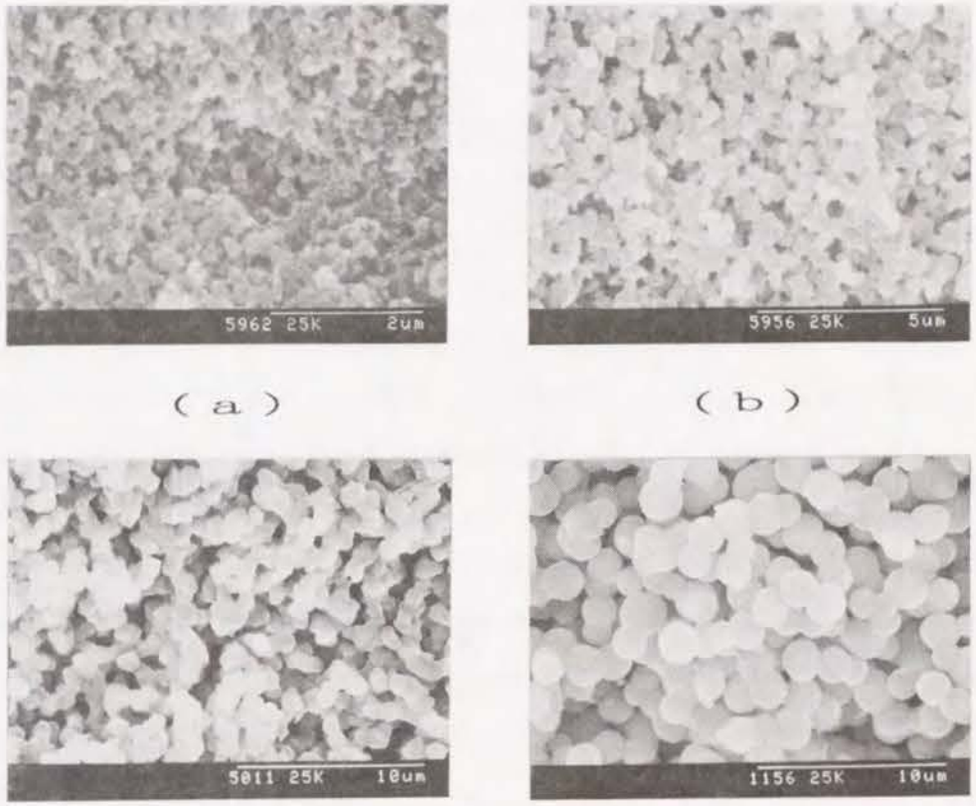

(a) (b)

(c) (d)

Figure 5.9 Variations in gel morphology of PS50-system with C at 60°C.
(a) C=0.142, (b) 0.150, (c) 0.158, (d) 0.174.

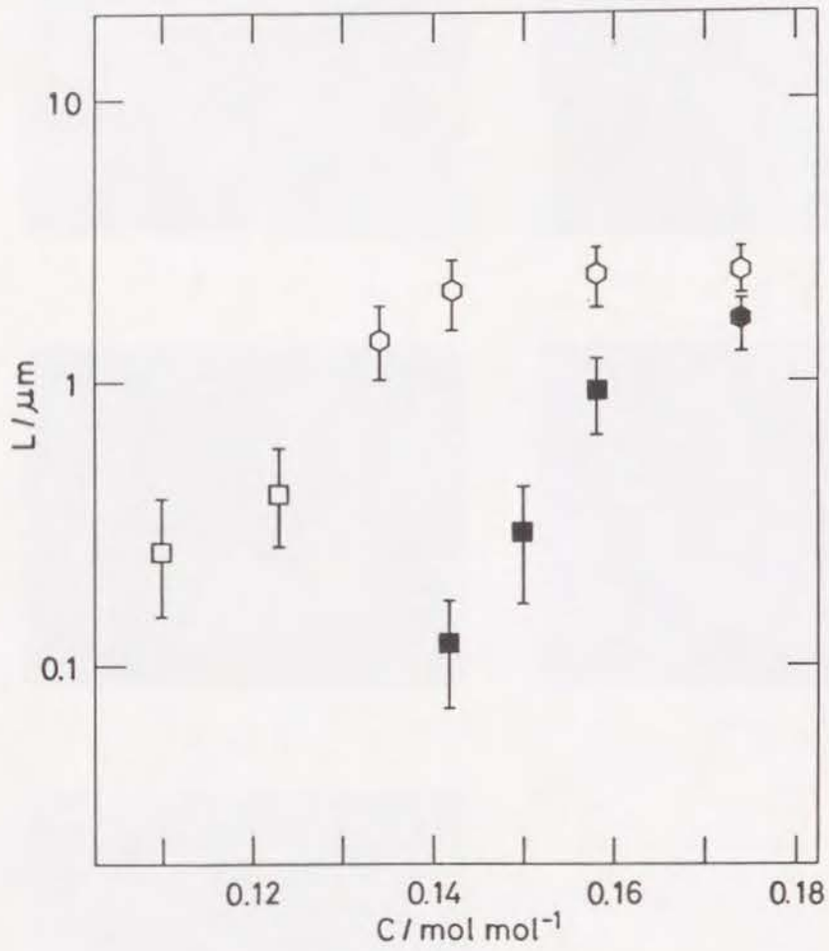

Figure 5.10 Variations of periodic size L with NaPSS content C in PS50-containing system; □, ○:40°C, ■, ●:60°C. Hexagons indicate the particle aggregates.

5.3.4 Effect of Solvent Composition

In the remaining two sections, the effects of compositional parameters except NaPSS concentration are shown for the PS5-containing system. In contrast to the catalyst concentration which is known to significantly affect the polymerization rate of silica[4], relatively small changes in the concentrations of silica, methanol and water, are expected to influence mainly on the mutual solubility of the constituents. From this viewpoint, the effects of solvent composition on the resultant gel morphology under constant acidity of water phase were investigated especially focusing on the role of water content.

For the acid-catalyzed and water-rich TMOS systems it has been confirmed by gas-chromatographic analysis that the hydrolysis and polycondensation reactions expressed as eqs. (1) and (2) are almost completed shortly after the mixing and that the concentrations of water and methanol is essentially constant until the gelation occurs[5].

$$n\mathrm{Si(OCH_3)_4} + 4n\mathrm{H_2O} \rightarrow n\mathrm{Si(OH)_4} + 4n\mathrm{CH_3OH} \quad (1)$$

$$n\mathrm{Si(OH)_4} \rightarrow n\mathrm{SiO_2} + 2n\mathrm{H_2O} \quad (2)$$

Totally, per 1 mole of TMOS, 4 moles of methanol increases and 2 moles of water decreases from the starting composition. In Figure 5.11, relations between the calculated solvent compositions and the morphology of resultant gels are shown. Since the concentration of NaPSS is fixed relative to Si, the SiO_2 concentration in the triangle is always proportional to that of NaPSS. With a small increase in the water to methanol ratio, the size of interconnected structure drastically decreased. In the case of lower water ratio, the phase separation resulted in sedimentary and supernatant layers, while in the opposite case relatively dense translucent gels were obtained.

The dependence of L on water content was examined in some more detail around the concentration range shown as S-3 in Table 5.2. Figures 5.12 and

5.13 show the changes in morphology and that of L with water content, r, the molar ratio of water to Si atoms in the starting solution. At both temperatures the decrease of L with increasing r is evident exceeding two orders of magnitude against ca. 10% change of r, and their upward concave manner is more significant than in Figure 5.4.

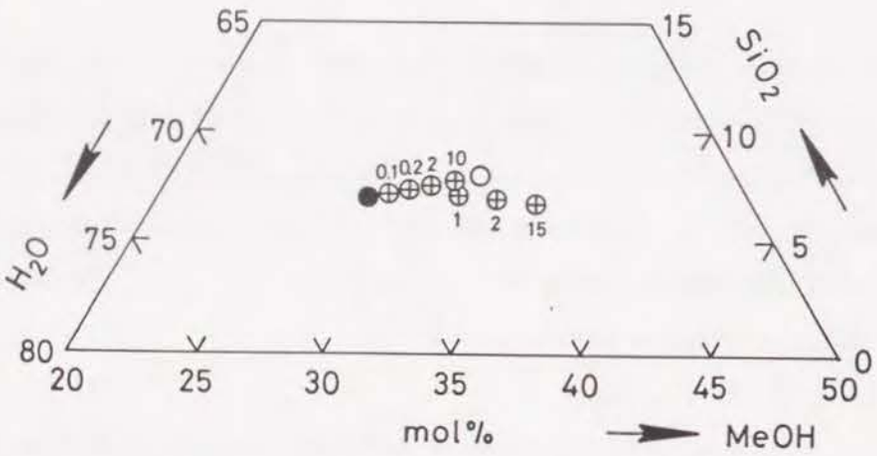

Figure 5.11 Variations of gel morphology of PS5-system with solvent composition at 60°C. Starting compositions were S-2 and S-3 in Table 5.2. C is fixed at 0.187. For the composition calculation, see text.
●:translucent gel, ⊕:interconnected structure, ○:particle aggregates.

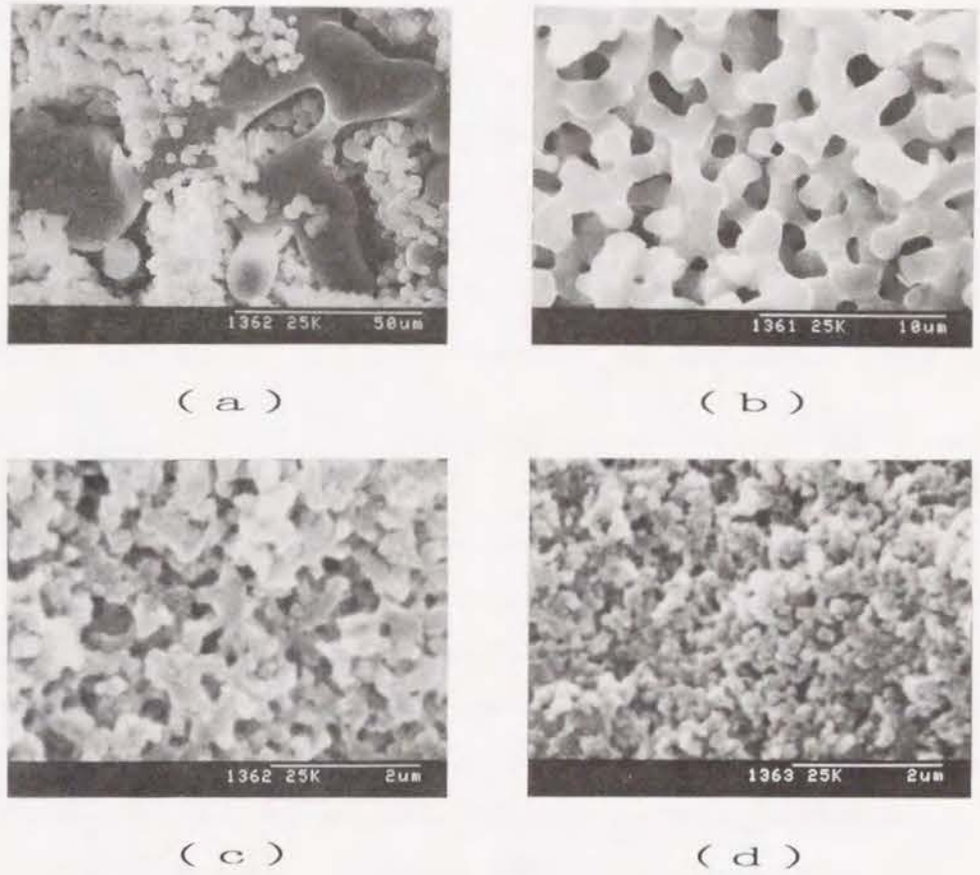

(a) (b)

(c) (d)

Figure 5.12 Variations of gel morphology of PS5-system with molar ratio of water to TMOS r, at 60°C. The molar ratio HNO_3/H_2O was fixed at 0.0173, C at 0.187 (Composition S-3 in Table 5.2);
(a) r=7.85, (b) 8.19, (c) 8.53, (d) 8.87.

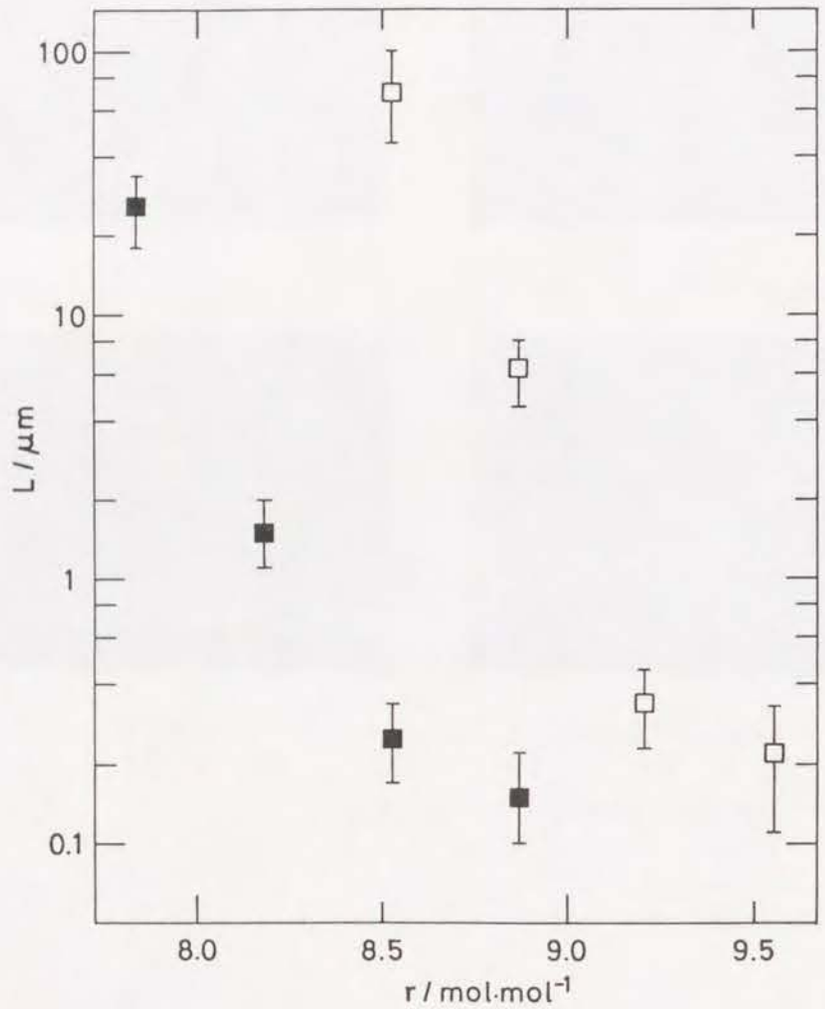

Figure 5.13 Variations of periodic size L with water to TMOS ratio r in PS5-system. Starting compositions are S-3 in Table 5.2;
□:40°C, ■:60°C.

5.3.5 Effect of Catalyst Concentration

Figure 5.14 shows the effect of nitric acid concentration on L for PS5-containing system under fixed C and the other compositions of solvent phase. At 60°C, with a decrease of nitric acid concentration, the L first increased and then decreased steeply, while t_g monotonously increased from 20min at 2.0 moldm^{-3} up to 120min at 0.1 moldm^{-3}. At 40°C, almost the same results were obtained although the gels with sedimentary and supernatant layers formed between 0.05 and 0.8 moldm^{-3}.

5.4 DISCUSSION

5.4.1 Spinodal Phase Separation in Polymerizing System

As has been discussed in detail in Chapter 1, the chemical bond can be viewed as equivalent to the attractive interaction among constituents. The "equivalent temperature T_{eq}" is defined as T_{eq}=J/β where -J and β respectively denote the interaction energy per one pair of monomers and the correlation strength between monomers, decreases as the polymerization reaction proceeds (β increases). In addition, amorphous sol-gel and liquid-glass transitions are quite similar in that both are related to the percolation of random network in three dimension. Hence, the gel-forming reaction is physically equivalent to the finite-rate cooling of glass-forming systems[7]. The cross-linked systems are ready to phase separate in the spinodal mechanism, when "cooled" either physically or chemically below the binodal temperature due to the reduced mobility[6]. The rate of polymerization determines that of T_{eq} change, thus can be regarded as the cooling rate. $T_{eq,g}$ can be compared to the glass transition temperature. The segregation strength determines the T_{eq} at which the system becomes "not-stable" in the overall polymerization process, hence it corresponds to the binodal temperature.

Even if the coexisting polymer has relatively poor solubility in solvent

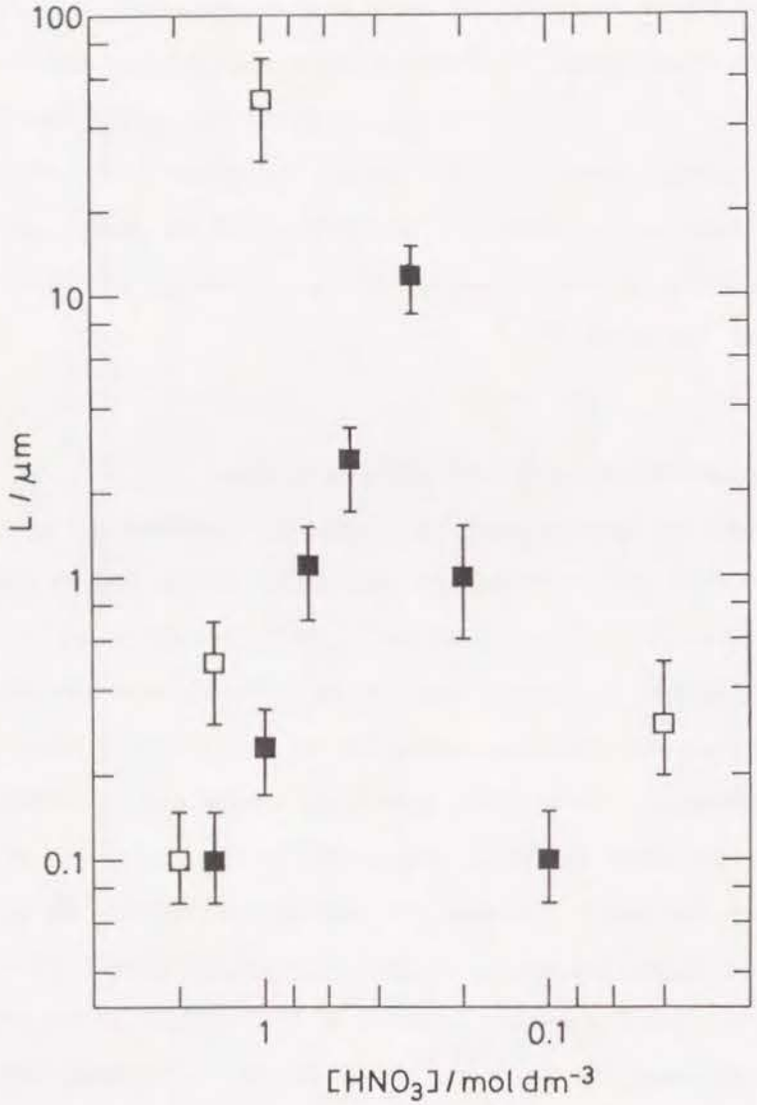

Figure 5.14 Variations of periodic size L with nitric acid concentration expressed by that in water phase; Starting compositions are S-4 in Table 5.2.
□:40°C, ■:60°C.

phase, the overall process of free-energy change with the polymerization of silica is just the same as in highly compatible systems. However, $T_{eq,b}$ changes relative to $T_{eq,g}$ far more steeply with varying compositional parameters than in, for example, HPAA-system as well as the effective quench depth will strongly depend on the polymerization rate in the case of $T_{eq,b}$ being larger than $T_{eq,g}$. As a result, the interconnected structure can be fixed as gel morphology in quite limited ranges of reaction parameters.

5.4.2 Structural Evolution of Spinodally Phase Separating System

The phase separation by spinodal mechanism proceeds in three successive stages as described in Chapter 1. It has been proved for the extremely low-mobility systems like polymer blends the initial stage is experimentally detectable[8]. Indeed, the growth of fluctuation amplitude at the fixed wavelength was observed in HPAA-system as the phase separation occurred in loosely crosslinked gel network. In NaPSS-systems, the situation changes as can be seen in the LS profile during the structure formation (Figure 5.1(a)).

In the case that the system is near the critical composition (that corresponds to the critical consolute point, i.e., a maximum of the free energy-composition curve) the interconnected (percolated) structure developed in the initial and intermediate stages of spinodal phase separation increases its periodic size without breaking up the continuity also in the late stage. For the off-critical compositions, the increase in the periodic size is followed by the breaking-up of the interconnected structure into fragments (percolation-cluster transition) in the late stage, and the breaking-up occurs earlier as the compositions deviates from the critical one at fixed temperature[9]. Therefore, when the phase separation proceeds before the gel-formation, a slight difference in the reaction parameter would be enhanced through the coarsening process in the final gel morphology. If the changes in the reaction parameter

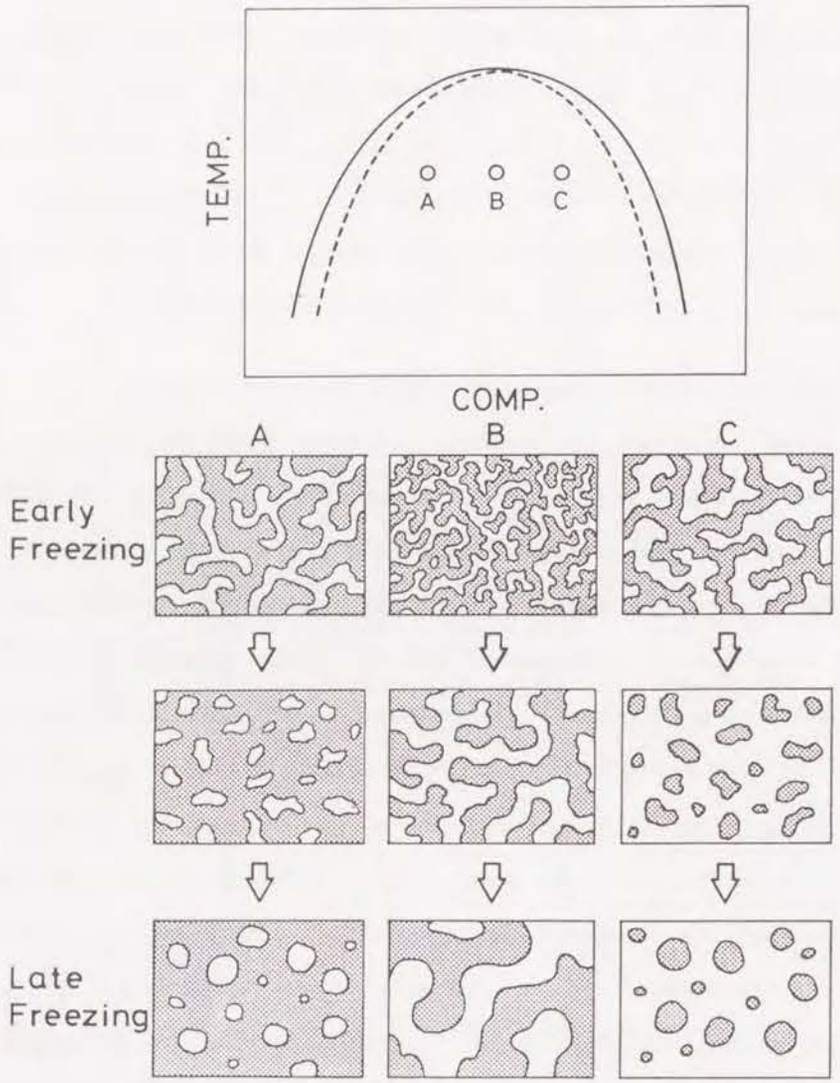

Figure 5.15 Various possible structures in the coarsening stages of spinodal phase separation. At off-critical compositions, the breaking-up of the interconnected structure (percolation-cluster transition) occurs earlier than at near-critical compositions. Earlier freezing of the coarsening structure by gelation results in the finer structure with higher connectivity.

leads the system to off-critical condition, the final structure tends to be discontinuous. It is the moment of freezing of the phase separating structure during these kind of structural evolution that finally determines the morphology of the solidified material, so that the polymerization rate also plays an important role. Figure 5.15 gives schematic correspondence of composition (quench depth), moment of freezing and resultant structure.

5.4.3 Effect of Molecular Weight of NaPSS

The present system containing PS5 as polymer component seems to lie in the near-critical condition when polymerized between 40 and 60°C with particular composition and catalyst concentration shown in Figures 5.2, 5.3, 5.6 and 5.14, where the interconnected structure is preserved in the solidified gel against the changes in various reaction parameters.

The PS1- or PS50-containing samples showed micron-range fragmented domains in the solidified gel structures (Figures 5.5 and 5.8) when prepared at 40°C. Accepted that the solutions containing PS5 corresponds to the near critical condition of the present NaPSS-silica-solvent system, PS1- and PS50-containing systems respectively fall on the NaPSS-poor and NaPSS-rich region in the miscibility gap. In other words, the respective suitable amounts of PS1 and PS50 to cause the phase separation in parallel to the gelation of the silica-rich phase ($T_{eq,b} = T_{eq,g}$) occupy substantially lower and higher volume fractions than in the case of PS5.

When the reaction temperature is increased, the above situation changes to affect the final gel morphology. It is especially evident in the case of PS1-containing system in which the interconnected structure formed instead of isolated pores in substantially higher C-range. The increased temperature improves the solubility of NaPSS as well as accelerates the polymerization reaction. The higher solubility contributes to increase the amount of NaPSS

required to cause the phase separation which accompanies the increase in volume fraction of NaPSS-rich phase, and the rapid gelation freezes the percolated structure in the earlier stage of coarsening process. Judging from the experimental results, PS1-containing system seems to be in "near critical" condition at 60°C. In PS50-containing system, on the other hand, as the increased NaPSS content leads the system further off-critical condition, only the earlier gel formation contributes to increase the connectivity within phase-separated domains in the final gel structure. And the experimental results suggest the significance of the latter effect on the connectivity between domains. For the variation of L with C in the above systems, the explanation will be given in the next section.

5.4.4 Effect of Compositional Parameters on Gel Morphology

Now we concentrate on the structural evolution in the "near critical" mixtures in which the coarsening tends not to result in the discontinuous domain formation. In the present strongly acidic system, when the phase separation occurs in weak segregation condition, the developed structures are frozen without effective coarsening by gelation due to the low mobility. On the contrary, those phase separate in a stronger segregation condition tend to be frozen after a growth of periodic size through the coarsening because the sol-gel transition occurs only near $T_{eq,g}$. Therefore, the difference in the periodic size with varying reaction conditions is more or less enlarged in the solidified gels by the incorporation of the coarsening process.

Since NaPSS is insoluble in pure methanol, the solubility limit of NaPSS decreases in a methanol-water mixed solvent as the relative water concentration (r) is reduced. In the same way, the incompatibility of the system increases as the added amount of NaPSS (C) increases. Hence, when started from the NaPSS-poor or water-rich conditions, $T_{eq,b}$ increases to approach

and pass through $T_{eq,g}$ with increasing C or decreasing r, provided that $T_{eq,g}$ is essentially unaffected by the small changes in C or r. As discussed in Chapter 1, the increase in $T_{eq,b}$ relative to $T_{eq,g}$ decreases the effective chemical cooling rate and results in the decreased quench depth which leads to the increased periodic size. At the same time, the phase separated structure will experience longer coarsening process which enlarge the periodic size before being frozen by gelation. As a result, the L increases steeply with increasing C or decreasing r.

The increased temperature accelerates the polymerization reaction as well as improves the mutual solubility of the constituents, both contribute to increase the chemical cooling rate at the fixed composition (decreased $T_{eq,b}$ relative to $T_{eq,g}$). The decrease in the slope of L vs. C with increasing temperature is attributed to the effect of the earlier freezing of the phase-separated structure by the accelerated polymerization. The above discussion on L vs. C and on the effect of temperature is also valid for the isolated and interconnected pores in PS1-containing system. In contrast, the change in the slope of L vs. C is not so remarkable in PS50-system where the domains are developed in the gel network incorporating the quite slow diffusion of higher molecular weight NaPSS chains. This suggest the possibility of controlling the coarsening process by the choice of molecular weight of polymer component, which has to be confirmed by future investigations.

Because the above variations in morphology with reaction conditions could be explained simply in terms of the solubility of NaPSS, it can be regarded as a dominant factor to determine the compatibility of the present system, which is in good accordance with SAXS results shown in the next chapter.

5.4.5 Effect of Catalyst Concentration

The catalyst concentration is an exceptional compositional parameter because it simultaneously affects both the solubility of ionic polymers and the rate of polymerization of silica more than the experimentally available range of reaction temperature does. The polymerization rate of colloidal silica is reported to be proportional to the concentration of hydronium ion below pH=2[4], and the analogous results have been reported in the alkoxy-derived systems[10]. This coincides with the fact that the observed gelation time increased with decreasing catalyst concentration. On the other hand, the degree of dissociation of ionic polymers is a function of solution pH, and is closely related to their solubility. In general, an increased dissociation leads to an enhanced solvation and increased solubility. Although the exact data are not available for the dissociation behavior of NaPSS in a strongly acidic aqueous solution, it can be reasonably assumed for the strong acid such as polystyrene sulfonate that the degree of dissociation and the solubility steeply increase with increasing pH in such a low pH range as around 1 or 2.

In the concentration range indicated in Figure 5.14, with increasing pH the polymerization rate decreases, while the solubility of NaPSS is expected to increase steeply from certain pH value. At relatively low pH condition, the pore size increases with pH reflecting the depressed chemical cooling rate while the solubility is less dependent on pH, then it abruptly starts to decrease due to the steep increase in the solubility which overcomes the decreasing polymerization rate and results in the increased chemical cooling rate due to the large decrease in $T_{eq,b}$ against $T_{eq,g}$ as discussed in the previous sections. The schematic relation between the polymerization rate and the solubility in the experimental pH range is illustrated in Figure 5.16. The quench depth of the phase-separating system is graphically expressed by the distance between two curves.

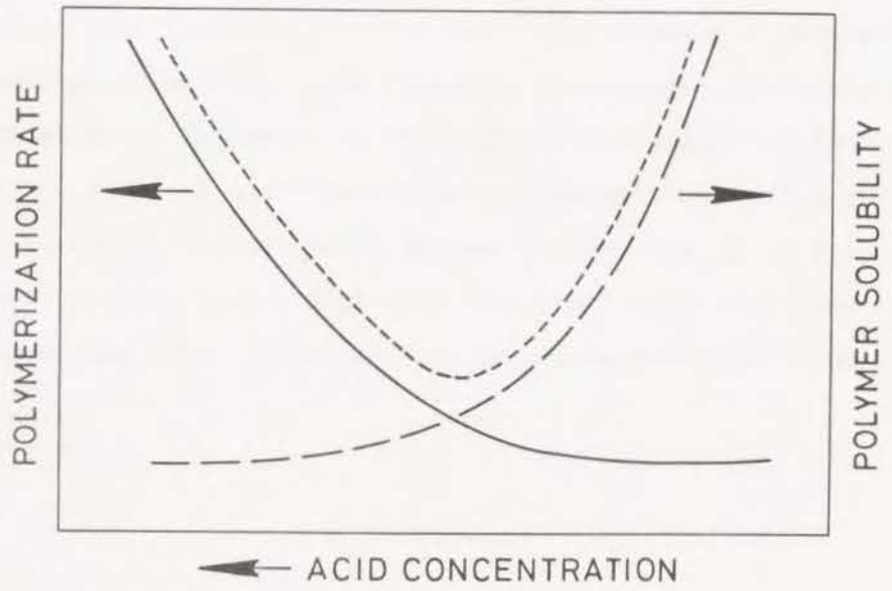

Figure 5.16 Catalyst concentration dependence of polymerization rate (solid line) and solubility (broken line) of NaPSS. The chemical cooling rate (dotted line) is high when either of the above two is high. With increasing pH from zero toward the isoelectric point, the chemical cooling rate passes a minimum which corresponds to the maximum in L in Figure 5.14.

5.5 CONCLUSIONS

(1) In the systems containing hydrolyzed TMOS and NaPSS under strongly acidic conditions, the interconnected structure was found to form as a result of spinodal phase separation induced by the "chemical cooling" of the system, which was fixed as the solidified gel structure by the subsequent gelation of silica-rich phase.

(2) The preliminary LS measurement showed that the periodic wavelength grew with time and then was "frozen" in the gel structure, which exhibited the similarity to "chemically cooled" organic polymer systems.

(3) The variation in the periodic size of interconnected structures with NaPSS and water content was well explained by their influence on the "chemical cooling rate" mainly through the solubility of NaPSS in the reacting solution.

SUMMARY OF CHAPTER 5

Phase separation which occurs in parallel to the hydrolysis and gelation of TMOS solution containing NaPSS has been investigated. Phase separated gel morphology including the interconnected structure in a length scale from 0.1 to 100μm has been directly observed by SEM. Although the effects of various reaction parameters on the gel morphology could be explained similarly to HPAA-containing systems, the dependence on any preparation condition was much stronger than that in HPAA-system reflecting the poor solubility of NaPSS in methanol-water mixed solvent.

REFERENCES

[1] K.Nakanishi and N.Soga, *J. Non-Cryst. Solids*, **108**(1989), 157-162.

[2] T.Hashimoto, J.Kumaki and H.Kawai, *Macromolecules*, **16**(1983), 641-648.

[3] H.Matsuoka, S-.R.Chen, H.Ishii, N.Ise, K.Nakanishi and N.Soga, submitted to *Bull. Chem. Soc. Jpn.*

[4] R.K.Iler, *The chemistry of silica*, Wiley, New York, 1979.

[5] M.Yamane, S.Inoue and A.Yasumori, *J. Non-Cryst. Solids*, **63**(1984), 13-21.

[6] P.G.deGennes, "*Scaling Concepts in Polymer Physics*" (Cornell University, Ithaca, N.Y., 1979), Chapter V.

[7] J.W.Cahn and R.J.Charles, *Phys. Chem. Glasses*, **6**(1965), 181-191.

[8] M.Takenaka, K.Tanaka and T.Hashimoto, *Contemporary Topics in Polym. Sci., vol. 6, Multiphase Macromolecular Systems Symposium*, W.M.Culberston ed., Plenum Press, 1989.

[9] T.Hashimoto, M.Itakura and H.Hasegawa, *J. Chem. Phys.*, **85**(1986), 6118-6128.

[10] E.J.Pope and J.D.Mackenzie, *J.Non-Cryst. Solids*, **87**(1986), 185-198.

CHAPTER 6

ANALYSIS OF POLYMERIZATION BEHAVIOR BY SMALL ANGLE X-RAY SCATTERING

6.1 INTRODUCTION

In Chapter 5, the phase separation in hydrolyzed tetramethoxysilane (TMOS) solutions containing sodium polystyrene sulfonate (NaPSS) was described. In this chapter, a system containing tetraethoxysilane (TEOS) as silica source was adopted because the applicable temperature and gelation time range could be extended compared with NaPSS-TMOS system. First, the composition range in which the analogous phase separation and gelation to those in NaPSS-TMOS system occur was determined. Secondly, the effects of several reaction parameters on the phase separation behavior were studied in detail in almost the same way as was done in the preceding works. Finally, the small angle x-ray scattering (SAXS) technique was applied to analyze the effect of coexisting NaPSS on the polymerization and phase separation processes of reacting sols in a microscopic scale.

6.2 EXPERIMENTAL

TEOS, product of Shin-Etsu Chemical Co., was used as silica source. NaPSS aqueous solutions, product of Toso Co., having the molecular weight range from 50,000 to 100,000 (PS5) was used as polymer component. Nitric acid was used as a catalyst for hydrolysis.

The sample gels were prepared as follows. First, the NaPSS aqueous solution was diluted to an appropriate concentration and nitric acid was added. In most cases the molar ratio of nitric acid to water was fixed at 0.0173 which corresponds to ca. 0.9 moldm^{-3} acidity. Then TEOS was added to above solution in a short time. Immediately the container was sealed, and after stirring for 5 min the resultant homogeneous solution was kept at con-

stant temperatures for gelation. After gelation, the gel samples were aged at the same temperature, rinsed off the organic phase with water and ethanol, and finally dried at 60°C.

SAXS measurements were carried out for the solutions of selected compositions, from just after the hydrolysis until the time of gelation. The data were collected by an apparatus equipped with a position sensitive proportional counter (PSPC), Kratky U-slit and rotating anode-type x-ray source (CuKα; λ=0.154nm)[1]. The adoption of PSPC together with relatively high scattering intensity of the samples made it possible to obtain the time-resolved scattering profiles with high accuracy.

The sample sols for SAXS measurement were prepared in exactly the same way as described above. As soon as the stirring was finished, a little portion was injected into a 1.5mm diameter silicate glass capillary. The sample cell was kept at 40±2°C in a water-ciculating thermostat during the measurements. The other portion of the sample sol was kept in a sealed vessel to gel at 40°C for SEM observation.

Scanning electron microscope (S-510, Hitachi Co.) was employed for the observation of the resultant gel morphology. Difference in the degree of shrinkage in the drying stage was neglected because the silica content of starting solutions differed less than 7% of mean value under the present experimental conditions.

6.3 RESULTS AND DISCUSSION

6.3.1 Sol and Gel Formation in Systems Containing TEOS

An effect of difference in the kind of alkoxysilane could be observed at the hydrolysis stage of the preparation process. For a few minutes after the addition of TEOS, the solution showed heterogeneous appearance, with droplets of TEOS being dispersed in the aqueous phase. Under vigorous stirring, the

size of TEOS droplets gradually became small to form emulsion with homogeneous appearance. Soon after this stage, the solution became transparent accompanied by a heat evolution. In several systems with relatively low water content, the solution once turned transparent became slightly cloudy again before the heat evolution and following re-dissolution.

Above changes in the appearance of solution suggest that the mixing and hydrolysis reaction of NaPSS-TEOS system proceed in a following sequence. (i) TEOS starts to hydrolyze from the surface of small enough droplets, (ii) Evolved ethanol improves the mutual solubility between TEOS and water in the solution, and give transparent appearance, (iii) NaPSS starts to precipitate to form fine powders with further evolution of ethanol, (iv) Polymerization of hydrolyzed TEOS evolves water and causes re-dissolution of precipitated NaPSS. As has been observed in NaPSS-TMOS system, samples with relatively low water content were observed to phase-separate from transparent solution into two liquids shortly after the stirring was finished.

The gelation behavior of sols thus prepared was almost the same as that has been reported in Chapter 5 for the systems containing TMOS. The increase in turbidity of the sol was observed either before or after gelation. The composition range in which the interconnected structure were obtained is shown in Figure 6.1 for the systems containing TMOS and TEOS with fixed molar ratio of NaPSS/Si and HNO_3/H_2O. The solution compositions were calculated assuming the complete hydrolysis and condensation of alkoxysilane species which means 2 moles of decrease of water and 4 moles of increase in alcohol per 1 mole of alkoxysilane from the starting compositions. The system containing TEOS requires about twice as much water as in the case of TMOS, reflecting the lower solubility of NaPSS in ethanol-water mixed solvent than in that of methanol-water.

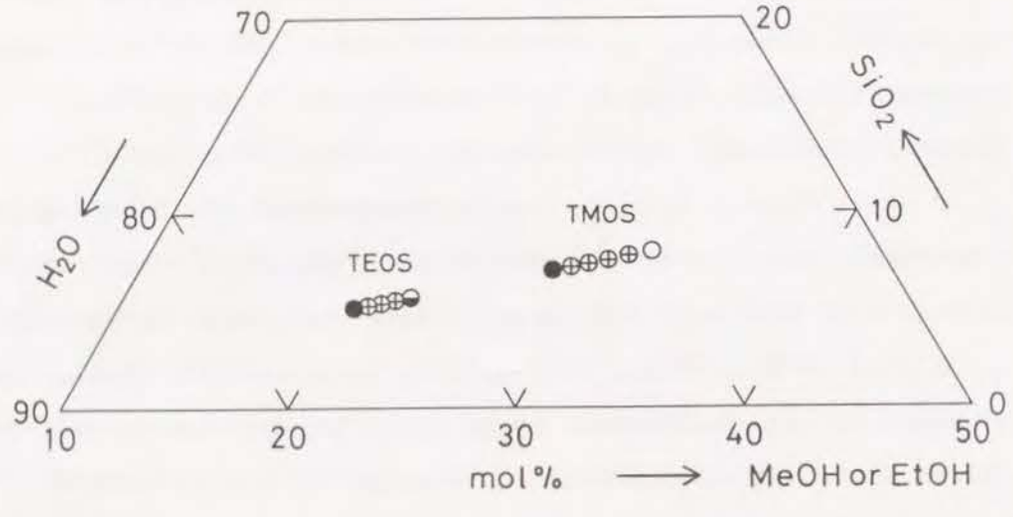

Figure 6.1 Composition ranges of gel formation with interconnected pore structure ; The moler ratio of NaPSS/Alkoxide is fixed at 0.177, HNO_3/H_2O at 0.0173 and reaction temperature at 60°C.

● :translucent gel, ⊕ :interconnected structure,

◒ :macroscopic two-phase, ○ :particle aggregates.

6.3.2 Effects of Concentration of NaPSS and Water.

Figure 6.2 shows the variation in the thickness of silica skeleton, L, with NaPSS concentration expressed by C, molar ratio of monomeric unit of NaPSS to TEOS. The molar ratio of water to TEOS, denoted by r hereafter, was fixed at 15.7, and that of catalyst to water at 0.0173. At 40°C, the dependence of L on C is the strongest and the maximum value of L exceeds 50μm. In contrast at 80°C, the L changes gently with C and the continuity of gel skeleton disappears when L exceeds 5μm.

Figure 6.3 shows the dependence of L on r, under the conditions of C≒0.186. Steep decrease in L with an increase of r can be recognized at any temperature. The formation of particle aggregates at lower r at 40°C indicates that the change in volume fractions of phase separated domains can be induced equivalently by increasing C and by decreasing r.

These results show almost similar feature to those obtained for TMOS system described in Chapter 5, although the solution composition is considerably different. At least under fixed catalyst concentration, the difference in starting alkoxide seems to affect the phase separation and gelation behavior only through the solubility of NaPSS in the solutions containing corresponding alcohols. Under strongly acidic and water-rich conditions, even less reactive TEOS is known to be almost fully hydrolyzed long before gelation[2,3], which supports the above presumption.

6.3.3 Effect of NaPSS on Polymerization of Silica Evidenced by SAXS

Due to large differences in the scattering intensity between silica and other components, SAXS measurement of the reacting solution is expected to give the exclusive information about the growth process of silica polymers out of the other components. As can be seen in Figures 6.2 and 6.3, relatively small changes in compositional parameters induce drastic changes in the

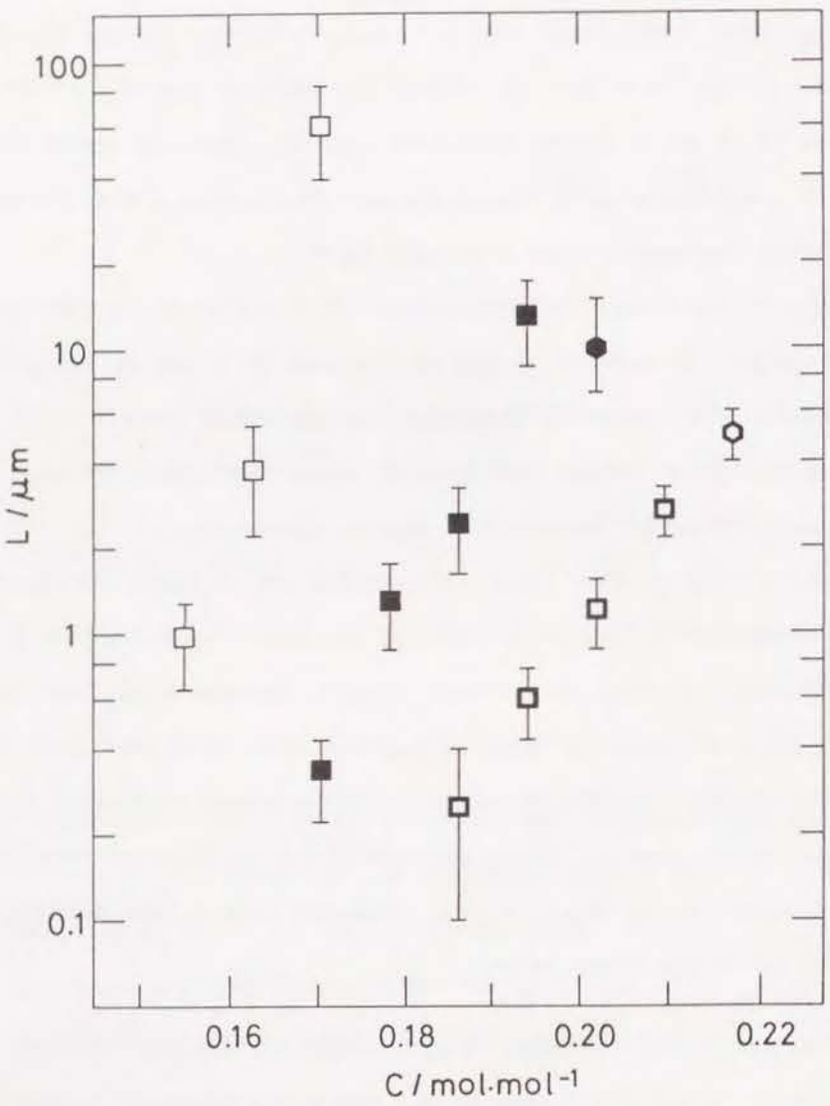

Figure 6.2 Dependence of average pore size L on NaPSS concentration C in TEOS system at different temperature. r=15.4 □:40°C, ■, ●:60°C, ◘, ✪:80°C. Hexagons indicate particle aggregates.

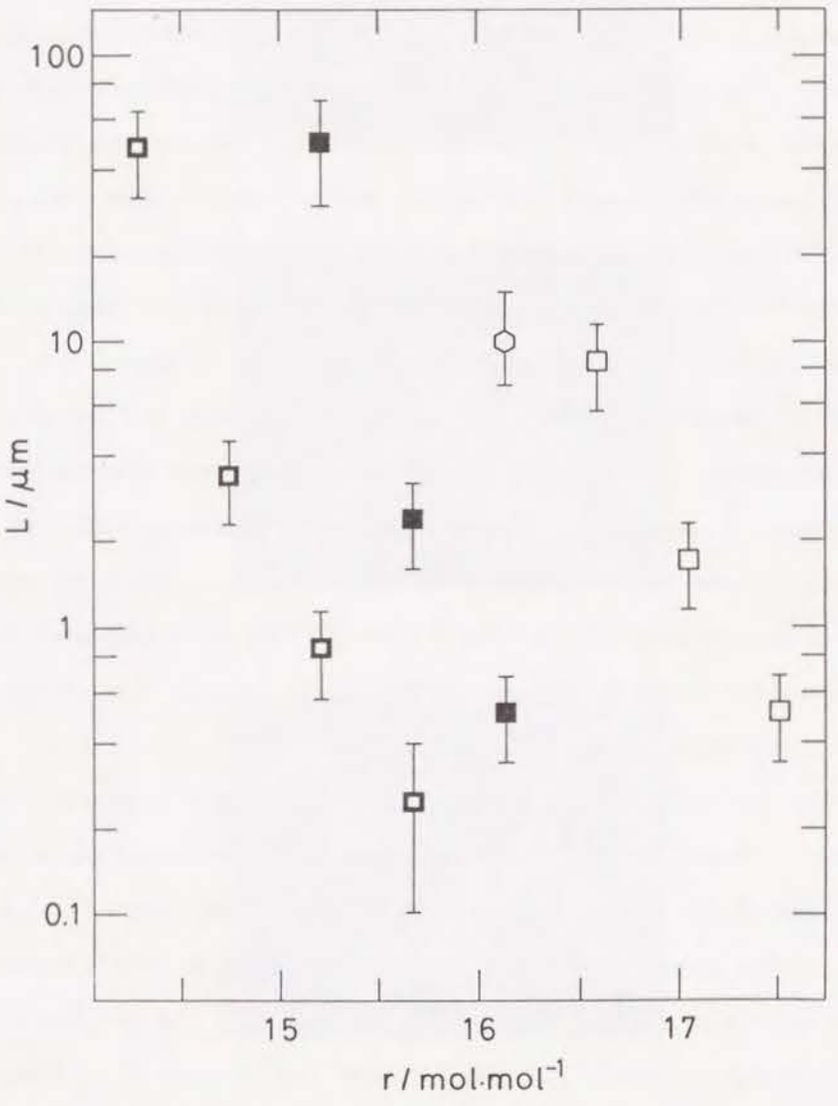

Figure 6.3 Dependence of average pore size L on water content r at different temperature. C=0.186. Symbols are the same as in Figure 6.2.

resultant gel morphology. For example at 60°C, about one order of increase in L can be realized with only 5% of increase in C or decrease in r. Generally, a large changes in C and r are thought to affect the polymerization reaction of silica by influencing the collision frequency and the chemical composition of solvent phase. However, small changes in composition itself are expected to have negligible effect in such water-rich conditions. Hence, the samples for SAXS measurement were chosen out of the NaPSS concentration range which resulted in the interconnected structure at 40°C (C1, C2, C3), while the polymer-free solution (C0) was used as a reference. Selected SEM photographs of the dried gels used in the SAXS measurement are shown in Figure 6.4.

The SAXS profiles obtained were analyzed in Guinier and Porod regions to obtain information about the radius of gyration R_g and the structure of silica aggregates, respectively. Figure 6.5 shows the time evolution of R_g of the scattering entities evaluated from the Guinier region. Since R_g estimated by scattering measurement reflects the z-averaged degree of polymerization, in the polydispersed systems R_g represents the nearly maximum size of the polymers even though their number is relatively few.

The time evolution of R_g shows different features depending on the NaPSS content. In the sample without NaPSS, as has been reported in several preceding reports[4,5], after a certain induction period R_g started to increase with an increasing growth rate, then gradually leveled off and showed little change through the sol to gel transition of the system. The samples containing moderate amount of NaPSS (C1 and C2) show the increase of R_g from much earlier stage of the reaction, and the saturated values were almost the same irrespective of the NaPSS content. The sample containing the largest amount of NaPSS (C3) showed almost analogous growth process in the initial stage, however, the saturated value was much larger possibly exceeding the detectable limit of the present measuring system.

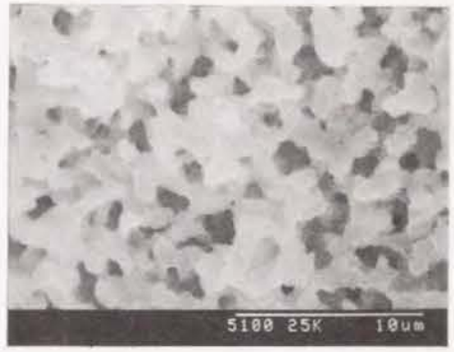

(a)

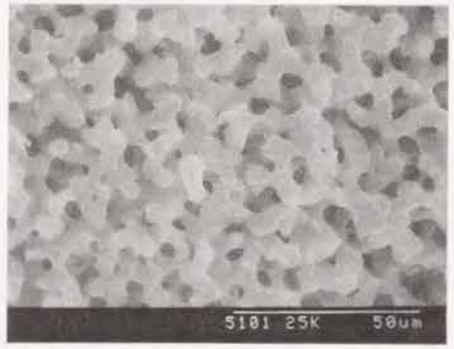

(b)

(c)

Figure 6.4 SEM photographs of dried gels prepared from the identical solutions for SAXS measurements with various amount of NaPSS at 40°C; (a) C1 (C=0.155), (b) C2 (C=0.163), (c) C3 (C=0.171).

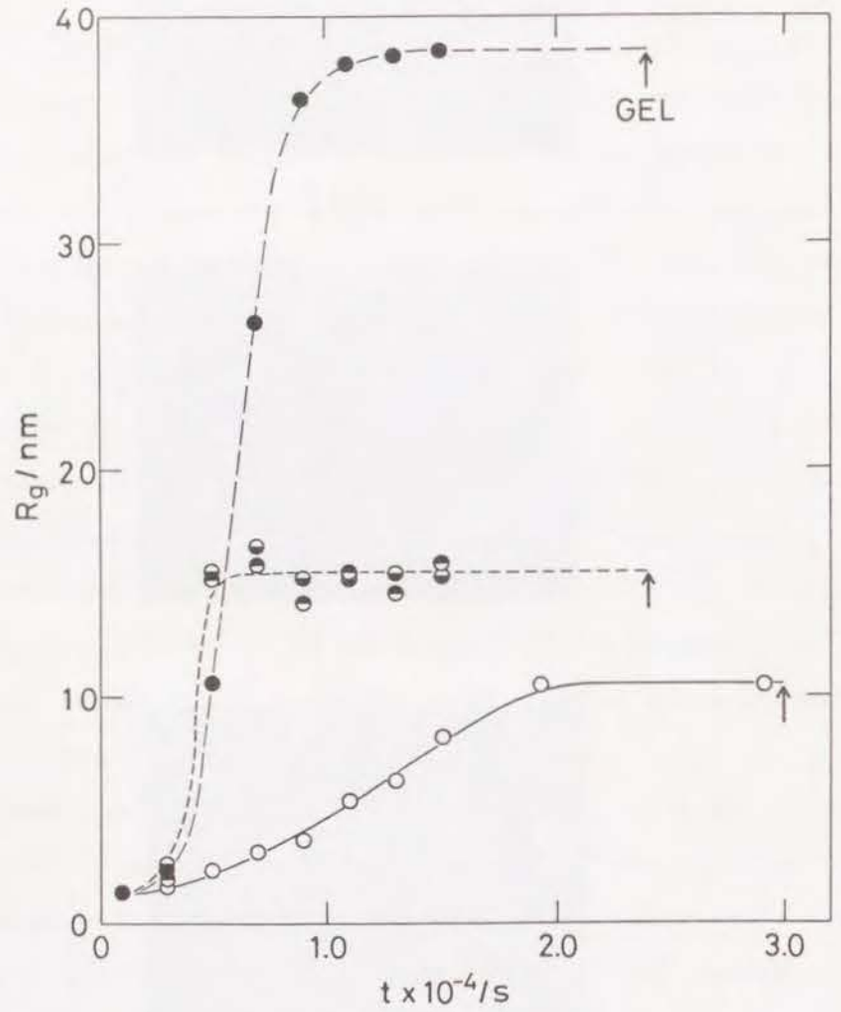

Figure 6.5 Time evolution of Guinier radius R_g for silica sols containing various amount of NaPSS at 40°C; ○:C0, ◒:C1, ◓:C2, ●:C3.

The analysis in the Porod region (power law region) also revealed the difference in growth processes. Figure 6.6 shows log-log plots of the scattering intensity against the scattering vector q at different stages of the reaction for the selected samples. The changes in the scattering profiles can always be recognized at the times which correspond to the inflection points (burst up) of R_g's. In C0 sample, linear profile (power law profile) extends towards lower q region after the moderate inflection in R_g accompanying the gradual decrease in the slope down to -2.2 as has been reported previously[4]. In the samples C1 and C2, the profiles seem to consist of relatively narrow power law portion with the slope of about -1.5 in higher q region and slightly upward convex portion in the medium q region. The power law portion shows slight extension towards low q region as polymerization proceeds, while the slopes remain almost constant. Since the apparent power of medium q range is around -1 which corresponds to no physically real three dimensional scatterers, this type of profile could better be interpreted as the scattering from significantly polydispersed system[7]. The C3 sample shows no change in the profile in high q region even after the saturation of R_g, and the relative scattering intensity in the lower q region becomes exceptionally higher than those in other samples, which is consistent with the formation of larger size (>20nm) scatterers.

6.3.4 Growth Model for Polymer-Containing System

It has been reported for the polymer-free systems that the time evolution of scattering profiles of alkoxy-derived silica shows moderate feature without abrupt change in R_g or Porod slopes irrespective of the kind of catalyst used[4,5]. An emergence of the "break" in Porod plot during gelation process has been reported in the systems of colloidal aggregation[7] or Si-Al esters[8]. With a postulation that the compactness of the structural units

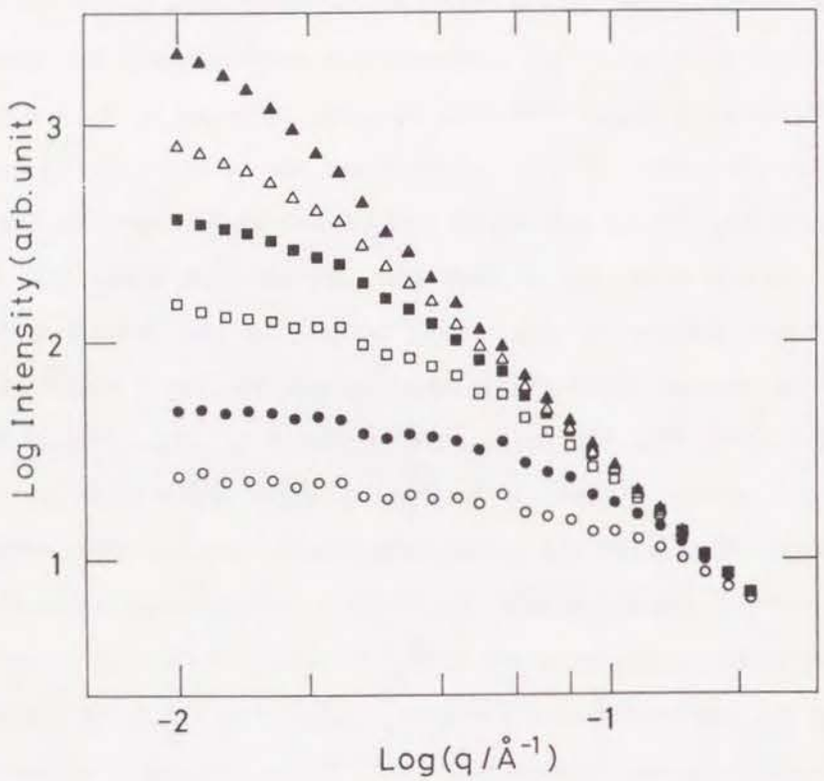

Figure 6.6(a) Time evolutions of log-log plotted scattering profiles for C0.
○ :1000s, ● :3000s, □ :5000s, ■ :9000s, △ :13000s, ▲ :19240s.

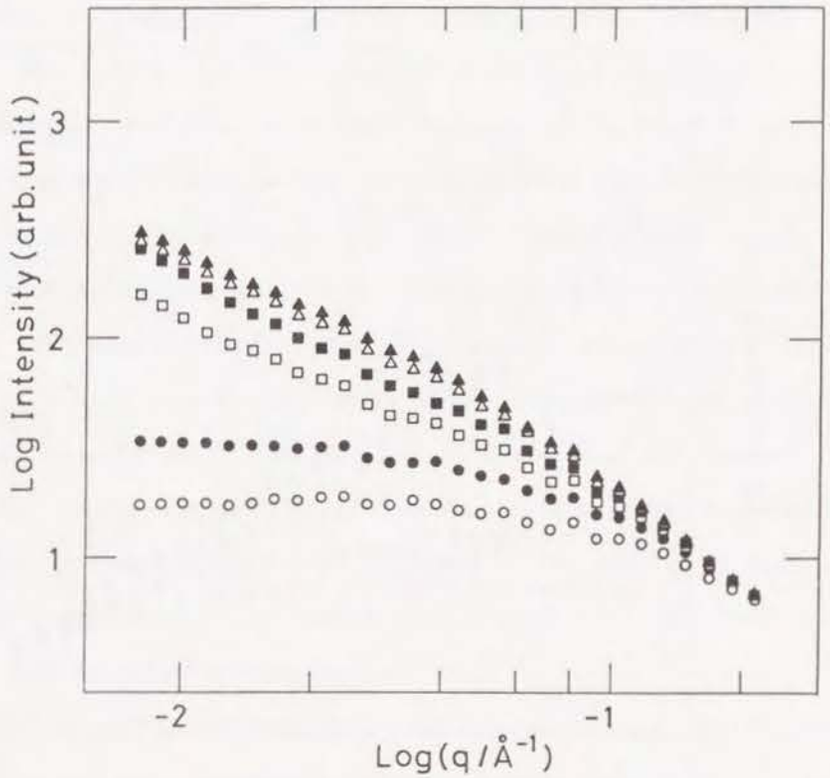

Figure 6.6(b) Time evolutions of log-log plotted scattering profiles for C1.
○ :1000s, ● :3000s, □ :5000s, ■ :7000s, △ :11000s, ▲ :15000s.

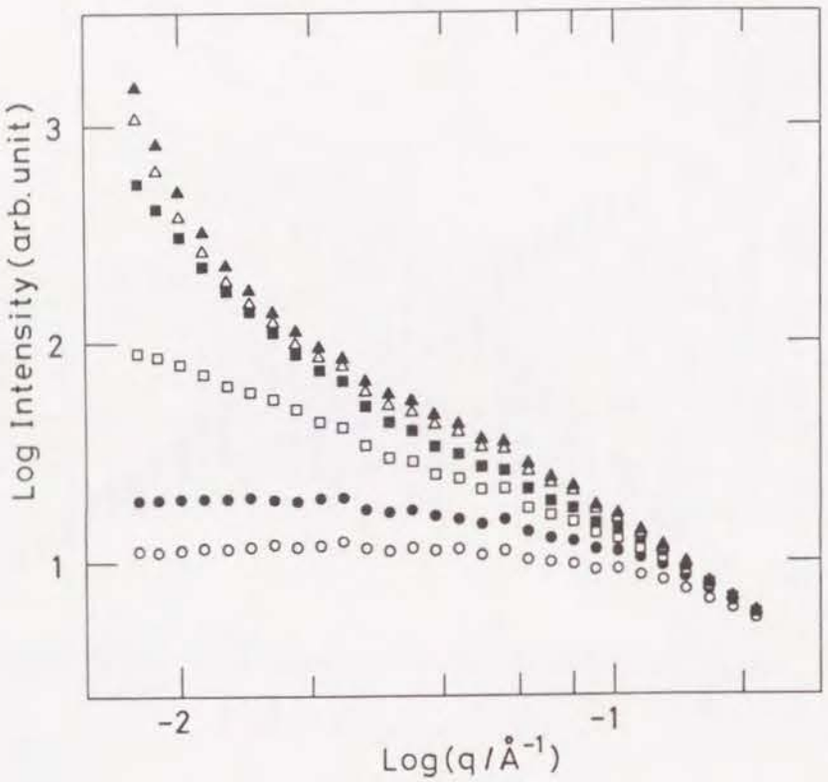

Figure 6.6(c) Time evolutions of log-log plotted scattering profiles for C3. ○:1000s, ●:3000s, □:5000s, ■:7000s, △:11000s, ▲:15000s.

having the size of corresponding q-range can be evaluated by volume fractal dimension d_v directly related to the Porod slopes α ($\alpha = -d_v$), the "breaks" are interpreted as an indication of compact clusters or particles which build up more ramified aggregations in both cases. The position of the "break" is regarded as a measure of the cluster- or particle-size. Comparing our results with the above two cases, the abrupt change in Porod profile in NaPSS containing samples is indicative of the transition of the system from that with homogeneous low molecular weight polymers to that with polydispersed agglomerated clusters. The unusually low volume fractal dimensions of 1.5 in the samples with NaPSS suggest that the initially generated structural units start to build up highly ramified and significantly polydispersed agglomerates during the system pass through such kind of transition. Gel bodies consisted of structural units with such low fractal dimensions are thought to contain substantial internal space filled with solvent and to show sensitive change in the drying process which will be reflected to the density or surface area of the dried gels. Experimental evidences of this kind of interaction between solvents are described in Chapter 7.

The polymerization behavior in the present system can be modelized as follows. In the initial stage, the primary clusters with R_g of about 1.5nm are formed in all samples just after the hydrolysis and show no marked growth. Then the clusters start to agglomerate in the following stages of polymerization, which are reflected to both the increase in R_g and the change in Porod profile. The main factor which induce instability into the homogeneous dispersion of silica clusters may be the coexistence of NaPSS molecules which are incompatible with silica clusters due to their polymeric character. That is, the system turns into microscopically two-phase, one rich in polymerized silica and the other in NaPSS. Since the volume fraction of silica polymer is still very low in the initial stage of polymerization, the agglomeration of silica is much

more likely to occur than the precipitation of NaPSS-rich droplets. This growth model can be also supported by the fact that the coexistence of NaPSS accelerates the total gelation process. The same kind of accelerated gelation by NaPSS has been observed also for other polymers and the colloidal silica system and can be explained in the same way[10].

As can be seen in the experimental results, the metastable size of agglomerates exists, which is constant for a certain range of C but probably diverges for higher C-values. The gradual change in the Porod profile observed under constant R_g indicates the eventual growth of smaller agglomerates and subsequent narrowing of the size distribution. Comparison between Figures 6.4 and 6.5 tells us that the interconnected structures free of silica particles or voids in the skeletons can be obtained from the solutions containing metastable agglomerates. This suggests that the micron-range interconnected structure in the reacting solution forms as a result of interaction between silica agglomerates and NaPSS molecules, and that under constant temperature the difference in the segregation tendency of NaPSS rather than that in polymerization rate affects the periodic wavelength determined by the chemical cooling rate. The divergent growth of R_g in C3 samples suggests that the polydispersed silica spheres stuffed in large sized interconnected structures (>10μm) at least partly result from an agglomeration reaction. The polydispersity may be related to the critical droplet formation near the spinodal of the system. More extreme case of this macro-scale agglomeration certainly causes the sedimentation of silica agglomerates having much fewer bridging bonds, which can be observed as macroscopic liquid-liquid phase separation long before the gel formation.

6.4 CONCLUSION

For the systems containing NaPSS and TEOS, analogous phase-separation and gelation behaviors to those in NaPSS-TMOS systems were observed. SAXS measurements revealed the marked difference in their polymerization process compared with a polymer-free system. It was further suggested that the formation of micron-range interconnected structure requires the existence of agglomerated silica clusters which interact with NaPSS macromolecules, and that the periodical sizes are predominantly determined by the segregation tendency of NaPSS in the reacting solution.

SUMMARY OF CHAPTER 6

Phase separation of gelling silica sols has been investigated using tetraethoxysilane as silica source for the systems containing sodium polystyrene sulfonate (NaPSS). Reported are the dependence of periodic size of interconnected structure on several important reaction variables such as solution composition and temperature. The results are compared with those of NaPSS-tetramethoxysilane systems, and an explanation in terms of the solubility of NaPSS is given for the difference in their phase separation behavior. Small angle x-ray scattering measurement of polymerizing solutions suggested the formation of highly ramified silica polymers in NaPSS-containing samples. The segregation tendency of NaPSS was found to be the dominant factor in determining the micron-range periodic size fixed in the gel structure.

REFERENCES

[1] N.Ise, T.Okubo, S.Kunugi, H.Matsuoka, Y.Yamamoto and Y.Ishii, *J. Chem. Phys.*, **81**(1984), 3294-3306.

[2] J.C.Pouxviel, J.P.Boilot, J.C.Beloeil and J.Y.Lallemand, *J. Non-Cryst. Solids*, **89**(1987), 345-360.

[3] M.Yamane, S.Inoue and A.Yasumori, *J. Non-Cryst.Solids*, **63**(1984), 13-21.

[4] T.Lours, J.Zarzyki, A.Craievich, D.I. dos Santos and M.Aegerter, *J. Non-Cryst. Solids*, **100**(1988), 207-210.

[5] D.W.Schaefer and K.D.Keefer, in "*Better Ceramic Through Chemistry*", eds. C.J.Brinker, D.E.Clark and D.R.Ulrich, Elsevir-North-Holland, N.Y., 1984), 1-13.

[6] P.J.Martin and A.J.Hurd, *.J. Appl. Crystal.*, **20**(1987), 61-78.

[7] D.W.Schaefer, J.E.Martin, P.Wiltzius and D.S.Cannell, *Phys. Rev. Lett.*, **52**(1984), 2371-2374.

[8] J.C.Pouxviel and J.P.Boilot, in "*Ultrastructure Processing of Advanced Ceramics*", eds. J.D.Mackenzie and D.R.Ulrich, (Wiley-Interscience, N.Y., 1988), 197-209.

[9] H.Matsuoka, S.-R.Chen, H.Ishii, N.Ise, K.Nakanishi and N.Soga, *Bull. Chem. Soc. Jpn.*, in press.

CHAPTER 7

PORE SURFACE CHARACTERISTICS OF MACROPOROUS SILICA GELS PREPARED FROM POLYMER-CONTAINING SOLUTION

7.1 INTRODUCTION

In the previous chapters, the experimental evidences on the formation of micron-range interconnected porous gels from alkoxy-derived silica sols containing water-soluble organic polymers have been shown. Their micron-range porosity could be controlled by changing reaction parameters such as compositions or temperature of the solution. Concerning the nanometer-range porosity in ordinary silica gels, it has been demonstrated that the aging or solvent exchange treatments in the wet state induce the structural evolution due to various solid-solid or solid-liquid reactions which occur on the internal surfaces[1,2]. Reversible changes in the nanometer-range pore size distribution measured by thermoporometry with solvent exchange have recently been reported in titania and zirconia systems[3,4]. Since the polymerization of polymer-containing hydrolyzed alkoxysilane generates highly ramified polymers[5], the effect of chemical treatment is expected to be enhanced than that in ordinary gels with rather compact structural units.

In this chapter, the effect of solvent exchange on the nanometer-range pore structure of the heat-treated xerogels has been extensively described. A model concept of good- and poor-solvents against the swellable structural units of wet silica gels was employed in order to explain the drastic changes in the internal surface characteristics with soaking treatments.

7.2 EXPERIMENTAL

7.2.1 Gel Preparation

Sample gels were prepared using polyacrylic acid (denoted as HPAA, molecular weight: 90,000, Aldrich Chemical Co.) and tetraethoxysilane (TEOS, Shin-Etsu Chemical Co.) as starting materials. The starting solution was prepared in the molar ratio TEOS:HPAA:H_2O:HNO_3 = 1:0.177:9.22:0.16 in the following procedure. After the hydrolysis at room temperature for a few minutes, the starting solution was kept at 80°C for 1 hr in a sealed container where gelation occurred after 35 min, followed by the aging treatment at 40°C for 20 hrs. The aged gel exhibited syneresis resulting in more than 10% of linear shrinkage. The gel sample after appropriate leaching and drying showed well-defined interconnected porous structure with the diameter of ca. 2μm.

7.2.2 Leaching and Soaking Treatments

The wet gels thus prepared were immersed in either pure ethanol or equi-volume mixtures of ethanol and aqueous solutions with various pH's in order to leach out the HPAA phase, finally soaked in various organic solvents or aqueous solutions. The leaching and soaking treatments were carried out at room temperature by immersing $3cm^3$ of a wet gel piece in $30cm^3$ of each solution. The external liquids were thoroughly renewed every 2h. In most cases, leaching steps consisted of three times of successive immersion. For the reference sample shown as zero leaching time in Figure 7.2, the drying and heat-treatment were performed without any leaching and soaking treatment. The composition and apparent pH of solutions used in the leaching or soaking steps are listed in Table 7.1.

Table 7.1 : Aqueous components of the solutions used in leaching steps. Leaching treatments were performed with 50 vol/vol% mixture of each aqueous component with pure ethanol. The apparent pH values of mixture solutions measured with a glass electrode are shown.

Notation	Aqueous Component	Apparent pH
A	1M HNO_3	0.80
B	0.1M HNO_3	1.58
C	0.01M HNO_3	2.48
D	Distilled Water	5.72
E	0.005M NH_4OH	9.80

7.2.3 Surface Characterizations

Preliminary experiments showed that the surface characters of heat-treated gels depended not only on leaching and soaking but also on drying and heating processes. In order to minimize the effect of the latter ones, the following standardized procedure was adopted. After finishing the soaking steps, the wet gels were dried in an air-circulating bath at 40°C to remove the liquid phase by evaporation. For the liquids with higher boiling point, the complete drying required a few days or higher temperature. For the surface area measurements, the dried or half-dried gels were heat-treated at 600°C for 5h in most cases. As described in the following section, the 5h holding assured the complete decomposition and removal of organic components as well as the settled values of surface area reflecting the thermally stabilized structure. Adsorption experiments of N_2 gas at liquid N_2 temperature were carried out for the roughly crashed samples using the steady-flow type apparatus equipped with TCD detector (GAB-10, Yanaco). Samples were degassed at 200°C for 30 min under dry nitrogen flow prior to each measurement. The experimental errors in the surface area calculated from the data taken at three different relative pressures were proved to be less than 10% for all the samples. The reliable lower limit of surface area was $5m^2g^{-1}$.

The small angle x-ray scattering (SAXS) measurements were performed for the several selected samples in order to analyze the fractal nature of structural units of silica skeletons. The heat-treated gels were ground and sieved to obtain 0.5mm granules and were aligned in the scattering cell. Details of SAXS equipment are reported elsewhere[6].

The distributions of pore diameters larger than 6nm were determined by mercury porosimetry (PORESIZER-9310, Micromeritics Corp.) and those smaller than 100nm with an automatic nitrogen adsorption pore size analyzer (ASAP-2000, Micromeritics Corp.), for the selected samples.

7.3 RESULTS

7.3.1 Effects of Leaching and Soaking Conditions

The measured values of BET surface area decreased with increasing period of heat-treatment at 600°C, especially for the samples soaked in ethanol-rich solvents. The 5h treatment was adopted for all the samples to assure the settled values of surface area.

Figure 7.1 shows the dependence of BET surface areas S_{BET} on the apparent pH of leaching solutions and their changes by additional soaking treatments in pure ethanol. In the lowest pH condition, S_{BET} has the highest value and retains modest value after a single soaking in ethanol. In higher pH conditions, however, S_{BET} decreases and passes through a minimum at the condition roughly corresponding to the isoelectric point of polymerized amorphous silica (pH=1.5-2.0)[7], then increases to a certain value showing only weak dependence on pH. In these cases, S_{BET} decreased below the detectable limit after a single ethanol soaking. The decrease in S_{BET} from several hundreds down to few square meters per gram corresponds to the drastic reduction of surface roughness in nanometer-range. To be more exact, the gel skeletons of samples which showed very low surface area were originally

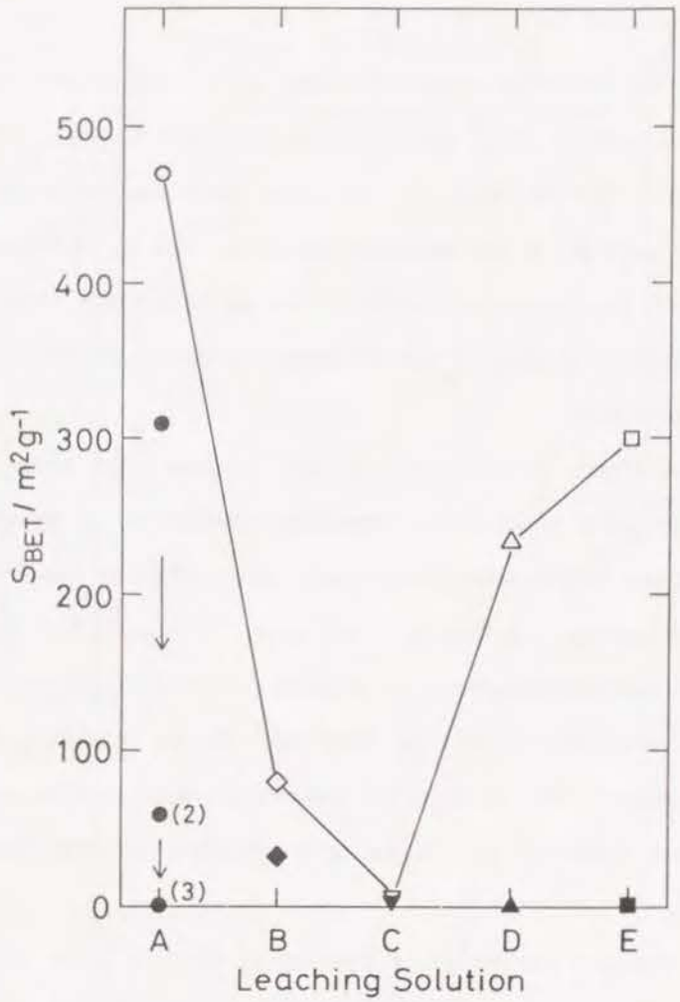

Figure 7.1 Dependence of BET surface area S_{BET} of heat-treated (600°C, 5h) gels on composition of leaching solutions and subsequent soaking treatments with pure ethanol. Open and closed symbols respectively denote before and after the soakings in ethanol. Numbers in parentheses denote the repetition of soaking in ethanol. Solution compositions are shown in Table 7.1.

composed of so fine structural units as could be almost completely sintered at 600°C for 5h.

Obviously the effect of ethanol soaking is to "smoothen" the gel surface and make it sinterable during the heat treatments. The fact that the same effect can be seen for the aqueous solutions with isoelectric condition indicates the close analogy of the phenomenon with that in swellable organic gel systems in which the degree of swelling can be controlled either by chemical affinity or by ionic character of the solvents as well as by the charge density on the gel-network[8,9].

Figure 7.2 shows the recovery of the surface area once depressed by the leachings in pure ethanol by soaking treatments in aqueous solutions. Also for this effect, acidic solution is much more efficient than the neutral or basic ones for obtaining the high surface area. It should be noticed that the changes in the surface structure of present silica gels shown in Figures 7.1 and 7.2 are reversible as far as the leaching/soaking treatment is carried out for "wet" gel state. This is in good accordance with the report on the reversible swelling behavior of titania gels studied by the thermoporometry technique[7].

Figure 7.3 shows the effect of soaking in various polar organic solvents on the surface area. The abscissa shows the solubility parameter of each solvent, δ_s, which is defined as a square root of cohesive energy density, commonly used to estimate the compatibility between solvents or solvent and polymers. Comparison has been made for the samples pre-soaked under neutral conditions (Solution D) in order to avoid possible complexity arising from the condensation reactions between hydroxyl-containing solvents and accompanying changes in the nature of the gel surface. There seems to exist steep transition of the surface structure around δ_s = 15, which results in several hundred-fold changes in S_{BET}.

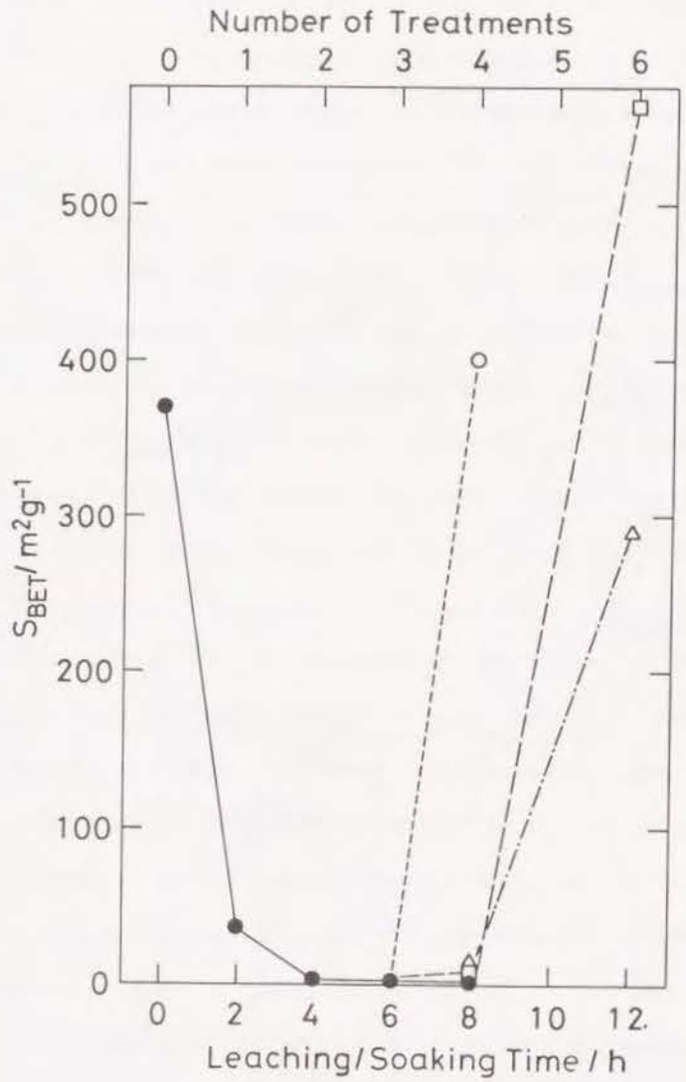

Figure 7.2 Change in BET surface area S_{BET} of heat-treated gels with soakings in aqueous solutions after leaching treatments in ethanol. ○ :solution A, △ :D, □ :E.

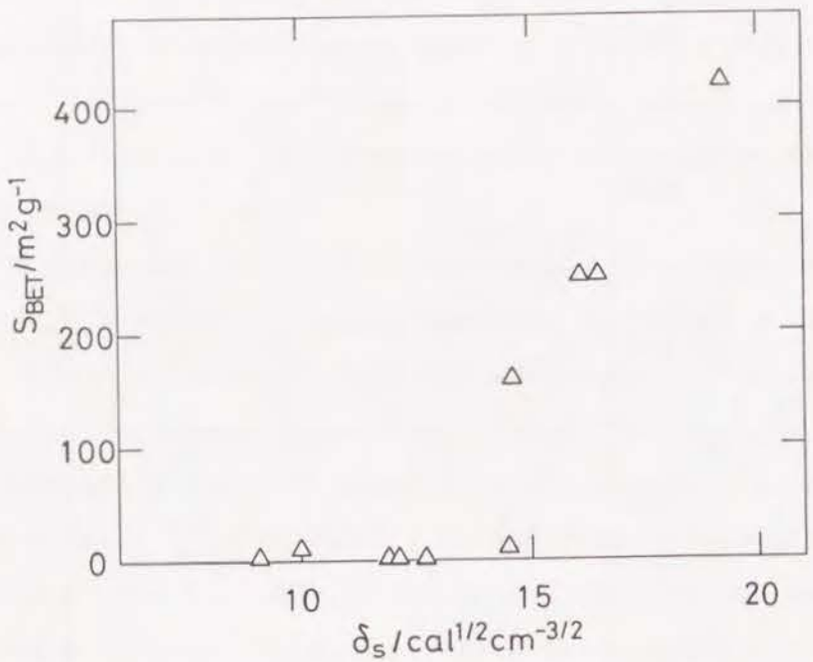

Figure 7.3 Dependence of BET surface area S_{BET} of heat-treated gels on solubility parameter of organic solvents used in the soaking treatments.

7.3.2 Surface Structure Evidenced by SAXS

Figure 7.4 shows the log-log plotted SAXS intensity vs. scattering vector q of the selected gel samples after different leaching-, soaking-, and heat-treatments. The treatment conditions and corresponding measured values of Porod-region slope are listed in Table 7.2. The profiles can be classified into two groups based on the q-dependence in higher q region, one with single power-law profile and another with upward convex curve. Hereafter, gel samples with relatively high (>100 m^2/g) surface area and Porod-region profile with upward convex shapes will be denoted as H-type gels, whereas those with low surface area and single power-law profile as L-type gels. A possible interpretation of the upward concave curve is to regard it as combined power-law slopes indicative of the existence of relatively compact units building up the ramified aggregated structure. The scattering vector corresponding to the intersection or crossover of the slopes is a measure of the size of the structural units[6]. Although there remains another possibility of the upward convex profile to be viewed as the polydispersed porous structure[10], the existence of a certain kind of density fluctuation in the gel structure in a length scale of few nanometers might well be assumed.

Following the power-law analysis of upward convex profile, the slopes α of the H-type gels in high q region fall in $-4 < \alpha < -3$ while in low q region $\alpha <= -2$, which indicate the gel structure consisting of ramified aggregation of small compact units with surface fractal character[6]. Further decrease of α at higher temperature implies the partial densification or sintering of structural units. In contrast, the L-type samples show α-values of around -2 even treated at considerably different temperatures. Discrete structural unit cannot be defined in this case, and again the silica particles aggregate in a highly ramified manner.

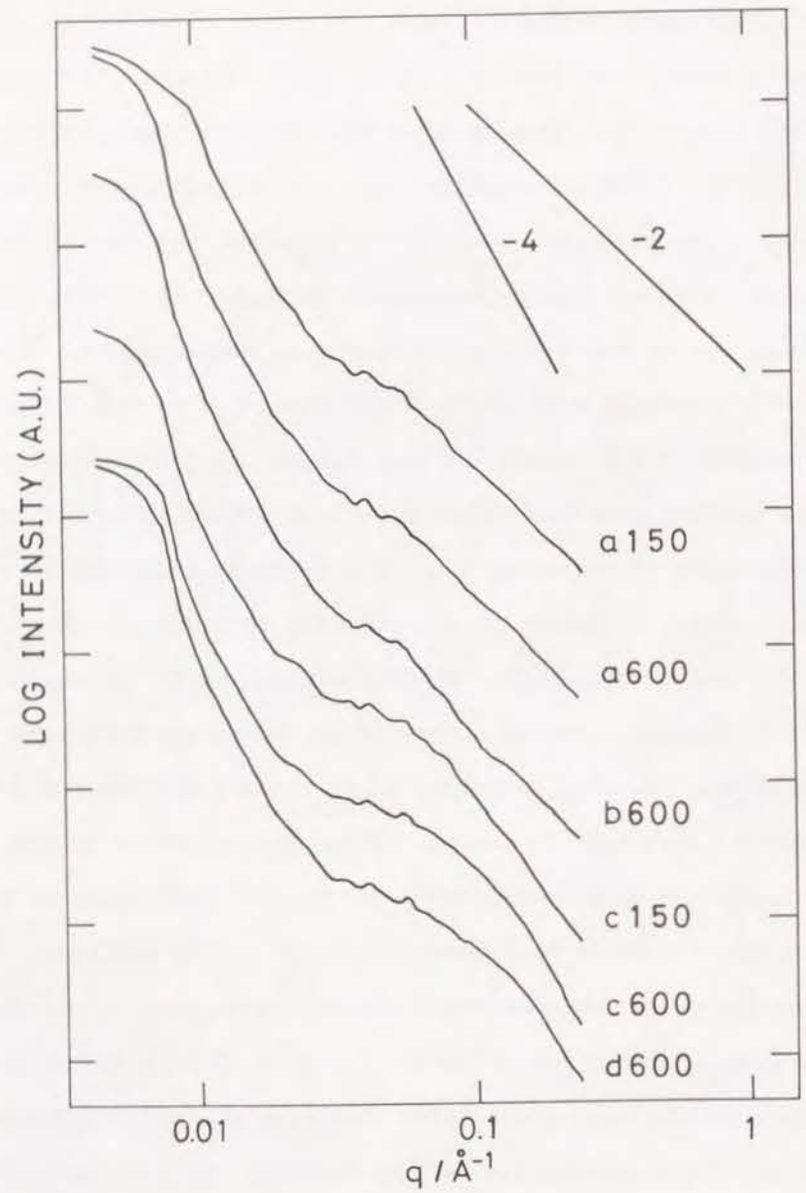

Figure 7.4 Log-log plotted SAXS profiles of gels leached, soaked and heat-treated in various conditions. The abscissa is scattering vector q defined by $q=(4\pi/\lambda)\sin(\theta/2)$ where λ is the wavelength of incident beam, and θ is the scattering angle.
The intensity is arbitrarily shifted for clarity.

Table 2 : BET specific surface areas and Porod region slopes α of gels after various leaching/soaking and heat-treatments.

Sample Name (Type)	Leaching Condition	Soaking Condition	Heat-Treatment	S_{BET}/m^2g^{-1}	α
a 150 (L)	EtOH, 2h*3	None	150°C, 24h	-	-2.1
a 600 (L)	EtOH, 2h*3	None	600°C, 5h	<5	-2.0
b 600 (L)	liq.D, 2h*3	EtOH, 2h	600°C, 5h	<5	-2.1
c 150 (H)	EtOH, 2h*3	1N HNO_3, 2h	150°C, 24h	-	-2.9
c 600 (H)	EtOH, 2h*3	1N HNO_3, 2h	600°C, 5h	400	-3.7
d 600 (H)	liq.D, 2h*3	None	600°C, 5h	230	-3.4

7.3.3 Pore-Size Distribution

Figure 7.5 shows the pore-size distribution of gels denoted as **b**600 and **d**600 in Table 7.2. The data of mercury porosimetry and nitrogen adsorption are combined in the form of cumulative specific pore volume. It can be clearly recognized that pores in both micro- and macro-pore region exists in **d**600 in good accordance with the high surface area. In contrast, **b**600 has no pores smaller than 1μm after the sintering of micro-pores although the total pore volume slightly exceeds that of **d**600.

7.4 DISCUSSION

7.4.1 Structural Evolution by Soaking Treatment

The drastic changes in specific surface area and in SAXS profile suggest that the surface structure can be modified by the soaking treatments of the wet gels. The facts that high surface area is always accompanied by the Porod-region profile with shoulder in higher q and that low surface area by single power-law profile can be explained assuming the existence of discrete and isolated surface structural units in the H-type samples. Considerably high surface area of the L-type sample with shorter heat-treatment duration ($300 m^2 g^{-1}$ for 600°C, 2h) indicates that the structural units have similar surface roughness to that of H-type gels at lower temperature. The main difference between H- and L-type gels is, therefore, the sintering tendency of their surface structural units at 600°C.

Gel surfaces consisted of loose packing of compact units tend to be densified by increasing intra-particle bondings rather than inter-particle ones. Hence, the H-type gels can retain high surface area even after prolonged heat-treatments. In contrast, gels with no discrete structural units and with self-similarity in substantially broad length scale are likely to densify accompanying the collapse of smaller pores, and leave smooth surfaces. The above

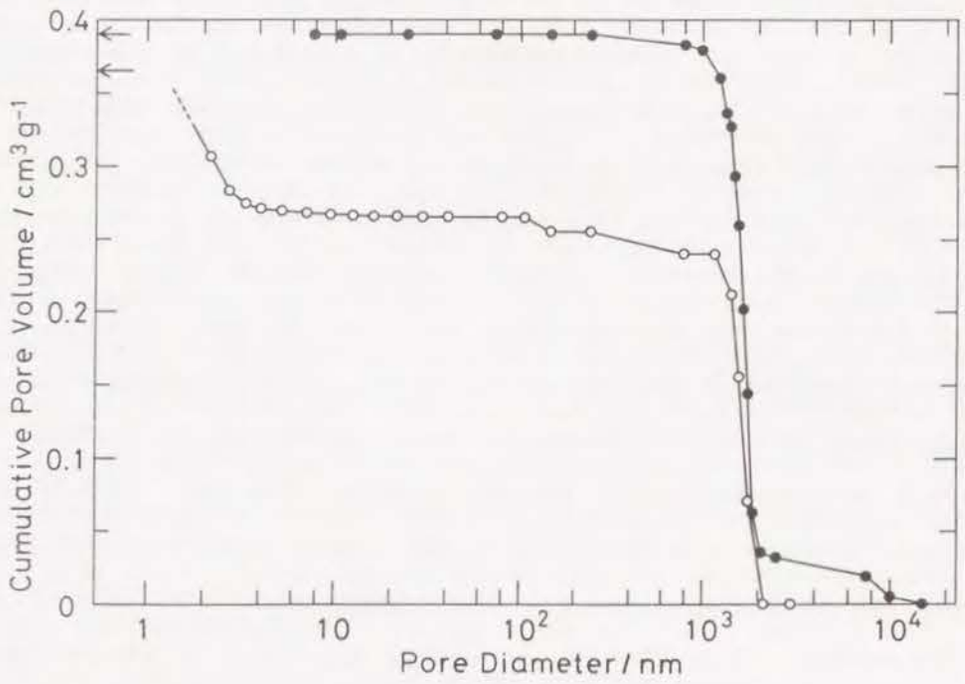

Figure 7.5 Pore size distribution of heat-treated (600°C, 5 hrs) gels soaked in different conditions. Pores larger than 10 nm were measured by mercury porosimetry, those smaller than 10nm by nitrogen adsorption-desorption method. Arrows indicate the respective total volume of nitrogen-accessible pores. ○:d600, ●:b600.

described difference is readily seen in the pore size distribution in nanometer range (see Figure 7.5).

7.4.2 Comparison with Organic Polymer Gel - Solvent Systems

Concerning the surface structure evolution by soaking treatments, important variables seem to be pH and solubility parameter of the external solutions. Organic gels initially swollen by a solvent and in one-phase state are known to easily be made cloudy due to microscopic phase separation with a relatively small change in temperature or solvent quality[7]. Gel networks have such low mobility that they cannot adjust themselves to the instantaneous change in the chemical interaction between solvent phase, which often drives the system into unstable region in a phase diagram. When the phase separation proceeds by the spinodal mechanism, the compositional fluctuations spontaneously develop in a microscopic scale, resulting in the uniformly distributed micro-domains within the gel network. The same kind of phase separation is expected to take place in the present silica - solvent systems because the swelling phenomena are already observed in many inorganic gel - solvent systems. This kind of micro-phase separation in wet-gel network seems to explain well the experimental results on the changes in microporosity with various exchanged solvents reported for the other inorganic systems[8]. (See Appendix)

With the drying proceeds, the spacial difference in network density increases to form porous structure in the dried gel. Therefore, gels under "swollen" state on drying tend to retain only fine pores corresponding to a molecular scale and show homogeneous or self-similar structure in an extended length scale. Those under "phase-separated" state give heterogeneous structure in the length scale of their domain size, which results in the meso- or macro-porous structure.

7.4.3 Factors Determining the Pore Surface Characteristics

Provided that the wet-gel network of the present macroporous silica system "reversibly swells", factors affecting the surface structures of dried or heat-treated gels can be consistently specified. Firstly, the phase separation of wet-gel occurs when the solubility parameter of the external solvent exceeds 15. This may imply that the silica gel network has relatively high polarity compared with ordinary hydrophilic organic polymers. The reason why the solvents with substantially low solubility parameter give L-type gel structure remains unclear, although an insufficient exchange of less polar solvent with polar ones in the vicinity of polar surface silanols may give an acceptable explanation. Secondly, the wet-gel tends to phase-separate under strongly ionic conditions. Especially under acidic conditions, this effect is obvious even if a considerable amount of ethanol coexists in the solution. This can be related with the protonation of ethanol and surface silanols which induces the electrostatic effects. This is in good accordance with the reports of Tanaka et al. which indicate the higher tendency of phase separation in ionic gels than neutral ones[8].

The reason why the wet-gel networks in the present samples are so sensitive to the change in solvent quality of the external solutions remains also unclear. It could partly result from the highly ramified manner in which the silica clusters aggregate in organic polymer-incorporated alkoxy-derived system. The peculiarity in the polymerization behavior has been reported for the systems containing sodium polystyrene sulfonate by measuring the SAXS of reacting solutions (Chapter 6 [5]) and almost the same results have been obtained also for the present system[11]. This point will be made more clear by measuring the detailed pore size distribution and skeletal density.

7.5 CONCLUSIONS

(1) The BET surface area of heat-treated silica gels obtained from HPAA-containing solution showed drastic changes with leaching and soaking treatments in the "wet" stage.

(2) SAXS measurements for several dried gels revealed that they can be categorized into H-type with discrete structural units and L-type with self-similarity in an extended length scale. Experimental results of pore size distribution and surface area measurement could well be explained by the above structural pictures.

(3) The origin of the formation of structural units in the "wet" state was found in the phase separation of the silica gel network between the external liquids with poor solubility. Highly ionic solutions acted as poor solvent. These facts indicated the close analogy of the present silica gel system to the organic ones. The discrete structural units of H-type gels could have originated from the phase-separated domains with higher density.

APPENDIX: An Alternative Interpretation of Thermoporometry Data for Wet Titania and Zirconia Gels

According to Quinson et al., the reversible change in the pore structure in wet titania or zirconia gels are interpreted in relation to the polarizability of the solvents filled in the pores[8]. Although their argument based on the thermodynamic interactions between an oxide and a solvent to affect the pore surface configuration seems to give a reasonable explanation to the experimental results, their assumption of "rigid" inorganic gel network sounds rather ambiguous. In fact, they observed a reversible swelling detectable by macroscopic volumetry which strongly suggest the "soft" character of the gel network having the correlation length considerably shorter than that in loosely crosslinked organic systems.

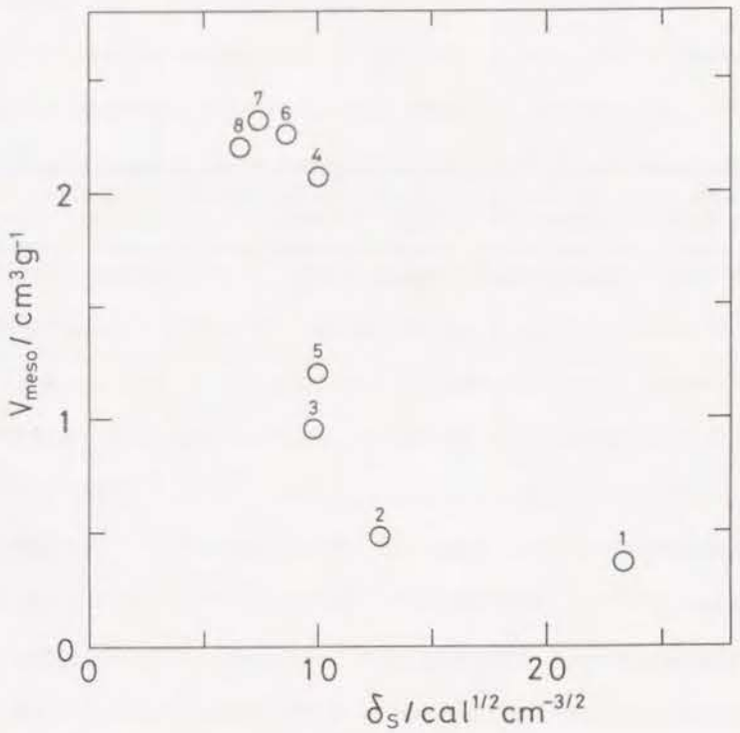

Figure 7.A1 : Mesopore volume plotted against solubility parameter of pore liquids. Numbers correspond to those listed in Table 7.A1

Table 7.A1 : Mesopore volume of reversed-micelle-polymerized titania gel treated with various solvents measured by thermoporometry.

Solvent	Solubility Parameter δ_s $((cal\ cm^{-3})^{1/2})$	Mesopore Volume V_{meso} $(cm^3\ g^{-1})$
(1) Water	23.4	0.370
(2) Ethanol	12.7	0.480
(3) Acetone	9.9	0.955
(4) Nitrobenzene	10.0	2.070
(5) 1,4-Dioxane	10.0	1.195
(6) Carbon Tetrachloride	8.6	2.260
(7) Heptane	7.4	2.318
(8) Decane	6.6	2.200

An alternative interpretation in terms of the solubility parameter of the solvents suggests that the same kind of swelling-deswelling transition exists in those micelle-polymerized titania or zirconia gels. Figure 7.A1 shows the mesopore volume measured by thermoporometry re-plotted against the solubility parameter of the solvents used to fill the pores. It is obvious that the large change in mesopore volume occurs when δ_s exceeds 10. Following their discussion, the increased mesopore volume is brought by a reorganization of micropores into larger spaces due to interfacial energy requirements. This can alternatively be explained in such a way that the swelling of micro-phase separated domains reorganize the micropores and makes them into larger pore space. Since their gels were prepared under relatively limited water condition, it is natural their solubility parameter to be substantially lower than that of silica gel prepared in our study. The swelling experiments of wet titania gel performed in the literature[7] showed very small volume change on swelling. This may due to the high cross-linking density or to the stiffness of the network in inorganic gels. However, it is possible for the structural units of the network in the length scale of from several to tens nanometers to interact as polymeric unit with external solvent to cause swelling accompanied by the substantial softening of the network leading to the drastic change in the mesopore structure, as has been shown for silica system in the present study. The most powerful tool to check this presumption should be SANS or SAXS measurements of gels in wet state.

SUMMARY OF CHAPTER 7

Nitrogen adsorption method, together with small angle x-ray scattering (SAXS) technique, has been employed to analyze the pore surface characteristics of macroporous silica gels with micron-range interconnected morphology. Broad variations were observed in the specific surface area and pore-size distribution of heat-treated gels by the soaking treatments in the wet state in several kinds of organic solvents or in aqueous solutions with various pH's. These effects could be related to the swelling phenomenon of loosely cross-linked structural units of silica network analogous to that well-known for organic polymer systems.

REFERENCES

[1] J.F. Quinson, N. Tchipkam, J. Dumas, C. Bovier and J. Serughetti, *J. Non-Cryst. Solids*, **100**(1988), 231-235.

[2] T. Kawaguchi, H. Hishikura and J. Iura, *J. Non-Cryst. Solids*, **100**(1988), 220-225.

[3] J.F. Quinson, N. Tchipkam, J. Dumas, C. Bovier, J. Serughetti, C. Guizard, A. Larbot and L. Cot, *J. Non-Cryst. Solids*, **99**(1988), 151-159.

[4] J.F. Quinson, J. Dumas, M. Chatelut, J. Serughetti, C. Guizard, A. Larbot and L. Cot, *J. Non-Cryst. Solids*, **113**(1989), 14-20.

[5] K.Nakanishi, N.Soga, H.Matsuoka and N.Ise, submitted to *J. Am. Ceram. Soc.*

[6] D.W. Schaefer and K.D. Keefer, in; "*Better Ceramic through Chemistry*", eds. C.J. Brinker, D.E. Clark and D.R. Ulrich, (Elsevir-North-Holland, New York, 1984), 1-13.

[7] P.G. deGennes, in ; "*Scaling Concepts in Polymer Physics*", (Cornell University Press, Ithaca and London, 1979), Chapter V.

[8] T. Tanaka, D. Fillmore, S.-T. Sun, I. Nishio, *Phys. Rev. Lett.*, **45**(1980), 1636-1639.

[9] T.Tanaka, *Phys. Rev. Lett.*, **40**(1978), 820-823.

[10] J.E.Martin and A.J.Hurd, *Appl. Cryst.*, **20**(1987), 61-78.

[11] H.Matsuoka, H.Ishii and N.Ise, unpublished data

SUMMARY

The present thesis has described the studies on the phase separation in the polymer-incorporated alkoxy-derived silica sol-gel systems as a basis for controlling macro- or micropore morphology of gel-forming oxide materials. The contents of respective chapters are summarized as follows.

In Chapter 1, the phase separation in the acid catalyzed alkoxy-derived silica systems containing polyacrylic acid was studied. The occurrence of spinodal phase separation was clearly evidenced by the light scattering measurement, and the formation of well-defined micron-range interconnected porous morphology was observed. Steep decrease in the mobility of gelling silica network was considered to be responsible for the remarkable increase in scattering intensity after the settlement of peak position. Experimental results on the effects of HPAA concentration and solvent composition suggested that the relative rates of phase separation and gel-formation are the most important factors to determine the quench depth and resulting periodic size of the interconnected gel morphology.

In Chapter 2, using the same system as in Chapter 1, the effects of solvent composition, molecular weight of polyacrylic acid and reaction temperature on the phase separation and gelation behavior were examined through the morphology observation by SEM. All the effects could well be explained by considering the respective influences on the factors which determine the phase separation and gel-formation behavior such as segregation strength and volume fraction of polymer, polymerization rate of silica and total mobility of the phase separating system.

In Chapter 3, the phase separation behavior was studied in an extended acid catalyst concentration range for the same system as the previous chapters. In spite of the considerable differences in the polymerization rate and

gel-forming behavior of silica, analogous phase separation and gelation to that in the highly acidic systems has been observed even under the pH condition higher than the isoelectric point of silica. The difference in the weight- and number-average molecular weights of silica polymers at gel-formation well explained the changes in the relations between reaction conditions and gel morphology.

In Chapter 4, the addition effects of various organic solvents on the porous gel structure have been investigated for the acid-catalyzed HPAA-TEOS system. The changes in the segregation tendency of HPAA and in the polymerization rate of silica influenced the overall phase separation and gelation processes leading to the wide variety of resultant gel morphology. The efficiency of additional solvents which reduce the segregation strength and accelerate polymerization, such as formamide, to form finer interconnected structure in an extended composition range was demonstrated.

In Chapter 5, phase separation behavior in the acid-catalyzed NaPSS-TMOS has been investigated. Macroporous gel morphologies including the interconnected structure in a length scale from 0.1 to 100μm were observed by SEM also in the system containing alcohol-insoluble polymer. Although the effects of various reaction parameters on the gel morphology could be explained similarly to HPAA-containing systems, the dependence of morphology on any preparation condition was much stronger than that in HPAA-system reflecting the poor solubility of NaPSS in methanol-water mixed solvent.

In Chapter 6, the effect of kind of starting alkoxysilane was studied employing NaPSS-containing systems. Small angle x-ray scattering measurements of polymerizing solutions suggested the formation of highly ramified and larger silica polymers with an incorporation of NaPSS. The segregation tendency of NaPSS was found to be a dominant factor in determining the micron-range periodic size fixed in the gel structure. The possibility of inclusion of

the nucleation-growth mechanism in the large sized periodic domain formation was also suggested.

In Chapter 7, nitrogen adsorption-desorption method, together with SAXS technique, has been employed to analyze the pore surface characteristics of macroporous silica gels with micron-range interconnected morphology. Broad variations were observed in the specific surface area and pore-size distribution of heat-treated gels by the soaking treatments in the wet state in several kinds of organic solvents or in aqueous solutions with various pH's. The effects could be related to the swelling phenomena of loosely crosslinked structural units of silica network analogous to those well-known for organic polymer systems.

From the present series of studies, the possibility of tailoring both the macro- and micro-porosity of gel-forming oxide materials has been demonstrated. Since the mechanism of morphology formation will not be specific to the organic polymer - silica systems, various kinds of gel-forming oxides, including multicomponent systems, will possibly be tailored in a similar manner. The fixation of the transient structure formed through the non-equilibrium phase separation route has extensively been utilized in polymer alloying technology. Further investigations on the generality and specificity of the inorganic gel-forming systems compared with those composed of organic polymers are required to extend the compositional variation and the controllable length scale of the material morphology, which promises one the goal of low-temperature tailoring of inorganic material structures.

AKNOWLEDGEMENTS

The present thesis has been carried out at Department of Industrial Chemistry, Faculty of Engineering, Kyoto University, under the direction of Professor Naohiro Soga.

The author expresses his sincere gratitude to Professor Naohiro Soga for his continuous encouragement and valuable suggestions throughout the work. Useful discussions with Prof. T.Hanada and Prof. K.Hirao are also appreciated. Helpful advice on the experiments from Dr. H.Kozuka, Dr. K.Tanaka, Mr. S.Tanabe are gratefully acknowledged.

The author is grateful to Professor H.Odani and Professor S.Sakka, Institute for Chemical Research, Kyoto University, for valuable discussions on the physical chemistry of polymers and science of sol-gel processing.

The collaborations of Dr. T.Inoue, Institute for Chemical Research, and Professor T.Hashimoto and Mr. M.Takenaka, Department of Polymer Chemistry, Faculty of Engineering, in the performance of light-scattering measurements are gratefully acknowledged. The author is also indebted to Professor N.Ise and Dr. H.Matsuoka in carrying out all the SAXS measurements.

The author wishes to thank Dr. M.Fukuda of Toso Company for supplying the NaPSS solutions, and Mr. T.Kawaguchi, Ms. M.Yamamoto and Mr. Y.Sagawa, Advanced Glass R&D Center, Asahi Glass Company, for providing polyacrylic acids with various molecular weights and performing nitrogen adsorption and mercury porosimetry measurements.

Finally, hearty thanks are made to Norihiko and Toshiko Nakanishi, his parents, for their continuous understanding, encouragement and prayer.

S.G.D.

Kazuki Nakanishi